

UNIVERSITY OF MANITOBA

Heat Recovery From Horizontal Tubular Condensers
of Refrigeration Systems

by

Thambiyah Nitheanandan

A Thesis

Submitted to the Faculty of Graduate Studies
in Partial Fulfillment of the Requirements for the
Master of Science Degree in Mechanical Engineering

Winnipeg, Manitoba

1988

Permission has been granted to the National Library of Canada to microfilm this thesis and to lend or sell copies of the film.

The author (copyright owner) has reserved other publication rights, and neither the thesis nor extensive extracts from it may be printed or otherwise reproduced without his/her written permission.

L'autorisation a été accordée à la Bibliothèque nationale du Canada de microfilmer cette thèse et de prêter ou de vendre des exemplaires du film.

L'auteur (titulaire du droit d'auteur) se réserve les autres droits de publication; ni la thèse ni de longs extraits de celle-ci ne doivent être imprimés ou autrement reproduits sans son autorisation écrite.

ISBN 0-315-44177-1

HEAT RECOVERY FROM HORIZONTAL TUBULAR CONDENSERS
OF REFRIGERATION SYSTEMS

BY

THAMBIAYAH NITHEANANDAN

A thesis submitted to the Faculty of Graduate Studies of
the University of Manitoba in partial fulfillment of the requirements
of the degree of

MASTER OF SCIENCE

© 1988

Permission has been granted to the LIBRARY OF THE UNIVER-
SITY OF MANITOBA to lend or sell copies of this thesis, to
the NATIONAL LIBRARY OF CANADA to microfilm this
thesis and to lend or sell copies of the film, and UNIVERSITY
MICROFILMS to publish an abstract of this thesis.

The author reserves other publication rights, and neither the
thesis nor extensive extracts from it may be printed or other-
wise reproduced without the author's written permission.

TABLE OF CONTENTS

	<u>PAGE</u>
ABSTRACT	iv
ACKNOWLEDGEMENTS	vi
LIST OF FIGURES	vii
LIST OF TABLES	x
NOMENCLATURE	xi
CHAPTER	
1. INTRODUCTION	1
1.1 General	1
1.2 Vapor Compression Cycles	2
1.2.1 Single Stage Vapor Compression Cycle	4
1.2.2 Compression Ratio	8
1.2.3 Choice of Refrigerants	10
1.3 Applications	15
1.4 Heat Recovery From Refrigeration Systems	22
1.4.1 Sensible and Latent Heat	22
1.4.2 Quality of Energy	25
1.5 Advantages of Condensing Inside Tubes..	26
1.6 Disadvantages of Condensation Within Tubes	28
2. FIELD STUDY	31
2.1 Introduction of Food Processing Plant Study	31
2.1.1 Description of the Plant	31
2.1.2 Resource Input	34

	<u>PAGE</u>
2.2 Description of the Methodology Followed in Performing the Energy Audit	41
2.2.1 Energy Use in the Refrigeration System	41
2.2.1.1 Testing Methodology	41
2.2.1.2 Component Analysis .	44
2.2.2 Energy Use in the Heating System	49
2.2.2.1 Methodology of Evaluating Hot Water Production	49
2.3 Energy Balance of the Plant	58
2.4 Advantages of Reclaiming Condenser Waste Heat	60
2.5 Recommendations and Conclusions of the Energy Survey	61
2.6 Need for a Condenser Design Procedure .	64
3. REVIEW OF LITERATURE ON CONDENSATION HEAT TRANSFER INSIDE TUBES	69
3.1 ASHRAE Recommended Correlations	69
3.1.1 Laminar Flow Model	71
3.1.2 Turbulent Flow Model	73
3.2 Correlations Based on Theoretical Analysis	76
3.3 Correlations Based on Empirical Methods	96
4. DEVELOPMENT OF DESIGN PROCEDURE	102
4.1 Flow Regime Concept	102
4.2 Creation of a Heat Transfer Data Base .	110

4.3	Assessment of Correlations With the Data Base	113
4.4	Selection of Correlations	123
4.4.1	Mist Flow Regime	125
4.4.2	Annular Flow Regime	135
4.4.3	Wavy Flow Regime	153
4.4.4	General	153
4.5	Development of a Design Procedure Based on the Theory of Successive Summation .	156
5.	APPLICATION TO FIELD STUDY	163
6.	CONCLUSIONS AND RECOMMENDATIONS	166
6.1	Conclusions	166
6.2	Recommendations	169
	REFERENCES	170
	APPENDICES - APPENDIX A	175
	Determination of State Points in a Vapor Compression Cycle	
	- APPENDIX B	181
	Algorithm of the Design Procedure	
	- APPENDIX C	182
	Computer Listing of the BASIC Program	

ABSTRACT

The objectives of the investigation are to evaluate recently published condensation heat transfer correlations and compare the results to the correlations recommended by ASHRAE for horizontal tubular condensers with condensation inside tubes under different flow regimes.

A design procedure based on two phase flow transitions developed by Soliman for mist to annular and annular to wavy flow are used because of simplicity and extensive data support. Three major flow regimes are defined by the above two transitional criteria for a horizontal condenser and suitable heat transfer correlations for each of the three regimes are selected.

Seven correlations available in the literature are compared with a data base from four different publications. Local condensation heat transfer coefficients of condensing vapors in the mist flow regime are predicted accurately by Soliman's correlation. In this regime, where the Weber number is greater than 40, the other six correlations are less precise.

In the annular flow regime, defined by Weber less than 40 and Froude number greater than seven for condensation inside horizontal tubes, the heat transfer coefficient is represented by a single correlation.

Flows with a Froude number less than seven are in the wavy flow regime and the heat transfer coefficient within

this regime is predicted adequately by the ASHRAE recommended correlation. The experimental data within this regime is limited.

A design procedure in the form of a computer program in BASIC language is developed based on the above results. The food processing industry has numerous applications in which the waste heat rejected by refrigeration systems can be used for preheating water. Heat exchanger designs for condensation heat transfer inside tubes provide an economical method of reclaiming this heat.

ACKNOWLEDGEMENTS

The author wishes to express his deepest gratitude to Prof. R.E. Chant for his continuing interest, encouragement and guidance without which this thesis would have been impossible. Special thanks are due to Dr. H.M. Soliman for his encouragement and helpful suggestions. Thanks are also due to Dr. R. A. Gallop.

Special thanks are due to Mr. E. Bertschinger, General Manager, Dunn-Rite Food Products Ltd. and his staff for giving an opportunity to conduct the energy audit. Special thanks are also due to Mr. M. Kapitoler for drawing the diagrams. Thanks are also due to Mrs. M. Webster for typing the manuscript.

The author is grateful to the Canadian Commonwealth Scholarships and Fellowships Plan for their financial support. Financial support was also received from the Institute for Technological Development under a research grant.

Finally, the author wishes to thank his parents in Sri Lanka for their sincere support and encouragement.

LIST OF FIGURES

<u>Figure</u>	<u>Page</u>
1.1 Pressure enthalpy diagram of an actual vapor compression cycle.....	3
1.2 Temperature entropy diagram of an actual vapor compression cycle	5
1.3 Components of a vapor compression refrigeration system	7
2.1 Diagrammatic arrangement of hot water production systems	32
2.2 Layout of refrigeration equipments	36
2.3 Successive stages in poultry processing	39
2.4 Dunn-Rite plant utility bills between July 1983 to August 1986	40
2.5 Dunn-Rite plant electricity use between July 1983 to August 1986	42
2.6 Dunn-Rite plant electricity demand between July 1983 to August 1986	43
2.7 Dunn-Rite boiler test	51
2.8 Dunn-Rite water use: November 18-21, 1986	56
2.9 Dunn-Rite gas use: November 18-21, 1986	57
2.10 Helical coil tube heat recovery unit	66
2.11 Bayonet tube or U-tube tank heater	67
3.1 Development of flow patterns in the direction of flow during condensation	70
3.2 Surface covered by the Condensing film over the film angle	79
3.3 Typical variation of h with the increase of film angle	86
4.1 Typical flow map developed by Baker [33]	104

4.2	Comparison of Azer <u>et al.</u> [23] correlation with his data Run No. 6 using 1967 and 1977 ASHRAE transport property values	122
4.3	Comparison of mist flow data with Traviss <u>et al.</u> [25] correlation	126
4.4	Comparison of mist flow data with Azer <u>et al.</u> [23] correlation	128
4.5	Comparison of mist flow data with Shah's [30] correlation	129
4.6	Comparison of mist flow data with Soliman's [32] correlation	130
4.7	Comparison of mist flow data with Tandon <u>et al.</u> [31] correlation	132
4.8	Comparison of mist flow data with Akers <u>et al.</u> [6] correlation	133
4.9	Comparison of mist flow data with Rosson and Myers [16] correlation	134
4.10	Comparison of annular and wavy flow data (for Condensation inside horizontal tubes) with Tandon <u>et al.</u> [31] correlation	137
4.11	Comparison of annular and wavy flow data (for condensation inside horizontal tubes) with Akers <u>et al.</u> [6] correlation	138
4.12	Comparison of annular and wavy flow data (for condensation inside horizontal tubes) with Rosson and Myers [16] correlation	139
4.13	Comparison of annular and wavy flow data (for condensation inside horizontal tubes) with Shah's [30] correlation	140
4.14	Comparison of annular and wavy flow data (for condensation inside horizontal tubes) with Traviss <u>et al.</u> [25] correlation	141
4.15	Comparison of annular and wavy flow data (for condensation inside horizontal tubes) with Soliman's [32] correlation	143
4.16	Comparison of annular and wavy flow data (for condensation inside horizontal tubes) with Azer <u>et al.</u> [23] correlation	144

4.17	Comparison of annular flow data (for condensation inside vertical tubes) with Soliman's [32] correlation	145
4.18	Comparison of annular flow data (for condensation inside vertical tubes) with Tandon <u>et al.</u> [31] correlation	146
4.19	Comparison of annular flow data (for condensation inside vertical tubes) with Shah's [30] correlation	147
4.20	Comparison of annular flow data (for condensation inside vertical tubes) with Traviss <u>et al.</u> [25] correlation	148
4.21	Comparison of annular flow data (for condensation inside vertical tubes) with Azer <u>et al.</u> [23] correlation	149
4.22	Comparison of annular flow data (for condensation inside vertical tubes) with Azers <u>et al.</u> [6] correlation	150
4.23	Comparison of annular flow data (for condensation inside vertical tubes) with Rosson and Myers [16] correlation	151
4.24	Comparison of Akers <u>et al.</u> [6] correlation with Shah's [30] correlation in the wavy flow regime .	154
4.25	Comparison of Akers <u>et al.</u> [6] correlation with wavy flow data	155
4.26	A counter flow heat exchanger	159

LIST OF TABLES

<u>Tables</u>	<u>Page</u>
1.1 Comparison of commonly used refrigerants based on -29°C evaporation and 43°C condensation for a Ton of refrigeration effect	9
2.1 Refrigeration system: refrigeration capacities and daily energy consumptions	35
2.2 Annual resource use and unit cost between September 1985 and August 1986	38
2.3 Daily water use of Dunn-Rite plant	54
2.4 Daily gas use on a typical winter processing day	55
4.1 Heat transfer data base	112
4.2 Number of calculated heat transfer coefficients falling within $+30\%$ of the heat transfer coefficient found experimentally	116
4.3 Comparison of Traviss <u>et al.</u> [25] correlation with Traviss's [49] data	117
4.4 Comparison of Azer <u>et al.</u> [23] correlation with Azer's [23] data	118
4.5 Comparison of thermophysical properties of R-12 reported in 1967 and 1977 ASHRAE Handbooks	120
4.6 Comparison of Azer <u>et al.</u> [23] correlation using μ valves reported in ASHRAE Handbook of Fundamentals 1967 with the data of Azer <u>et al.</u> [23]	121
4.7 Comparison of Tandon <u>et al.</u> [31] correlation with Azer <u>et al.</u> [23] data	123
4.8 Comparison of correlations within the three flow regimes	124
4.9 Comparison of Soliman's [32] correlation with Shah's [30] correlation for flows with a We greater than 40	131
4.10 Comparison of Shah's [30] correlation with Tandon <u>et al.</u> [31] correlation for flows with a We less than 40	152

NOMENCLATUREEnglish Symbols:

a	Gravitational component along an inclined tube, m/s^2
A	Heat transfer area, m^2
A_z	Cross sectional area, m^2
C	Constant
C_{pL}	Specific heat of liquid at constant pressure, $J/kg.K$
C_{pv}	Specific heat of vapor at constant pressure, $J/kg.K$
C_{pW}	Specific heat of the coolant, $J/kg.K$
D	Tube diameter, m
D_o	Outside diameter of the tube, m
D_i	Internal diameter of the tube, m
f_v	Fanning friction factor [13]
f_{v1}	Parameter defined by Equation 3.68
F	Parameter defined by Altman <u>et al.</u> [7], Pa
F_a	Force due to gravity, N
F_f	Force due to vapor friction, N
F_m	Force due to momentum change of condensing vapor, N
F_o	Total force due to gravity, vapor friction and momentum change, N
Fr	Froude number
F_{rT}	Parameter defined by Equation 3.37
F_s	Stress ratio between axial shear force to gravitational body force
$F(X_{tt})$	Parameter defined by Equation 3.61

F_2	Parameter defined by Bae <u>et al.</u> [20] and Traviss <u>et al.</u> [25]
g	Acceleration due to gravity, m/s^2
g_0	Gravitational constant
G	Total mass flux, $kg/m^2 \cdot s$
G_E	Equivalent mass flux for two phase flow defined by Akers <u>et al.</u> [6], $kg/m^2 \cdot s$
G_L	Liquid mass flux, $kg/m^2 \cdot s$
G_M	Mean vapor mass flux, $kg/m^2 \cdot s$
G_V	Vapor mass flux, $kg/m^2 \cdot s$
h	Local heat transfer coefficient, $W/m^2 \cdot K$
h_i	Tube side heat transfer coefficient, $W/m^2 \cdot K$
h_L	Dittus-Boelter single phase heat transfer coefficient, $W/m^2 \cdot K$
h_m	Mean heat transfer coefficient, $W/m^2 \cdot K$
h_o	Heat transfer coefficient at the top of the tube, $W/m^2 \cdot K$
h_s	Shell side heat transfer coefficient, $W/m^2 \cdot K$
h_1	Parameter defined by Equation 3.84, $W/m^2 \cdot K$
h_{π}	Heat transfer coefficient at the bottom of the tube, $W/m^2 \cdot K$
h_{fg}	Enthalpy of vapor relative to condensate film, J/kg
H	Heaviside unit function defined by Equation 3.73
j_g^*	Dimensionless gas velocity defined by Wallis [41]
J	Parameter defined by Equation 3.14
k_L	Thermal conductivity of liquid phase, $W/m \cdot K$
k_T	Thermal conductivity of the tube material, $W/m \cdot K$
k_V	Thermal conductivity of the vapor phase, $W/m \cdot K$

k_w	Thermal conductivity of fluid, W/m.K
K	Ordinate of Taitel and Dukler [40] map.
K_p	Parameter defined by Equation 4.6
L	Length of condenser, m
ΔL	Infinitesimal length of condenser, m
m_v	Mass flow rate of vapor, kg/s
m_w	Mass flow rate of coolant, kg/s
M	Parameter defined by Equation 3.46
Ga	Galileo number
N	Constant
Nu	Local Nusselt number
Nu_{an}	Nusselt number for annular flow
Nu_{st}	Nusselt number for stratified flow
Nu_{tr}	Nusselt number for transition zone
Nu_{π}	Nusselt number for the bottom of the tube
Pr	Reduced pressure
Pr_L	Prandtl number of liquid, Pr_L
ΔP_{TPF}	Frictional two phase pressure drop given by Forster and Zuber [8], Pa
q	Total heat transferred, J
Q_L	Liquid volume flow, m^3/s
Q_V	Vapor volume flow, m^3/s
R	Volumetric ratio
Re_e	Equivalent Reynolds number
Re_E	Equivalent liquid Reynolds number
Re_L	Liquid Reynolds number

Re_m	Reynolds number of the homogeneous mixture of vapor and liquid
Re_T	Total vapor Reynolds number defined by Equation 3.38
Re_v	Vapor Reynolds number
Re_w	Reynolds number of the single phase fluid
S	Perimeter of the tube, m
t_δ	Dimensionless temperature drop across the condensate film
T_O	Wall temperature, °C
T_V	Vapor temperature, °C
T_{V1}	Vapor temperature of the current section of the condenser, °C
T_{V2}	Vapor temperature at the infinitesimal section immediately next to the current section, °C
T_w	Coolant temperature, °C
T_{w1}	Coolant temperature in the current infinitesimal section, °C
T_{w2}	Coolant temperature in the adjoining section of the condenser, °C
T^+	Parameter defined by Equation 3.72
ΔT	Temperature drop across the condensate film, °C
ΔT_V	Temperature drop of vapor between inlet and outlet, °C
ΔT_w	Temperature increase of water between inlet and outlet, °C
ΔT_{LM}	Log mean temperature difference, °C
V_L	Superficial liquid velocity, m/s
V_V	Superficial vapor velocity, m/s
u_τ	Friction velocity, m/s

u_*	Friction velocity defined by Jaster and Kosky [26], m/s
U_i	Overall heat transfer coefficient based on the inside tube area, w/m^2s
We	Weber number
W_T	Total fluid flow rate, kg/s
x	Quality
x_1	Quality at the current section
x_2	Quality at the succeeding section
Δx	Infinitesimal change in quality
X_{tt}	Lockhart - Martinelli parameter [17]
Z	Axial distance from condensation starting point, m
Z_c	Parameter defined by Equation 3.83

Greek Symbols:

α	Parameter defined by Equation 3.51
β	Integral defined by Equation 3.16
δ^+	Dimensionless film thickness
ϕ_g	Parameter defined by Equation 3.70
ϕ_v	Lockhart - Martinelli pressure drop parameter
γ	A constant relating interfacial liquid velocity to the average velocity
Γ	Condensate rate per unit periphery at any point kg/m.s
λ	Parameter defined by Equation 4.2
μ_L	Dynamic viscosity of the saturated liquid, kg/m.s
μ_m	Viscosity of the mixture defined by Equation 3.90, kg/m.s
ν	Kinematic viscosity of liquid, m^2/s

θ	Angle of vapor flow vector with the horizontal
θ_m	Mean angle at which the mean heat transfer coefficient is found
$d\theta$	Infinitesimal film angle
ρ_L	Density of liquid, kg/m^3
ρ_v	Density of vapor, kg/m^3
σ	Surface tension, N/m
τ_0	Wall shear stress, N/m^2
Ω	Parameter defined by Equation 3.17
Ψ	Parameter defined by Equation 4.1
Ψ_m	Mean film angle

CHAPTER 1

INTRODUCTION

1.1 General

Heat recovery is reclaiming part or all of the waste heat energy, that may otherwise be rejected into the environment during a process. The strategy of recovering waste heat depends in part on the economics involved and the temperature of the fluid rejecting heat. Heat recovery systems have become economically attractive with the price escalation of primary fuels. As a result, greater emphasis is placed on energy conservation and maximum resource use. The sources of waste heat may be subdivided according to the temperature ranges; namely, the high temperature range (above 650°C), the medium temperature range (between 230°C and 650°C) and the low temperature range (below 230°C). High and medium temperature waste heat can be used for a number of purposes. For example, it may be used to produce process steam or mechanical work before the waste heat is extracted. The industrial uses for low temperature heat rejected is limited. However, the food processing industry offers a promising application because only in such industries are large volumes of low temperature water required for various operations such as meat, fish, poultry and vegetable preparation. Such industries are generally equipped with large mechanical refrigeration systems. These systems reject considerable amount of waste heat in the low temperature

range. Even though the rejected heat is at a low thermodynamic quality, the scope for economic recovery of the waste heat exist when a simultaneous demand for low temperature heat exists.

1.2 Vapor Compression Cycles

The vapor compression cycle is the most common cycle used to transfer thermal energy continuously from a refrigerated space to the environment. An actual vapor compression cycle is shown in Figure 1.1. The actual vapor compression cycle deviates considerably from the basic ideal vapor compression cycle and the Carnot cycle. The Carnot cycle is reversible but the ideal vapor compression cycle is comprised of irreversible processes.

In an ideal vapor compression cycle the irreversibilities are caused by isothermal evaporation and condensation processes, which require a finite temperature difference in the heat exchanger to transfer heat. Irreversibilities are also developed when fluids flow through tubes. The refrigerant flow through tubes are accompanied by pressure drop due to friction. Another major irreversibility occurs in the expansion valve.

In addition to the above, an actual vapor compression cycle includes the pressure losses encountered in the suction and discharge valves. There is an entropy increase

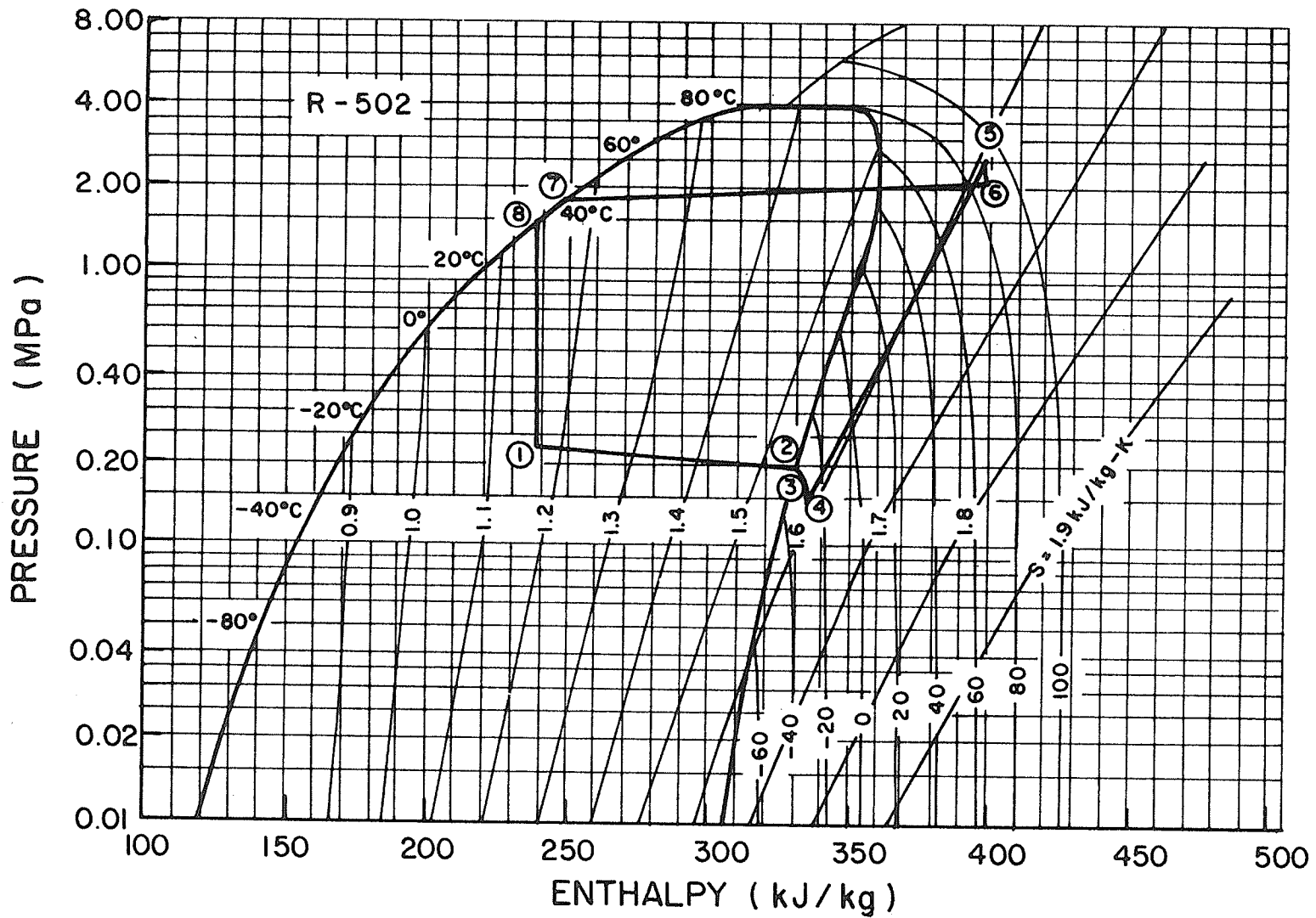


Fig. 1.1 Pressure enthalpy diagram of an actual vapor compression cycle

associated with these pressure losses. Fig. 1.1 illustrates these phenomena and the entropy growth associated with the pressure losses and compression process by the path from two to six.

In practice a coefficient of performance of refrigeration (COP) between 1.5 and 3 is attainable. This depends on the temperature difference between the evaporator and condenser that is T_1 and T_7 as shown in Fig. 1.2. The greater the temperature difference, the lower the COP, thus a one ton refrigeration machine using Refrigerant-502 (R-502) would remove heat at the rate of 3.52 kW (from a refrigerated space maintained at -20°C) during the cooling process. The power input to the compressor drive would be 2.4 kW and the heat discharged at a rate of 6.1 kW at 43°C . In this process approximately 38.6 g/s of refrigerant is circulated in the system. The actual COP is then 1.35. A complete analysis of a vapor compression cycle is given in APPENDIX A. The rate of heat gain, from the suction lines and the compressor walls, is approximately 0.18 kW. Fig. 1.2 gives the entropy changes involved in an actual vapor compression cycle.

1.2.1 Single Stage Vapor Compression Cycle

Single stage vapor compression cycles are used for refrigeration machinery when the difference between the evaporating and condensing temperatures does not exceed 70°C . If this difference is exceeded the COP decreases and

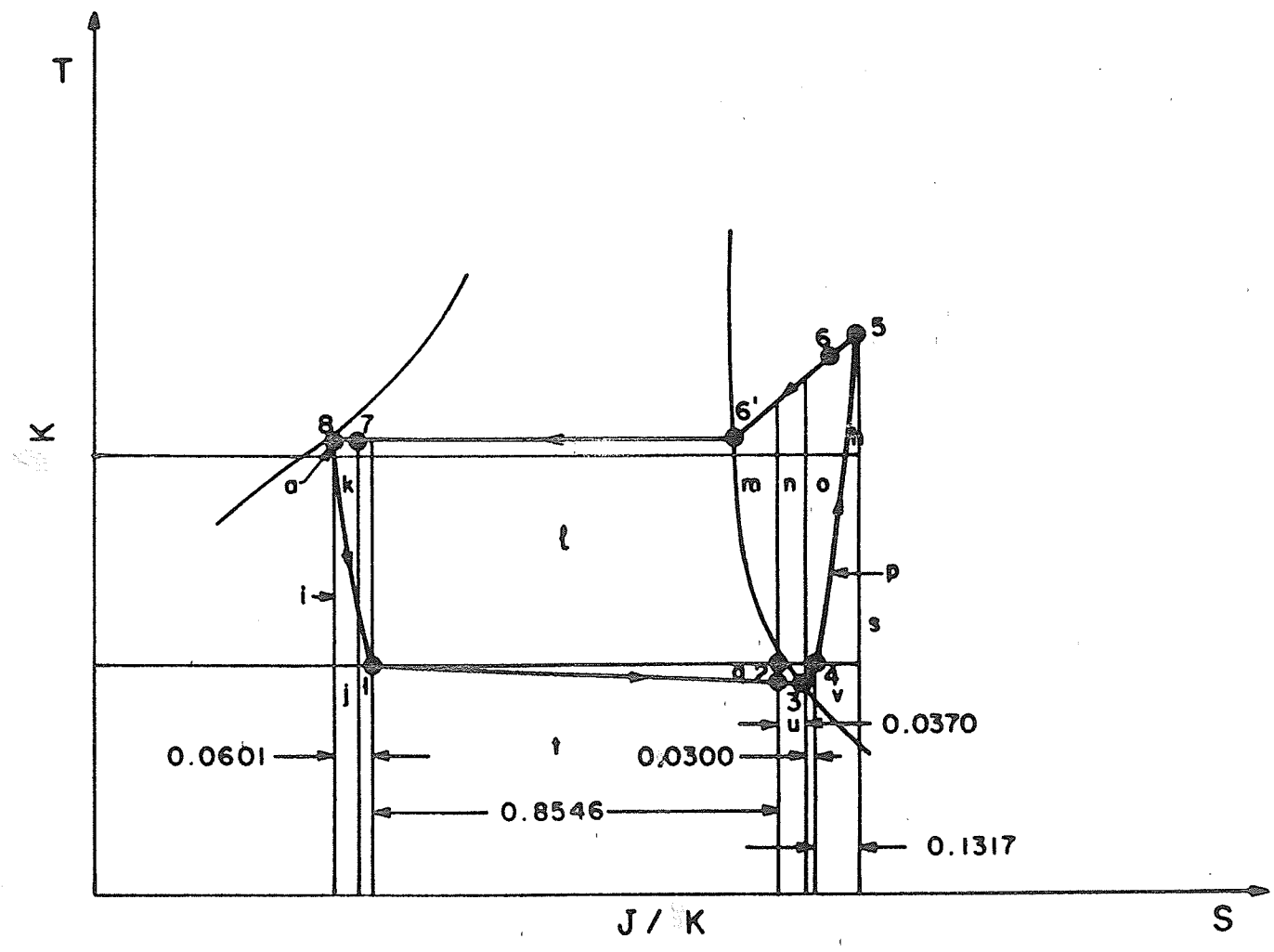


Fig. 1.2 Temperature entropy diagram of an actual vapor compression cycle

therefore the operation becomes less efficient.

In multistage vapor compression cycles the single stage vapor compression cycles of different refrigerants are coupled to increase the temperature difference between the evaporator and the condenser. Such methods can produce very low temperatures in the evaporators.

The combination and sequence of components required to achieve the cyclic operation of a refrigeration system is given in Fig. 1.3. The vapor compression machine consists of the compressor with drive motor, evaporator, condenser and expansion valve. These components are connected to a closed system by pipes in which a refrigerant with suitable thermodynamic properties circulates. This refrigerant is kept at such a pressure in the evaporator so that the evaporating temperature is below the temperature of the medium to be cooled. Because of the temperature difference, heat flows into the evaporator and the refrigerant evaporates while absorbing heat. The resulting vapor is drawn off by the compressor and compressed to a pressure such that the condensing temperature at this pressure is above the temperature of the medium receiving the waste heat. Because of the temperature difference, heat is discharged from the condenser and all the refrigerant vapor condenses while discharging heat. The liquid refrigerant is expanded in an expansion valve to the low evaporating pressure and can thus absorb heat again in the evaporator, thereby closing the cycle.

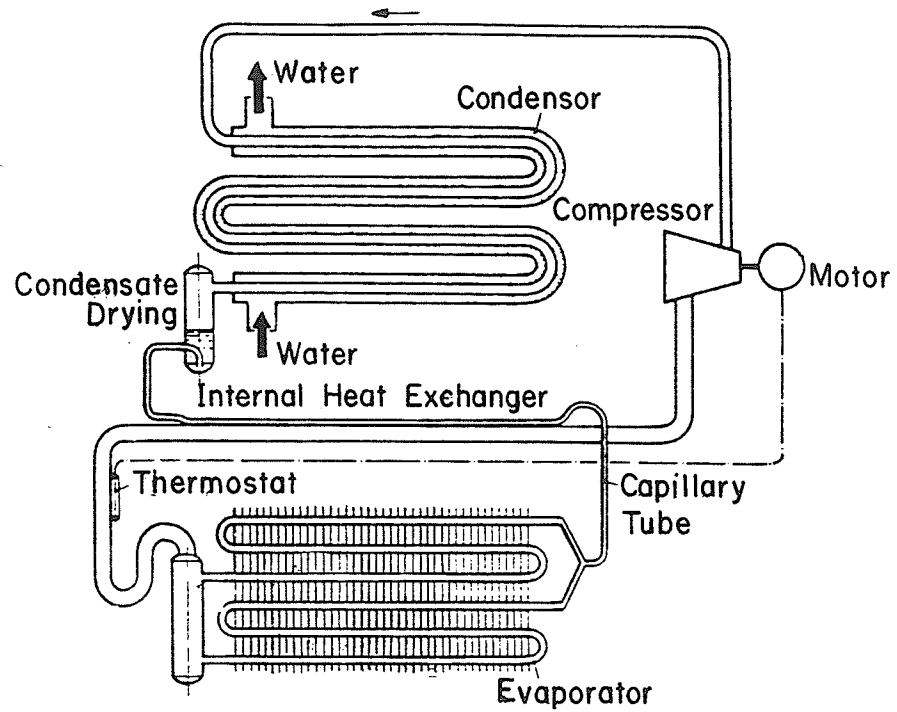


Fig. 1.3. Components of a vapor compression refrigeration system

1.2.2 Compression Ratio

The ratios of the absolute suction pressure to the absolute discharge pressure is called the compression ratio. Hence, for a given evaporator and condenser temperatures the compression ratio becomes a constant. However, in general increasing the discharge pressure or lowering the suction pressure will result in a low coefficient of performance. For example, with R-12 as the refrigerant a COP of 2.4 is obtained when the compression ratio is 9.9 (refer Table 1.1), however, if the compression ratio is increased to 13.1, by increasing the condensing pressure to 1378 kPa from 1041.1 kPa, the COP decreases to 1.3 resulting in a 46 percent reduction in performance. Similarly, when the compression ratio is increased to 16.8 by reducing the evaporating pressure from 103.4 kPa to 62 kPa the COP decreases to 1.9 giving a reduction of approximately 21 percent.

The selection of a suitable compressor depends on the capacity of the compressor. The capacity of the compressor is the volume of refrigerant a compressor can displace per unit time. The compressor must be able to displace all the vapor generated by the evaporator during a given time interval. The system will be in equilibrium only when the volume of vapor compressed becomes equal to the volume of vapor generated in the evaporator.

TABLE 1.1

COMPARISON OF COMMONLY USED REFRIGERANTS BASED ON -29°C EVAPORATION AND 43°C CONDENSATION FOR A TON OF REFRIGERATION EFFECT

Refrigerant Name	Evaporator Pressure (absolute) k Pa	Condensing Pressure (absolute) k Pa	Compression Ratio	Specific Volume of suction gas m^3/kg	Latent heat in the Evaporator kJ/kg	Net Refrigeration effect kJ/kg	Refrigerant Circulated kg/s	Liquid Circulated L/s	Compressor Displacement L/s	Compressor Power kW	Coefficient of Performance	Compressor discharge temperature $^{\circ}\text{C}$
R-12	103.4	1041.1	9.9	0.153	165.2	107.9	0.033	0.116	4.98	1.48	2.4	70
R-22	171.6	1660.5	9.7	0.130	226.7	148.4	0.024	0.093	3.09	1.54	2.3	92
R-502	208.1	1794.9	8.6	0.084	168.9	94.6	0.037	0.141	3.13	1.79	2.0	70

Atmospheric pressure: 101.3 k Pa

1.2.3 Choice of Refrigerants

Since the compression ratio is fixed by the evaporator and condenser temperatures the selection of a suitable refrigerant becomes important for high COP and low compressor power requirement.

A refrigerant is any substance which acts as a cooling agent by absorbing heat from another body or substance. In vapor compression cycles the refrigerant is the working fluid of the cycle which alternately vaporizes and condenses as it absorbs and gives off heat, respectively. To be suitable for use as a refrigerant in the vapor compression cycle, a fluid should possess certain chemical, physical and thermodynamic properties that make it both safe and economical to use.

The suitability of a refrigerant depends on the type of application. Hence, there is no single ideal refrigerant. A safe refrigerant must be nonflammable, nonexplosive and nontoxic. Most of the refrigerants in common use are both nonflammable and nonexplosive. These refrigerants are mildly toxic and therefore suitable precautions must be taken to prevent contamination of products and protect the health of the operators.

For economical use, the refrigerant must be capable of providing a high COP. The important properties of the refrigerant influencing the capacity and COP are:

- a) Latent heat of vaporization,
- b) specific volume of vapor,
- c) compression ratio,
- d) specific heat of refrigerant in both liquid and vapor states.

Except in small systems, a high latent heat value is desirable to reduce the amount of refrigerant circulated per unit of refrigeration capacity. When a high latent heat value is accompanied by a low specific volume in the vapor state, the efficiency and capacity of the compressor are greatly increased. This not only decreases the power consumption but also decreases the required compressor displacement. When the compressor displacement decreases smaller and more compact equipment can be used. However, in small systems, if the latent heat value of the refrigerant is too high, the amount of refrigerant circulated will be insufficient for accurate control of the liquid. Table 1.1 gives a comparison of three refrigerants for -29°C evaporator temperature and 43°C condenser temperature. It is evident from this comparison that a low specific volume of vapor and a high latent heat value found in the case of R-22 to reduce the compressor displacement, increases the capacity of the compressor.

Low compression ratios result in low power consumption and high volumetric efficiency, the latter being important in

smaller systems since it permits the use of small compressors. The effect of low compression ratios is not apparent in Table 1.1 due to the changes in the refrigeration effect with different refrigerants.

A low adiabatic compressor discharge temperature is highly desirable. When combined with a reasonable compression ratio, a low adiabatic discharge temperature greatly reduces the possibility of overheating of compressor and contributes to a maintenance free life of the compressor. A low discharge temperature becomes more important for hermetic motor compressors because with the increase in temperature the refrigerants tend to decompose chemically. Although R-22 gives a good compressor capacity for the conditions stipulated in Table 1.1, the discharge temperature reaches 92°C and therefore its use under these conditions becomes prohibitive.

A refrigerant with a high thermal conductivity in the vapor phase is desirable because the heat transfer rate can be improved in the heat exchangers, thereby reducing the size of heat transfer equipment.

A considerable amount of moisture and other contaminants will be drawn into the evaporator if the pressure is below atmospheric, thus an above atmospheric pressure is desirable in the evaporator and the low pressure side of the system. The use of R-12, as shown in Table 1.1, gives an absolute pressure of 103.4 kPa at the evaporator. A slight drop in

the evaporator temperature would cause a negative gauge pressure in the evaporator. Hence, the use of R-12 for the conditions given in Table 1.1 is not suitable.

Reasonably low condensing pressures under normal atmospheric conditions allow the use of light weight materials in the construction of the condensing equipment, thereby reducing the size, weight and cost of equipment. Although R-12 and R-22 gives low condensing pressures, as shown in Table 1.1, compared to R-502 the earlier mentioned disadvantages of R-12 and R-22 exclude their selection. As a result, R-502 offers a good choice under these conditions.

Freon-12 is the most widely used refrigerant especially in domestic refrigerators. It is nontoxic, nonflammable and nonexplosive. It is a highly stable compound even at high operating temperatures. If Freon-12 comes in contact with flame or heated electrical coil it decomposes releasing toxic gases. It has a boiling temperature of -29.8°C at atmospheric pressure. Freon-12 is oil miscible under all operating conditions. This simplifies the problem of returning the oil to the compressor and increases the efficiency and capacity of the system because the solvent action of the refrigerant maintains the evaporator and condenser heat transfer surfaces free of oil films.

Although the refrigeration effect per kg of R-12 is relatively small compared to other commonly used refrigerants it has a distinct advantage in small systems where accurate

control of liquid flow can only be done when a large volume flow rate is available. The disadvantage of a low latent heat value is offset by the high vapor density, so the compressor displacement required per ton of refrigeration is not much greater than the other common refrigerants.

R-22 (CHClF_2) has a boiling point of -40.8°C at atmospheric pressure. This was primarily developed for low temperature applications. The operating pressures and the adiabatic compressor discharge temperatures are higher than for R-12. Power requirements are approximately the same.

Although miscible in oil at temperatures found in the condenser, R-22 will separate from the oil in the evaporator. R-22 is especially advantageous over R-12 when small compressor displacements are required. The refrigeration capacity is approximately 60 percent greater than R-12 for a given compressor displacement. Hence, the pipe sizes are smaller for R-22 compared to R-12 and the amount of refrigerant required for a specific application is less.

R-502 is an azeotropic mixture of 48.8 percent by mass of R-22 and 51.2 percent of R-115. This was developed to replace R-22 in some low temperature, high compression ratio applications. It has been widely employed for the frozen food and cold storage temperature applications. R-502 is also well suited for heat pump applications. The particular advantage of R-502 over R-22 is its lower adiabatic discharge temperature. However, both the compressor displacement and

the power required per unit refrigerating capacity are higher for R-502, as are the operating pressures.

The relative costs of R-12, R-22 and R-502 are given below:

Relative Costs of Refrigerants

R-12	1.0
R-22	1.75
R-502	2.59

1.3 Applications

The preservation of food products is one of the most common uses of mechanical refrigeration. The quality of food products deteriorates when enzymes and microbes already present act on the food products. The activity of these deteriorating agents are reduced when the temperature of the commodity is lowered. Hence, mechanical refrigeration has become one of the least expensive methods of food preservation when the aim is to preserve the original nutritional value and sensory properties of the product.

The application of vapor compression refrigeration systems are numerous, however, they may be broadly classified

into the following:

- a) Domestic refrigeration,
- b) Commercial refrigeration,
- c) Industrial refrigeration,
- d) Marine and Transport refrigeration, and
- e) Air conditioning.

Domestic refrigeration represents a significant portion of the refrigeration industry, but because of the relatively small capacities, the heat rejected from the condensers has not been recovered economically. Consideration is now being given to use this waste to heat the ventilating air of energy efficient residences.

In commercial applications refrigeration equipment is used for processing, storing, displaying and dispensing of perishable commodities in retail stores, restaurants and hotels. Certain sports activities requiring ice surfaces are commercial ventures rejecting large quantities of heat from ice making machines. Such establishments require substantial amount of hot water for showering by participants and other domestic hot water uses for which the waste heat may be used.

Industrial refrigeration units are large and therefore the incorporation of a heat recovery system is often economically feasible. Typical industrial application of refrigeration are ice plants, large meat, fish, poultry and frozen foods packing plants as well as breweries, dairies and

industrial plants such as oil refineries, chemical plants, rubber plants, etc. Generally, the food industry uses large amounts of low temperature domestic and process hot water. Thus it is economical to use water cooled condensers to preheat the hot water requirements.

Marine and transportation refrigeration systems and the air conditioning systems offer little scope for condenser waste heat recovery. However, certain select situations especially with air conditioning units may become feasible.

The preservation of food products is one of the main concerns of industrial and commercial refrigeration, because of the time lapse before meat, vegetables and milk products reach the consumers. During the period of time the chances for bacterial contamination and growth is high. Bacterial contamination and growth in food products deteriorates quality which may cause possible food poisoning. The bacteria causing food poisoning are called pathogenic bacteria which do not multiply at temperatures below 4°C . The spoilage bacteria, called psychophilic bacteria, can survive even at temperatures as low as -4°C . However, both pathogenic and psychophilic bacteria become dormant at -10°C .

Meat processing plants usually require large refrigeration capacities because the initial refrigeration of carcass must be very rapid to reduce the live animal body temperature. The bulk of the beef chilling is done within 16 to 20 hours. Whereas a hog carcass is chilled within 8 to 12

hours. Such rapid temperature reduction is required to reduce the microbial growth that may occur on the carcass surfaces. In order to achieve rapid chilling of carcasses large refrigeration capacities and air circulation are required. Meat packing plants require hot water in large quantities. Beef carcasses are washed, immediately after they are cut, with 16 to 46°C water. Warm water is also used for washing down of equipment, floors, etc. Since the demand for large amounts of low temperature water are required at the same time as chilling of the products is required, an application of heat recovery from the refrigeration system exists in the meat processing plants.

A similar opportunity for the application of condenser waste heat exists in the poultry processing industry. Poultry is either ice chilled (1 to 2°C), deep chilled (-2°C) or frozen (-18°C or lower). Cooling of poultry carcasses, from its body temperature (24 to 35°C) during slaughtering, is done within 4 to 8 hours depending on the carcass weight. The heavier the bird the longer the time to reduce the temperature. Many poultry processing plants are able to process 5000 to 10,000 birds per hour. Therefore, large refrigeration capacities are required to handle the peak loads. As a result, the condensers reject an appreciable amount of heat which can be economically recovered. The recovered heat has number of alternate uses in the poultry processing industry. Hot water at 50 to 70°C is required for

scalding. This heating demand in the poultry industry may be met by either gas fired water heaters or by condensing steam. Hence, the use for the condenser waste heat at 65 to 80°C is available for preheating the hot water of the scalding in poultry processing plants, which also require large quantities of hot water for sterilization, cleaning and domestic use.

Fish processing plants, like poultry and meat packing plants, require a substantial amount of refrigeration capacity to preserve the quality of processed fish. Storage temperature of frozen fish ranges from -20°C to -30°C. Sea foods are very susceptible to high temperatures and poor handling practices. Hence, for longer shelf life fish must be stored at temperatures lower than -23°C. Compared to other meat products fish requires lower storage temperatures. The maximum storage life of fish varies with species but generally, it has been found, fish kept in refrigerated storage at 2°C lasts for 10 to 15 days. For storage of fish longer than 15 days the temperature must be lowered to -23°C or lower. The hot water demand in a fish processing plant is mainly for wash downs and domestic use.

The recovery of condenser waste heat from refrigeration systems has a number of uses in the dairy industry. The opportunities for its application lies at the dairy farm and at the milk processing plant level. In the farms, hot water is used for cleaning the milking and storage equipment.

Refrigeration systems are used to cool the milk from 32°C to about 4°C until it is delivered to a dairy plant for further processing. Most dairy farms have bulk milk tanks to receive, cool and hold milk. Tank capacities range from 750 to 12 000 litres. To maintain the quality of milk, fresh milk must be cooled to 10°C from 32.2°C within the first hour and from 10°C to 4°C within the next hour. During the second and subsequent milking, sufficient refrigeration capacity must be available to prevent the temperatures of the blended milk from rising above 7°C. Hence, it is clear that even at the farm level the refrigeration capacities required to handle milk are large enough for the application of an economically feasible condenser waste heat recovery unit.

In the dairy plants the milk obtained from the farms is standardized and blended for its milk fat content and then pasteurized by heating it to 63°C. Milk is held at this temperature for half an hour and then cooled rapidly within less than one hour to about 4°C. Rapid cooling is achieved by passing milk through evaporator plate heat exchangers of the refrigeration system. Because of the large volume of milk handled in these processing plants refrigeration capacities required are also large. In addition to the cooling load needed during pasteurization a further cooling load is required for butter, cheese, yoghurt, sour cream and ice cream manufacture. Hot water is required for the cleaning of equipment and for the employee domestic needs.

Vegetable and fruit packing plants also have refrigeration equipment and hot water demand. Vegetables are blanched with warm water before being packed and stored in refrigerators. This warm water requirement is substantial and temperature of water used ranges between 30-40°C. The desired refrigerator storage temperature for vegetables and fruits is 0 to 1°C. In addition to the control of temperature in the refrigerated space, vegetables and fruits require the control of relative humidity for longer shelf life. A low level of relative humidity increases moisture losses and thereby reduces the quality and freshness of vegetables and fruits.

Commercial food handling outlets have a promising opportunity to recover condenser waste heat from their refrigeration equipment. Display refrigerators are designed to merchandize food to maximum advantage, while providing as much refrigeration as is required for short term protection of the food. Generally the storage temperatures in such food display units range from -2 to 5°C for chilled products and -18 to -30°C for frozen foods and ice creams. Large refrigerated warehouses are also required in commercial handling outlets. The demand for domestic hot water also coexists and thus the opportunity for the application of waste heat recovery systems with food handling outlets.

Rinks use artificially made ice surfaces and sufficient refrigeration capacity to control humidity and temperature of

the air space is required. The freezing of an ice sheet is usually accomplished by the circulation of heat transfer fluid through a network of pipes located below the surface of ice. With a wet bulb temperature of 7°C and a 2.5 mm thick ice layer satisfactory ice is formed at -5°C for most of the sports activities. The ice sheet in the rink can be made faster if warm water is used rather than water at ambient temperature. Sports complexes of such nature require large amount of domestic hot water. Hence, the heat rejected from the air conditioning and refrigeration equipment can be used to meet part or all of the heating demand in ice rinks.

1.4 Heat Recovery From Refrigeration Systems

1.4.1 Sensible and Latent Heat

As previously shown the refrigeration process necessitates discharging heat from the condenser at a temperature higher than the ambient. Conventionally this heat may be rejected via a cooling tower or by means of an air or water cooled condenser directly to ambient air or water. The discharged heat may alternately be recovered and used for space heating, water preheating, or some other process. The heat is often of a comparatively low grade thus its use may be restricted to areas located conveniently in close proximity to the condenser. One of the main advantages of such an installation, however, is the fact that

replacement of the conventional condenser arrangement with one suitable for heat recovery is comparatively inexpensive, and a quick return on investment may be anticipated. The COP can not be optimized for the heating mode because the plant is normally installed for the refrigeration duty. However, producing some heating at a relatively low additional cost makes this point less significant.

In most of the food processing plants large amounts of waste heat can be recovered from refrigeration units. The rejected waste heat is at a temperature of about 40-90°C. The heating load of these food processing plants are large, a substantial fraction of this being spent for heating low temperature hot water for various processes and for domestic use. Therefore, the waste heat can be readily utilized to preheat the incoming, fresh, cold water. A saving of cooling water or fan power could be involved as well as the energy for heating the water. The demand for heating and the availability of condenser heat may not occur at the same time during the operating period, therefore, water storage may become necessary.

The heat rejected in a condenser is obtained from a condensing vapor. Vapors retain heat energy in two forms,

- a) Sensible heat, and
- b) latent heat.

The sensible heat of a vapor is available as superheat. The superheated vapor has low heat transfer coefficients compared to saturated condensing vapors. Hence, more condenser surface is required to remove equal amount of heat from a superheated vapor compared to a saturated vapor. Therefore, a minimal amount of superheat in the refrigerant is desirable to increase the COP and reduce the cost of condenser. However, in practice refrigeration systems cannot be operated without acquiring some superheat.

A comparison made between the heat transfer coefficients resulting from a condensing vapor and a superheated vapor flowing inside a tube shows that the heat transfer coefficients arising from a saturated condensing vapor to be 5-10 times higher than the heat transfer coefficients resulting from the flow of a single phase superheated gas. Therefore, a substantial portion of heat recoverable from a condenser lies in the latent heat. Under normal conditions the superheated vapor contributes about 15 percent of the total heat rejected in a condenser.

There are advantages of having superheat in the vapor. The water can then be heated to a higher temperature by the use of a counter flow exchanger. Generally under practical conditions an attempt is made to keep the superheat below 20-25°C.

1.4.2 Quality of Energy

The concept of quality of energy arises from the second law of thermodynamics. The thermodynamic function exergy takes into account the consequences of the second law of thermodynamics, in addition to those of the first law. The exergy is a generalized thermodynamic potential, equal to the maximum work which could possibly be extracted from a thermodynamic system in a given state. Hence, it is easier for designers to match the quality of energy supply and demand in engineering processes using exergy.

If high quality energy is spent to heat low temperature water the exergy loss is higher. For example, if 400°C steam is used to heat process water, flowing at the rate of 1 kg/s , from 4°C to 32°C with a heat transfer efficiency of 80 percent the exergy lost is 81.2 W . However, if a refrigerant condensing at 43°C is used, the exergy lost is only 7.4 W . The application of first law alone will result in the actual energy required to heat this water, which does not indicate the differences in the sources of heat.

The heating of process water with the high quality steam and low quality refrigerant leads to the same end result for the process water in the example. However, the unnecessary thermodynamic degradation of energy required to produce steam and the associated losses due to the high temperature potential of steam is a waste of resource. Hence, wherever there are alternate opportunities to produce low quality heat

instead of a high quality fuel, such avenues are worth exploring.

1.5 Advantages of Condensing Inside Tubes

The use of condensing refrigerants as a heating source in conventional refrigeration systems require few modifications. Majority of the conventional refrigeration systems use roof top condensers, where the heat is rejected to the ambient air. In order to modify such a system to incorporate a waste heat recovery system, a suitable water cooled condenser must be selected or designed.

Off-the-shelf water cooled condensers are generally shell and tube heat exchangers. Water is passed inside the tubes whereas the vapor is allowed to condense on the tubes. Such condensers require heavier shells to withstand the hoop stresses developed by the high pressure vapor. The absolute pressures normally found in the high pressure side of the compressors, used in the refrigeration industry, range from 20-40 kPa. As a result, the shell of a heat exchanger needs to be considered a pressure vessel. Consequently, the cost of equipment rises. If the vapor is condensed within the tube, the additional cost required to introduce heat recovery methods is probably lower. Copper tubes used in the heat exchangers are strong enough to resist the pressures of condensing vapors. Hence, the additional cost incurred in the design and manufacture of the shell can be avoided.

Under these conditions the shell can be made of standard commercial piping which will withstand the main water pressure.

In addition to being stronger, the shell requires leak proof methods for the assembly of pipes and fixtures when condensation takes place on the tubes. When vapor condenses within the tubes, as in air cooled condensers, the tubes can be soldered to the tube plates at the inlet and outlet ends of the condenser. This method is cost effective and leak proof. Because the tubes used to convey the vapor from the compressor to the condensers and the tubes used inside the condensers are all made of copper require a lower fabrication cost. It is also important to minimize the machine down time required for retrofitting. If the shell side is used for vapor condensation, dissimilar materials are encountered in conveying the vapor to the shell, and a gasket is required which introduces the possibility of leaks. As a result, inlet and outlet nozzles for the shell side fluid requires additional care and special attachments to prevent the leaks. Prevention of gaseous leaks are expensive. Therefore, using in-tube condensation process reduces the cost and care required in fabrication.

The weight of refrigerant required to fill the refrigeration system is increased several fold when shell side condensation is used. The shell side volume is many times larger than the tube side total volume, hence, an

increased mass of refrigerant is required to charge the system. This additional mass of refrigerant increases the first cost of the system.

1.6 Disadvantages of Condensation Within Tubes

When vapors condense inside or outside tubes the condensate film on the surfaces offers a thermal resistance to heat flow from the condensing vapor to the cooling medium. In case of condensation within the tube the liquid film forms an annulus around the tube. The hydrodynamic forces of the high velocity vapor prevents this liquid film from flowing to the bottom of a horizontal tube. As a result, the high local heat transfer coefficients found at the beginning of condensation drops rapidly. As the liquid film annulus thickens a greater film resistance to heat flow occurs. As the vapor mass velocity decreases along the length of the condenser the vapor momentum drops below a certain level where it can no longer maintain the annulus around the tube. Consequently the liquid flows down along the walls due to gravity and partially fills the bottom of the tube. This further retards the heat transfer from the vapor. The condensation progresses at a reduced rate until the entire vapor becomes condensed. As a result of the reduction in local heat transfer coefficient along the length of the tube the area required to condense a given quantity of vapor is increased. However, in case of shell side condensation

condensing vapor drips off the tube, thereby reducing the condensate film thickness on the tube. Therefore, the local heat transfer coefficient does not reduce. It has also been found by Young and Wohlenberg [1]* while condensing R-12 on a tube bank that the variation in heat transfer coefficient with tube position in the tube bank is not great. This is because the condensate film in the lower tubes is rippled and disturbed by drops from the upper tubes. These ripples increase convection and introduces a mass transfer in the condensate layer, thus increasing the rate of heat flow through the film.

In case of condensation within the tubes, as the condensing liquid fills the tube, near the outlet end of the condenser intermittent liquid and gas slugs may be formed. As more heat is removed from the vapor which is sandwiched in between alternate slugs of liquid, the vapor pockets collapse. This increases the hydrodynamic momentum of the liquid phase while rushing to fill the empty space created by the collapsing vapor. This, although a type of cavitation is not as severe as in pumps, develops implosive forces which erode the tube walls. Such cavitation does not occur in case of shell side condensation.

The major advantage of using shell side condensation is that, verified, reliable, generalized correlations are

* Number in brackets denote references at end of thesis.

available to predict condensation heat transfer coefficient outside the tubes. Therefore, the design procedures for condensation outside the tubes are well established.

However, in case of in-tube condensation there are no single general correlation available. Most of the correlations available in the literature are valid only for the ranges of parameters for which they were developed. When correlations are used outside their range of applicability, the deviations may be out by an order of magnitude. Therefore, an attempt is made through this work to develop generalized correlations to predict the process of in-tube condensation and to develop design procedures.

CHAPTER 2

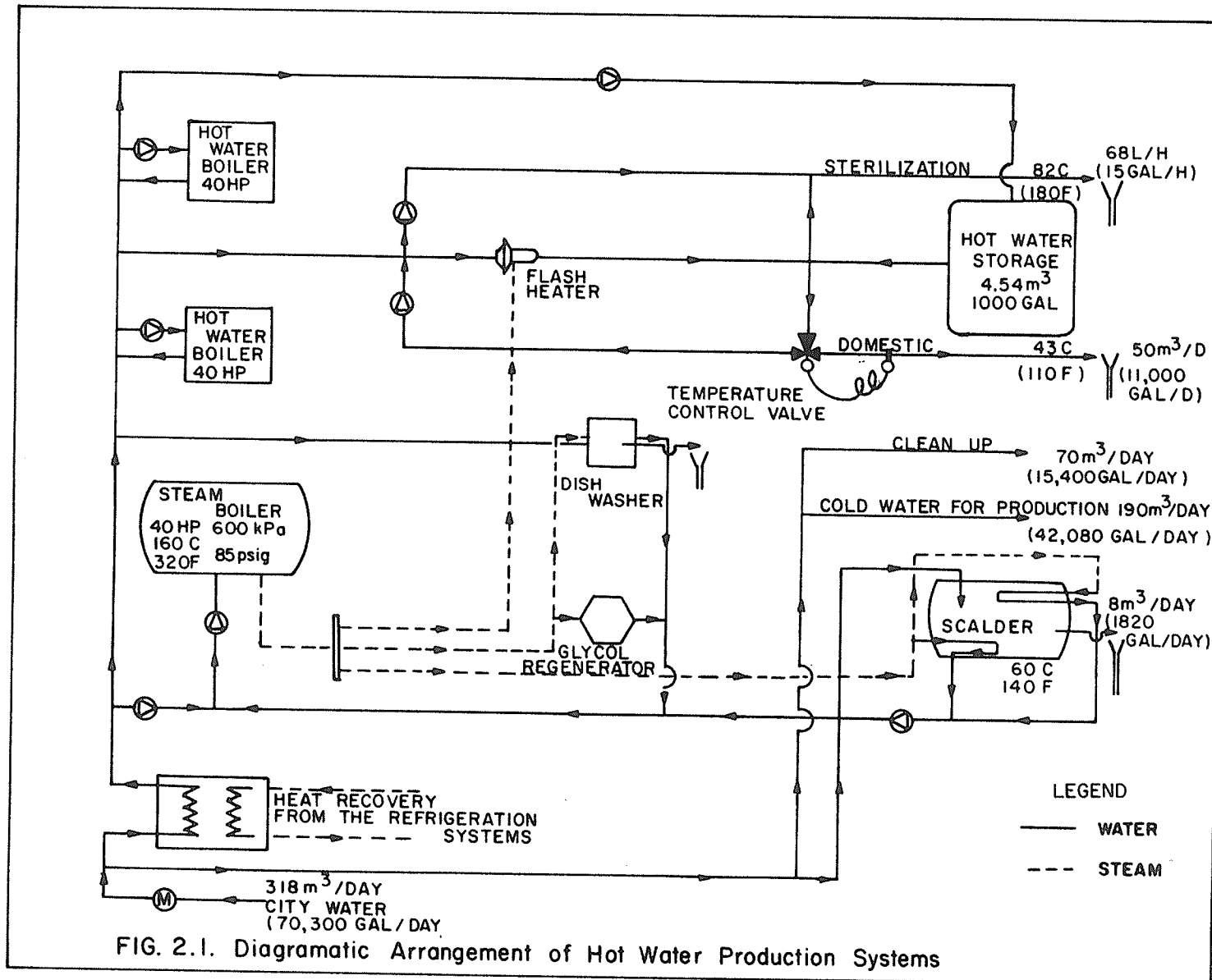
FIELD STUDY

The proper selection and application of waste heat recovery can not only conserve significant quantities of fuel but can also reduce the cost of an operation. In order to effectively utilize waste heat recovery techniques, an appropriate energy balance and profile of the characteristics should be determined for the industrial process of concern. The determination of process energy requirements are particularly important to the potential use of waste heat recovery. Hence, an energy survey in a poultry processing plant to evaluate the rate of refrigeration condenser waste heat rejection, the process heating loads and temperature ranges was undertaken. The heating loads were calculated and an overall energy balance of the plant completed (Fig. 2.1). An energy survey of this nature not only revealed what energy economies could be made in this particular plant but it also identified the relative merits and demerits of energy conservation in other similar industries.

2.1 Introduction of Food Processing Plant Study

2.1.1 Description of the Plant

The Dunn-Rite Food Products Ltd., Hamlin Road plant came into operation in 1980. It is housed in a building of approximately 2230 m², of which the office and staff



facilities occupy 465 m². The plant was designed to process 20,000 birds/day, however; the actual rate of production is 16,000 birds/day.

The installed water heating capacity of the plant is 1175 kW. The water heating facilities of the plant is as follows:

- a) Two 40 HP hot water boilers (total capacity 785 kW) for domestic and process water heating (refer to Fig. 2.1),
- b) A small 6 HP steam boiler (60 kW) supplies steam to a bag shrinker,
- c) An indirect-fired gas hot water heater (170 kW capacity) to meet the hot water required by a scalding tank which supplied water for the feather removing equipment, and
- d) A 40 HP steam boiler (capacity 390 kW) added in September 1984 replacing the indirect gas-fired heater of the scalding tank. With this addition a large steam dishwasher, a glycol regenerator and a flash water heater were also installed.

In addition to the above water heating facilities in the plant a number of indirect-fired unit gas heaters, with a total installed capacity of 530 kW, were used for space heating during winter months.

The total refrigeration capacity available in the plant was estimated to be 117.3 tons (412.4 kW). The refrigeration system of the Dunn-Rite plant is subdivided into groups as follows:

- a) Chilling system, consisting a
 - i) Giblet chiller
 - ii) Pre chiller
 - iii) Chill cooler,
- b) Ice maker,
- c) Quick freeze,
- d) Cooler,
- e) Deep freezer and
- f) Production room cooler.

Table 2.1 gives the details of the capacities of the compressors, the prime movers, the condensers, the evaporators, the total heat rejected by the condensers, electrical loads, etc. for each of the above groups. The layout of these equipments is given in Fig. 2.2.

2.1.2 Resource Inputs

The processing of poultry for human consumption involves a number of stages. At each stage varying amounts of water (both cold and hot) are required along with refrigeration and

TABLE 2.1

REFRIGERATION SYSTEM

REFRIGERATION CAPACITIES AND DAILY ENERGY CONSUMPTIONS

Name of Unit	Compressor Capacity, kW	Prime Mover Capacity, kW	Installed Condenser Capacity, kW	Total Heat Rejected, kW	Evaporator Capacity, kW	Electrical load per day, kWh (3)	Total Heat Rejected/day, MWh
Giblet Chiller(2)	13.74	8	17.29	17.58	-	72	
Pre Chiller(2)	13.74	8	17.29	17.58	-	72	1.09
Chill Tank(2)	66.98	50	92.59	85.56	-	450	
Ice Maker	27.78	38	45.71	79.7	-	380	0.8
Quick Freeze	154.7	74.6	210.96	215.65	-	383.7	1.1
Cooler	36.5	24	50.98	48.64	52.74(1)	513.7	1.04
Deep Freezer	43.77	56	76.18	69.15	43.14(1)	1612.8	1.99
Production Room	55.23	28	63.00	94.58	47.47(1)	252	0.95
Total	412.44	286.6	574.00	628.41	143.35	3746.2	6.65

(1) Evaporators installed in actual space

(2) Sub units of chiller tank system

(3) Product of total daily operational time and the rated power of the respective motors.

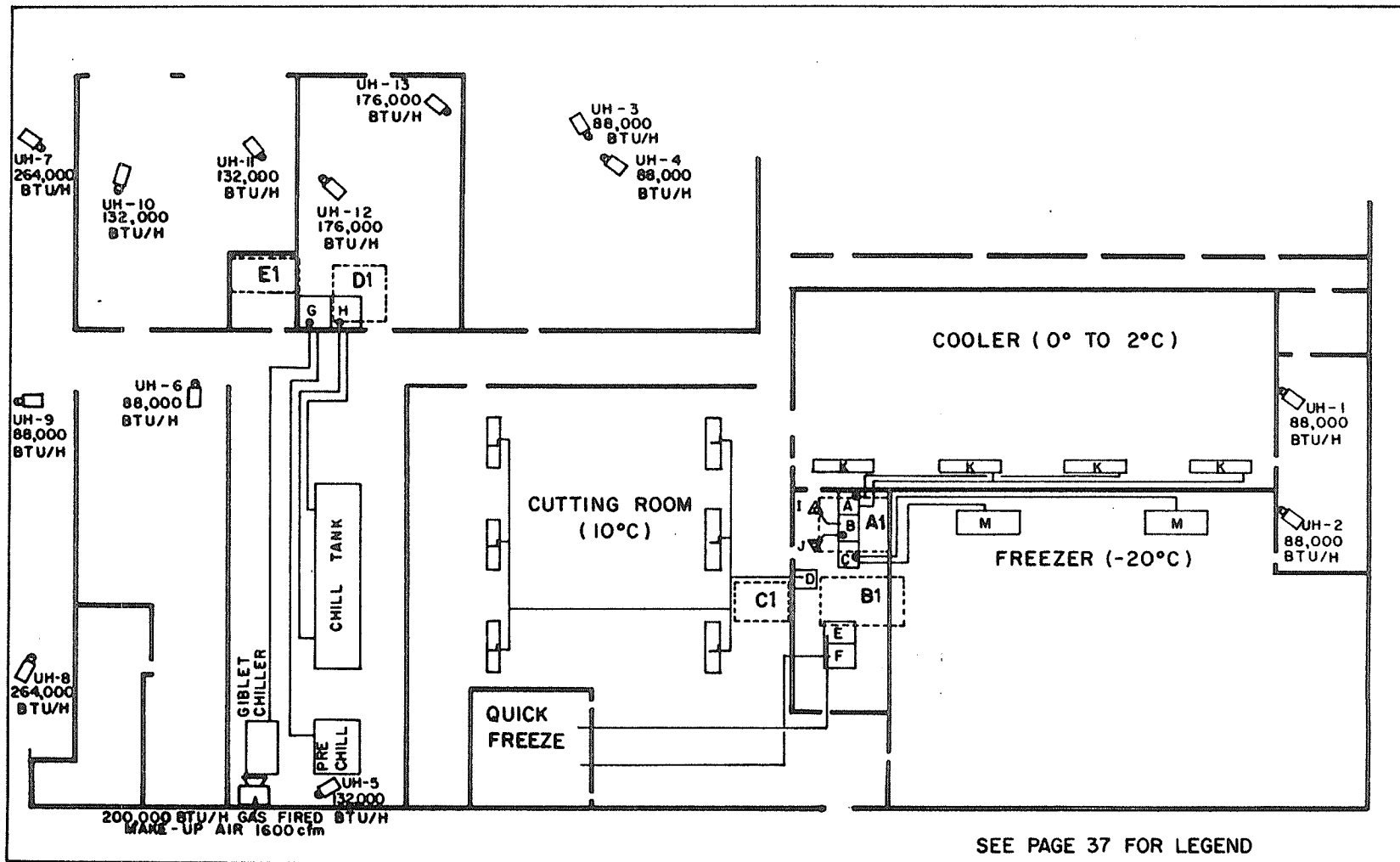


Fig. 2.2 Layout of refrigeration equipment

LEGEND

REFRIGERATION EQUIPMENT

COMPRESSORS

- A - COMPRESSOR UNITS WITH 12 KW MOTORS.
- B - COMPRESSOR UNITS WITH 19 KW MOTORS.
- C - COMPRESSOR UNITS WITH 28 KW MOTORS.
- D - COMPRESSOR UNITS WITH 28 KW MOTORS.
- E & F - TWO COMPRESSOR UNITS WITH 50 HP MOTORS.
- G - COMPRESSOR UNITS WITH 8 KW MOTORS.
- H - COMPRESSOR UNITS WITH 25 KW MOTORS.

EVAPORATORS

- K - EVAPORATORS. 4 NOS. (FOR A)
- L - UNIT COOLERS. 6 NOS. (FOR D)
- M - HORIZONTAL PRODUCT COOLERS. 2 NOS. (FOR C)
- I & J - ICE MAKERS. EVAP. TEMP. -18°C (0°F)

CONDENSERS

- A1 - AIR COOLED ROOF MOUNTED CONDENSER. (FOR A, B & C)
- B1 - AIR COOLED ROOF MOUNTED CONDENSER. (FOR E & F)
- C1 - AIR COOLED ROOF MOUNTED CONDENSER. (FOR D)
- D1 - AIR COOLED ROOF MOUNTED CONDENSER. (FOR G & H)

labour. Fig. 2.3 illustrates the successive stages in the process.

From the utility records the annual expenditures for a twelve month period starting from September 1985 to August 1986 were obtained. The records are summarized in Table 2.2.

Table 2.2

Annual Resource Use and Unit Cost Between September
1985 and August 1986

Item	Amount	Invoiced Amount	Unit Cost
Water	76,624 m ³	\$250,989.50	\$0.327/m ³
Electricity	1,552 Mwh	\$ 55,756.16	\$0.036/kWh
Gas	90,740 CCF	\$ 45,093.20	\$5.24/GJ
	TOTAL	\$351,839.00	

Water use is one of the major components of the production cost, followed by electricity. The electrical motors of the compressors consume a significant portion of the electrical energy. Gas is used for space heating during winter months and for water heating during production. During the winter months space heating requires about 60 percent of the total gas consumption per day. Utility bills between July 1983 to August 1986 reveals, in Fig. 2.4, a decrease in gas costs after 1984. The incorporation of the

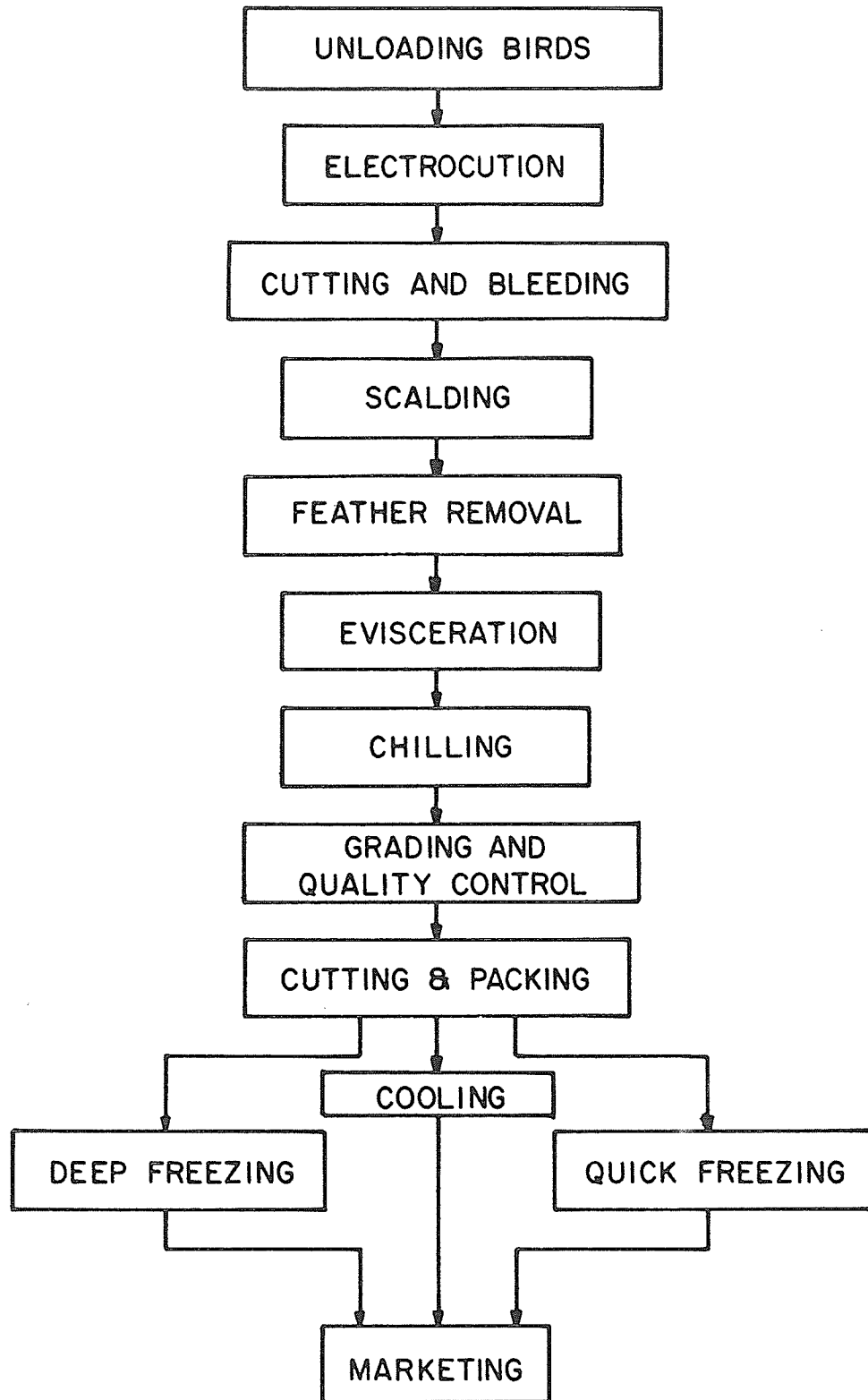


Fig. 2.3 Successive stages in poultry processing

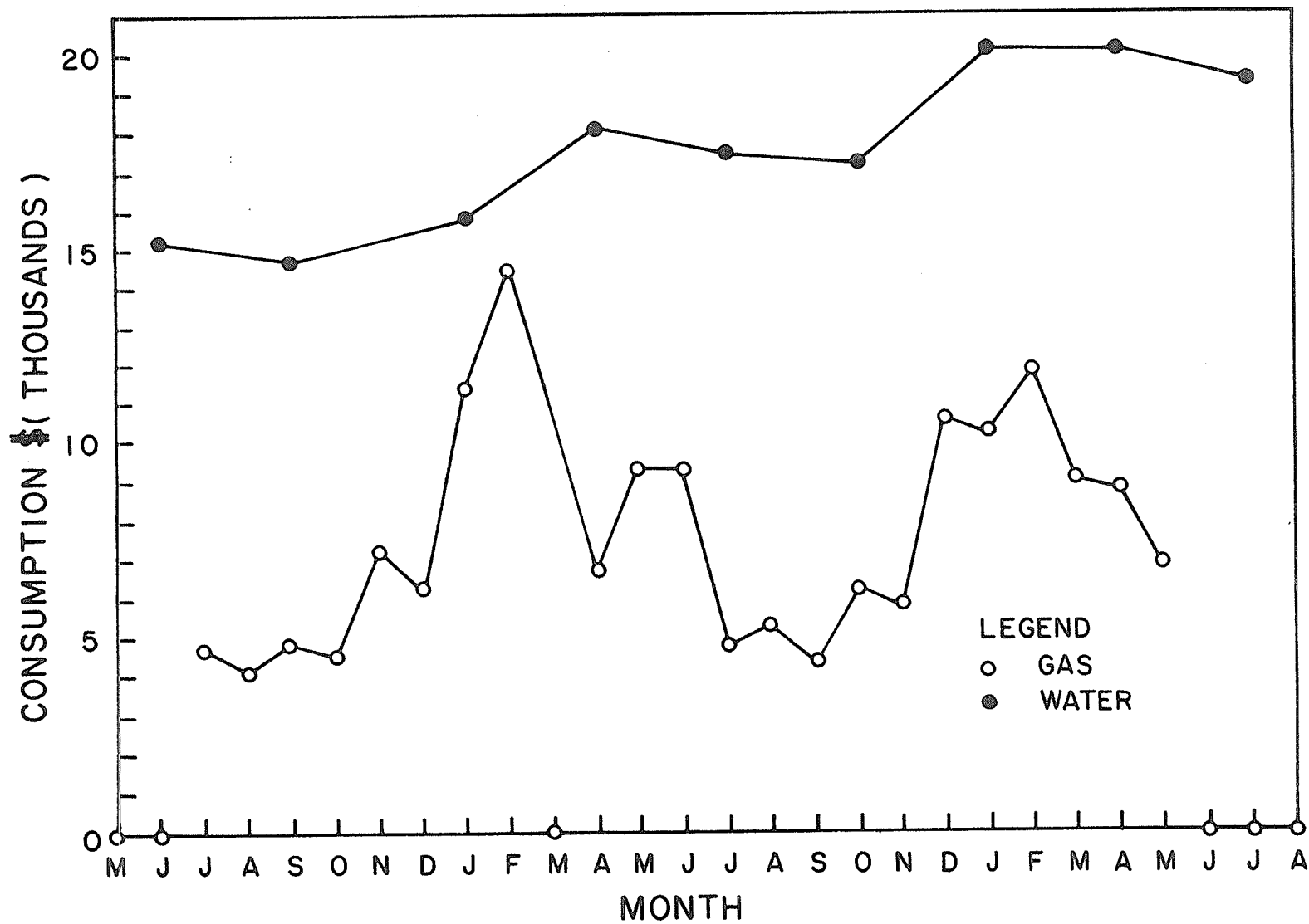


Fig. 2.4 Dunn-Rite plant utility bills between July 1983 to August 1986

more efficient steam boiler was attributed for this drop. Fig. 2.5 and 2.6 respectively show the electricity use and electricity demand charged by the utility supplier. Comparison of these figures show that the electricity consumption increases gradually over years. However, the same increase in the demand is not shown. The almost steady values shown in the demand curve coincides with the period in which the power factor correction was introduced.

2.2 Description of the Methodology Followed in Performing the Energy Audit

The energy inputs to the Dunn-Rite plant are of two forms; a) electrical and b) natural gas. Both of these energy inputs are utilized either for heating or for cooling. Therefore, to evaluate the total energy consumption of the plant the energy use in the refrigeration system and the energy use in the heating system were evaluated.

2.2.1 Energy Use in the Refrigeration System

2.2.1.1 Testing Methodology

The installed capacities of the evaporators, condensers and compressors were obtained from the manufacturer's catalogues. A refrigeration cycle analysis was performed on each system to establish the total heat rejected based on the evaporator and condenser temperatures, obtained from design

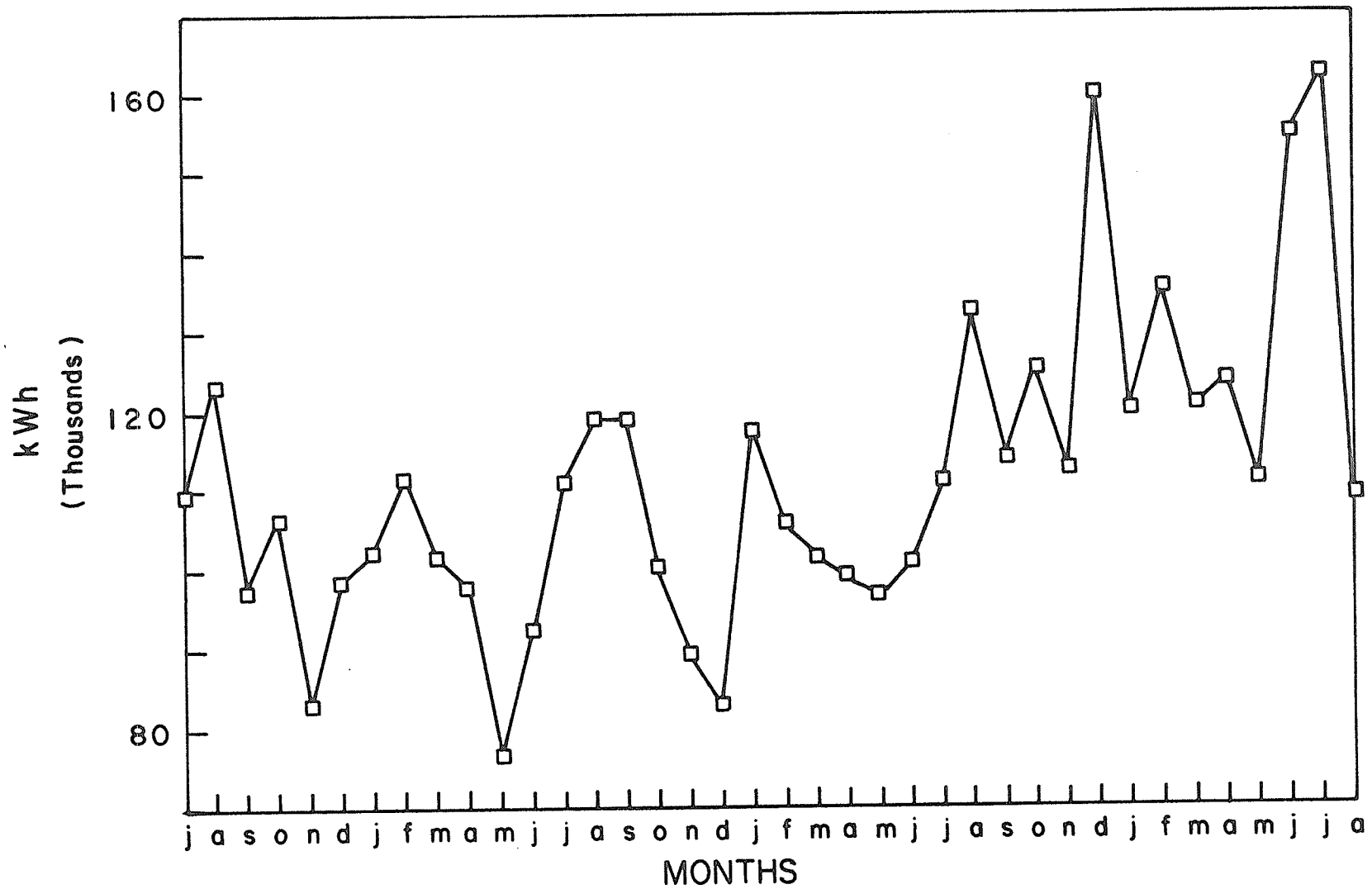


Fig. 2.5 Dunn-Rite plant electricity use between July 1983 to August 1986

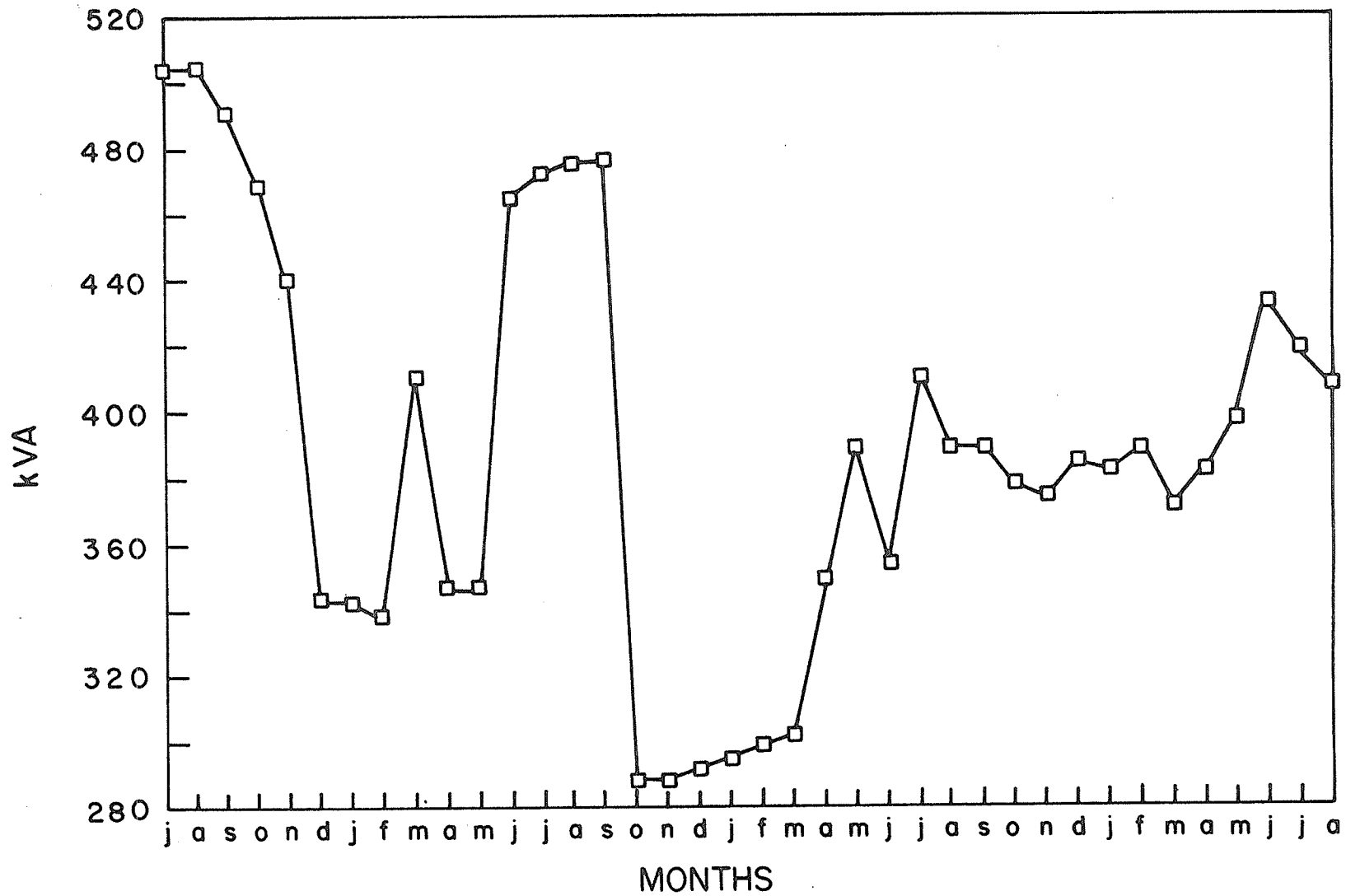


Fig. 2.6 Dunn-Rite plant electricity demand between July 1983 to August 1986

specifications supplied by the equipment supplier.

The operating times of the compressors were established by the use of a multichannel HONEYWELL analogue temperature recorder. Iron-copper thermocouple junctions were installed on the high pressure side of the compressors. The operating times were read from the charts and the power consumption calculated from input amperage within acceptable limits which was more convenient than using recording ammeters. The installed thermocouples showed a rapid increase in temperature when the compressor came into operation. A steady temperature was reached two minutes after the compressor started. Similarly, the temperature of the compressor output pipe dropped rapidly, within 3 to 5 minutes, after the motor was cut off. The rise and fall of the temperature of the compressor outlet established the on-off cycles of the compressor.

The compressor operating times were recorded for seven consecutive days and the duty cycles established. The daily operating times were obtained from the thermographs recorded by the multichannel chart recorder. The calculated daily electrical power consumption of the electrical load as shown in Table 2.1 were based on the total daily operating time.

2.2.1.2 Component Analysis

The components are comprised of the six subdivisions named in section 2.1.1, the description of the plant.

CHILLER TANK SYSTEM

This system is a combination of three units namely the GIBLET CHILLER, the PRECHILLER and the CHILL COOLER. Whole birds are passed through the latter two chillers successively after they are eviscerated and washed. The giblet chiller reduces the temperature of the organs from 32°C to 4°C. Such a reduction in temperature retards microbial growth and helps prevent deterioration. Birds are submerged into the chilling tank water maintained at 1°C and cooled quickly by agitating. The total amount of heat rejected per day by the chiller tank refrigerating system was estimated to be 1.9 MWh.

ICE MAKER

Two ice maker units produce the flaked ice required for storing the carcasses and for the packaging of the cut-up birds. The ice makers are operated mainly during packaging. The average period of operation per day was determined to be 10 hours. During the daily operating period both units rejected 0.8 MWh. The electrical load of the prime mover was steady during the operating period.

QUICK FREEZE SYSTEM

The quick freeze system is the only one using glycol as a secondary refrigerant. These large compressors (two of 37.3 kW) use R-502 as the refrigerant. The quick freeze unit

operated on a cycle - 20 minutes on and 15 minutes off, from 0630 till 1530 hours on working days. During an average working day 1.1 MWh of heat was rejected.

This quick freeze system is able to reduce the carcass temperature rapidly. Quick frozen products are superior to those which are slowly frozen. Quick frozen foods are cooled within a very short time, so that bacteria, mold and yeast growth during freezing is greatly reduced.

Since this is a brine refrigerating system the possibility of storing chilled brine produced during off peak electrical demand periods exists. Referring to Table 2.1 it is evident that this system has the largest prime mover capacity.

In addition the system is substantially oversized. The use of a cyclic operation with such large units causes substantial surges during start ups although they do not register on the meters. A more realistic mode of operation is to use both units until the system is brought down to the desired temperature in the morning and then use one unit to meet the requirement throughout the remainder of the process time (9 hours). Since the system is only operating 60 percent of the time in the cyclic mode one unit will meet the daily needs.

Cost savings can be realized by chilling the process water during the summer months (190 m³, Fig. 2.1), the

spare capacity of the system would reduce the temperature of this water to 2.5°C. This could be accomplished by inserting a heat exchanger in the glycol system on the return side of the chiller. The additional cost of electricity would be marginal particularly at run-off rates during the summer months.

To cool summer process water by another 1°C may be desirable from a process point of view but the cost of the necessary storage is prohibitive unless the same storage can be used in the winter months to reduce the electrical demand charges.

COOLER ROOM TEMPORARY STORAGE

The cooler room is a facility for storage of birds coming out of the chiller tank until they are bagged or cut and packaged. This room is maintained at an average temperature ranging between 0 and 2°C by four evaporators with an installed capacity of 52.74 kW. Two compressor units operate continuously, on an average, 5-1/2 hours followed by a 40 minute off period. The total heat rejected from the cooler room system per day was estimated to be 1.04 MWh/day.

DEEP FREEZE STORAGE

Two evaporators maintain the deep freeze storage room at -20°C. The evaporators and the compressors operate on a cycle consisting 30 minutes on and 15 minutes off which

continue throughout the day. On an average this system rejects 1.99 MWh/day. The two 22.4 kW compressors of the deep freeze system use R-502 as does the quick freeze system. The rest of the units use R-12 which is being used less because of the environmental concerns related to halogens and the atmosphere.

CUTTING ROOM COOLING

To maintain the chilled carcasses at an acceptable temperature the cutting room is held at a temperature of 10°C. Six evaporators with a total installed capacity of 47.5 kW maintain the room temperature. Condensers reject 0.95 MWh/day of thermal energy. The operating cycle of the cutting room compressor follows the same period as the compressors of the ice makers. Both of the units are required simultaneously for cutting and packaging of chilled birds.

The above six units draw 3.74 MWh per working day (see the column entitled "electrical load per day", Table 2.1), 43% of this is required by the freezer storage unit, 15.9% by the chiller tank system and 13.8% by the cooler room compressor motors.

The refrigerating units reject a total of 6.97 MWh on an average production day as shown in Table 2.1. The freezer storage unit contributes 30% (1.99 MWh) of the total heat rejected and the remainder is divided as follows: the

quick freeze system - 16.8%, the chiller tank system - 16.4% and the cooler room - 15.7%.

2.2.2 Energy Use in the Heating System

The energy for heating, in the Dunn-Rite plant, is supplied by natural gas. The gas is used for two main heating purposes - water heating and space heating. The space heating demand is a function of climate whereas the water heating demand is a function of number of birds processed.

2.2.2.1 Methodology of Evaluating Hot Water Production

Fig. 2.1 is a diagrammatic arrangement of the hot water production systems. The plant when moved from another location in 1980 had 1015 kW of water heating capacity consisting two hot water boilers (total capacity 785 kW) and a small steam boiler (60 kW) for the bag shrinker. These three boilers and the gas fired water heater of the scalding tank (capacity 170 kW) were adequate to meet the hot water and steam demand. However, in 1984 a 390 kW steam boiler was added. With this addition the gas fired water heater of the scalding tank was removed. Thus the total installed water heating capacity rose to 1235 kW. Hot water for the scalding tank is now provided by a shell and tube heat exchanger using steam as the heating medium with all the condensate being returned

to the boiler through a condensate receiver tank. In addition to the above modifications, a dishwasher, a glycol regenerator for the quick freeze system and a flash heater to provide 82°C water for sterilization purposes was added. All the new additions were housed in a sizeable building addition. As a result the hot water production system was extremely complex compared to a system designed especially for this plant.

The steam boiler efficiency was determined by both the heat loss method and input-output method. Since the major loss occurring in a boiler is through the stack, a furnace efficiency meter was used to determine the stack losses. The stack losses determined by this method at rated load was 20 percent. The input to the boiler was measured by shutting off all other appliances using gas and thus the gas flow to the boiler was determined in hundreds of cubic feet per hour (CCF/h) from the main gas meter readings. Similarly the output was measured by installing a 50 mm diameter hot water NEPTUNE flow meter, calibrated for 84°C, in the feed water inlet to determine the steam mass flow. By recording the inlet temperature of the feed water (84°C) and the outlet steam conditions, 620 kPa and 160°C the output of the boiler was determined. The ratio of output to input was 77.5%.

The temperature of the condensate from the scalding tank, boiler feed water flow rate and the gas flow rate are given in Fig. 2.7 for a 45 minute period. From the feed

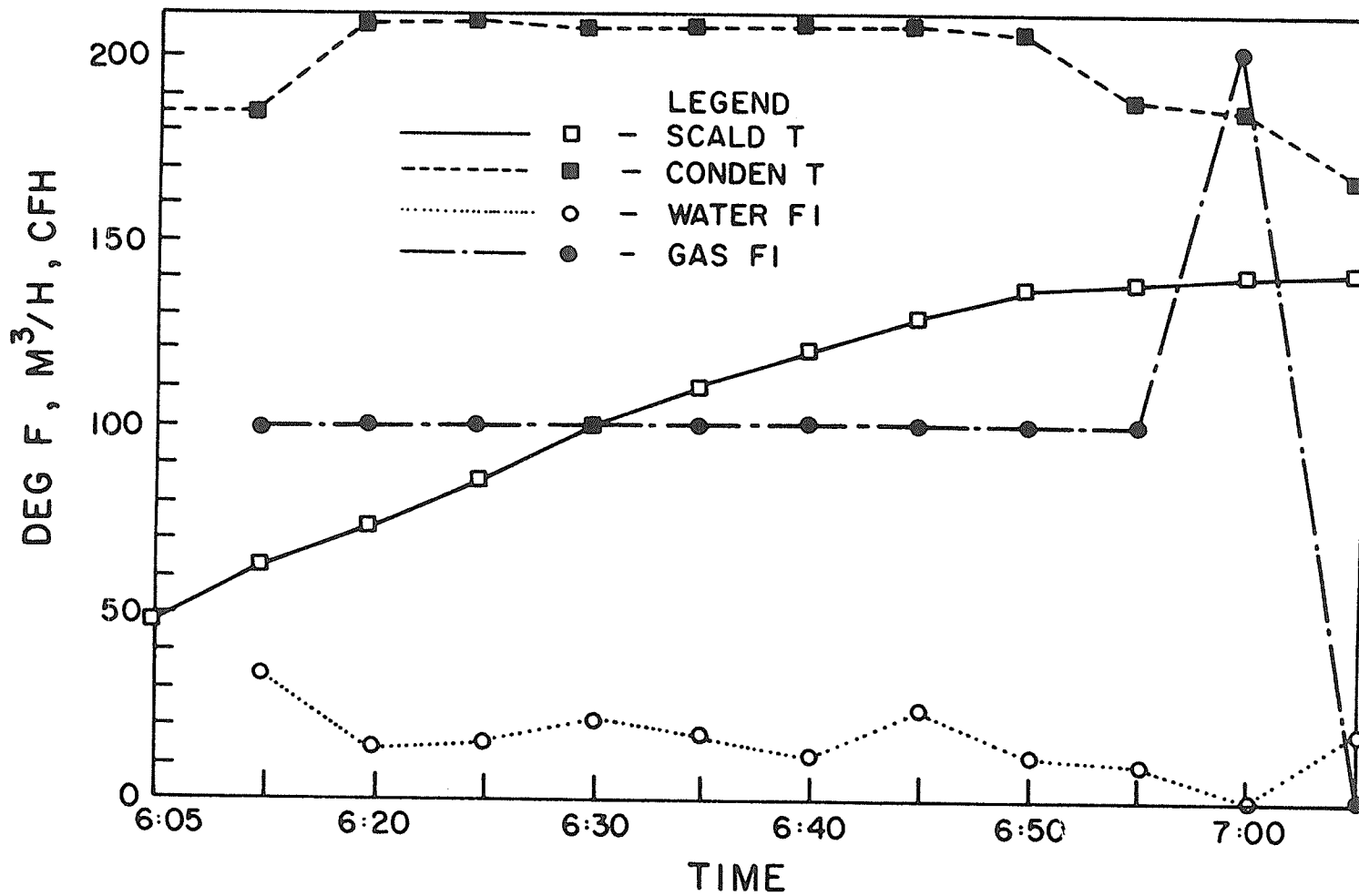


Fig. 2.7 Dunn-Rite boiler test

water flow rate and the gas flow rates it is evident that the boiler was operating at a steady state for at least 30 minutes period (between 0620 to 0650 hours). Calculations showed that within this period of time the boiler was at its rated load. The boiler manufacturer indicates an efficiency of 83% at rated load and guarantees 80% efficiency. Thus all efficiencies, determined and guaranteed were within acceptable limits.

The boiler was assumed to operate at an efficiency of 75% during normal operation since the manufacturer's performance curve showed little drop in performance of loads of 30% of rated and above. That is for all calculated heat balances and estimations a efficiency of 75 percent was assumed. This indicates that heat produced by the steam boiler costs $\$5.24/0.75 = \7.00 per GJ neglecting amortization of the first cost, maintenance and labour. This is about 24% lower than the cost of producing hot water using the old hot water boilers. The steam boiler referred to can not supply the peak load of the plant, but estimates indicates that it operates only at approximately 20% of capacity.

The efficiency of the old hot water boilers was determined by comparison. That is, the plant was run for an entire day on the steam boiler and then an entire day on the old boilers. The increase in gas consumption for an equal number of birds processed was noted and the ratio obtained.

The hot water production efficiency is 54% when operating on the old units. Hence, the unit cost of hot water produced by the old boilers is $\$5.24/0.54 = \9.70 per GJ. The introduction of the steam boiler has reduced the fuel cost, although steam boiler is not necessary to meet the process demands. The plant requires only a small amount of steam (i.e. only for the bag shrinker and the dishwasher) which can be supplied by the 60 kW boiler alone. The present method of producing hot water demands for processing (60°C), domestic use (43°C) and sterilization (82°C) is thermodynamically inefficient. The growth of entropy in reducing steam at 160°C to hot water at less than half its temperature is a wasteful processes. This is offset by the higher efficiency of the steam boiler which has reduced the fuel cost of producing hot water but the overall efficiency of the process could have been improved further if equipment was available to produce the hot water at the desired temperature.

A detailed analysis for the complete month of November, 1986 based on the daily number of birds killed and daily water consumption lead to a water use of 12.5 m^3 per 1000 birds with a standard deviation of less than 10%. That is $250 \text{ m}^3/\text{day}$ for a kill of 20,000 birds.

The breakdown of various water consumption rates based on the estimates associated with the production of 16,000 birds are given in Table 2.3.

Table 2.3
Daily Water Use Of Dunn-Rite Plant

	Use	Temperature °C	Flow m ³ /day
1	Domestic	43	50
2	Production	60	8
3	Production	4.5	192
4	Clean Up	4.5	70
Daily metered flow		-	320

This gives a gross water use of 20 m³ per 1000 birds. When domestic water use is subtracted from the gross water use the net water use for production becomes 12.5 m³ per 1000 birds processed.

The gas consumption of the plant is dependent on the water consumption patterns. Hence, once the water consumptions for various end uses were determined the gas use pattern could also be established.

November was a particularly cold month, 828.8 Degree Days (DD) below 18°C compared to a normal of 676 DD, and a study of the gas consumption for the weekends of the month yielded an estimate of the building heat losses to be 5 CCF per DD (0.528 MJ/DD).

The gas consumption calculated from the water end uses along with a knowledge of the building shell heat losses and the gas used for the heating of domestic water based on the

November 21st gas consumption, the packaging day when no birds were processed, lead to the breakdown of gas use for a typical winter processing day as shown below.

Table 2.4

Daily Gas Use on a Typical Winter Processing Day

ITEM	Gas, CCF	Gas, MJ
Production, birds killed = 16,000	83	8.76
Domestic, washing, etc.	22	2.32
Space heating load - 24 hrs (33 DD)	165	17.42
TOTAL	270	28.50

Detailed records were maintained during November 1986, these included the following:

- i) On November 20, from 0600 h the feed water flow, fuel flow, condensate temperature and steam temperature were read at five minute intervals for 45 minutes to determine the boiler efficiency.
- ii) For November 3rd to November 7th and November 18th to 21st inclusive water and gas meter were read at 15 minutes intervals to establish profiles of the water and gas use for each function of the plant (refer Fig. 2.7, 2.8 and 2.9).

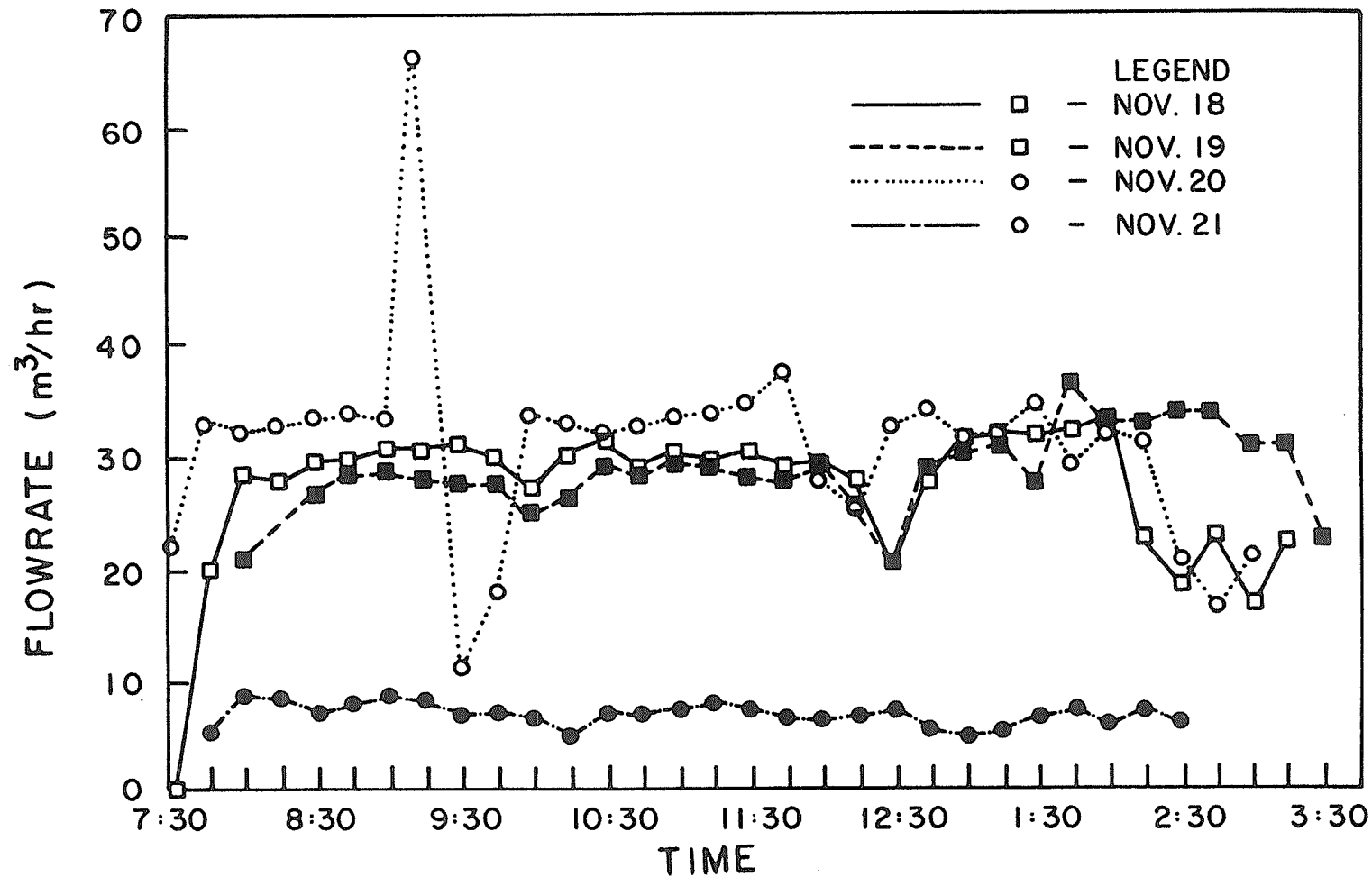


Fig. 2.8 Dunn-Rite water use: November 18-21, 1986

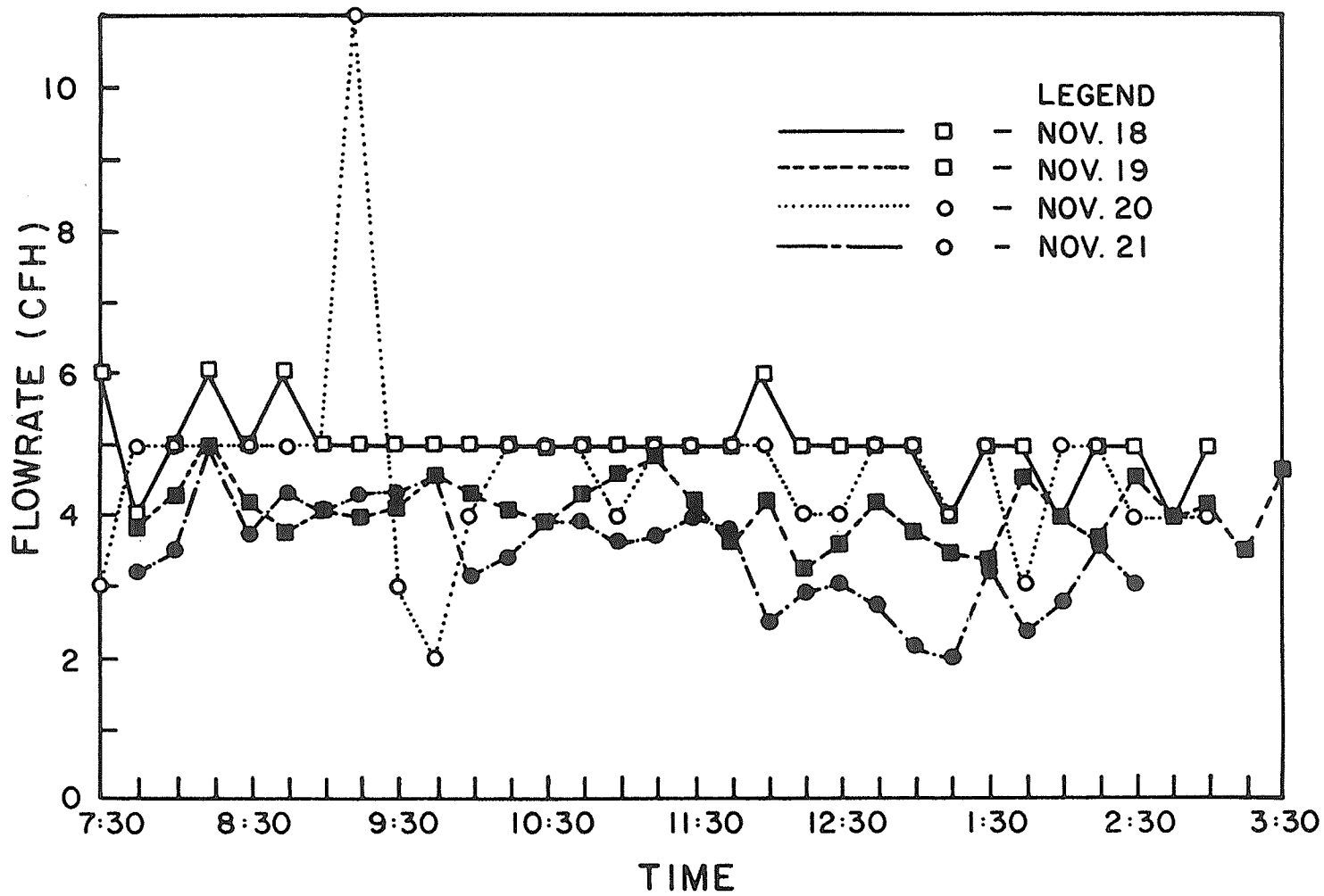


Fig. 2.9 Dunn-Rite gas use: November 18-21, 1986

iii) From November 3rd to November 28th the water and gas meters were read daily and the records of the birds processed obtained to establish the energy and water use per 1000 birds processed.

The results of the analyses based on these detailed records are shown on Table 2.3 and 2.4.

From the daily gas meter readings for the month of November 1986 and from the record of daily birds killed the average net gas consumption per 1000 birds was calculated to be 5.22 CCF, or 0.551 MJ per 1000 birds. The gross gas consumption (including requirements for the domestic water heating) was 6.6 CCF per 1000 birds and with the space heating totaled 16.9 CCF per 1000 birds.

2.3 Energy Balance of the Plant

Referring to Fig. 2.5 the average monthly electricity consumption between September 1985 and August 1986 was estimated to be 129 MWh. The daily electrical load required for the refrigeration equipment was estimated to be (Table 2.1) 3.75 MWh. For a month this accrued to 112.5 MWh. That is, 87% of the electrical load was used by the refrigeration equipment. The balance, 16.5 MWh was spent on lighting and sporadic use of power drills, lathes, etc. of the engineering maintenance department. Power factor correction and electric demand analysis was performed by a consultant and therefore

were not covered during this study. Power consumed by the electric motors less the energy removed by cylinder cooling and bearing friction losses is converted into an increase in enthalpy during the compression of the refrigeration cycle.

The annual gas use is given in Table 2.2 is 90 740 CCF or 9578 MJ. This gives a daily gas consumption of 252 CCF (26.6 MJ) based on the annual consumption figure. The daily gas consumption during November 1986 was 270 CCF (28.5 MJ). This is a realistic figure because during winter months the gas consumption is higher than the annual average because of the space heating. Out of this daily gas demand 31% (83 CCF or 8.76 MJ) is used for production and 8% for domestic use.

The gas demand for production and domestic use is only the gas consumed by the hot water and steam boilers. These boilers maintain the scalding tank water at 60°C and supply domestic water at 43°C. The quality of the energy at these temperatures is low and therefore the use of steam for this purpose is not justifiable. However, the use of steam can not be completely eliminated but the two old hot water boilers could be retired if part of the heat required for the scalding tank and domestic hot water production was supplied from the condenser waste heat. Thereby reducing the amount of steam required.

The estimated hot water heating demand was 2800 kWh. This figure was arrived by using the details given in Table 2.3 and an inlet water temperature of 4.5°C. The total hot water heating capacity available from the boilers is 1175 kW (section 2.1.1). Hence, the boilers need operate only 2.4 hours per day. Although there is excess heating capacity none of the boilers can meet the daily hot water demand alone. As a result the steam package boiler is operated less than 25% load over its operating time. This situation can be remedied by retiring the two hot water boilers except for standby and allowing the package boiler to handle the entire water heating load. Such a move requires careful scheduling of operations like dishwashing during off production hours to cut down the steam demand except for hot water production.

2.4 Advantages of Reclaiming Condenser Waste Heat

As shown in Table 2.1 the average daily heat rejected is 6.7 MWh, which is equivalent to 226 CCF (23.9 MJ) of gas. Referring to Table 2.4, the total gas demand to meet the production and domestic hot water is 105 CCF (11.1 MJ). When the daily heat rejected is compared to an average daily winter gas consumption of 270 to 300 CCF (28.5 to 31.7 MJ) recovery of a fraction of this heat is significant. It is generally not economical to attempt to reclaim more than 50 to 60% of the heat but with a boiler efficiency between 50 and 70% the reclaimable heat is estimated to be worth over

\$100 per day or \$20,000 per year. However, an estimated \$60 per day of this is usable (\$12,000/year) since it can only be used for preheating the domestic and production water. The annual rate of return of \$12,000 would justify a considerable capital investment to cover the initial cost of the heat recovery equipment. The equipment must be simple and maintenance free.

The heat rejected through a condenser consists of the heat absorbed from the refrigerated space plus most of the heat of compression. That is the heat put in by the prime mover as compressor work. Electric energy is thermodynamically a high quality energy and before this potential is ultimately lost to the environment (datum) subjecting it to maximum possible use conserves energy and resources. Hence, condenser waste heat recovery has an additional advantage beyond economic benefits - the advantage of resource utilization.

2.5 Recommendations and Conclusions of the Energy Survey

The following conclusions are drawn from the study.

- i) Sufficient heat could be reclaimed from the heat rejected to meet the entire need for the domestic and production water. However, since the domestic water is required at 43°C and the production water is required at 60°C the recovered heat is available

at approximately 32°C only 60% is usable without a sophisticated heat exchanger with a desuperheater section.

- ii) An extra storage tank may be required to accommodate the heat recovery equipment and to match the supply of the heat rejected with the hot water demand.
- iii) The introduction of a heat exchanger to preheat the make-up water for the more efficient steam boiler and preheat the hot water for storage would yield substantial yearly savings as indicated.
- iv) The reclamation of at least 60% of the condenser waste heat (as mentioned in (i) above) and making full use of the steam boiler would permit the older hot water boilers to be retired or relegated to standby.

In addition to the above conclusions a number of recommendations were made throughout this section, these are as follows:

- i) Since consultants were retained by the plant management to study the electrical loads and demand no consideration was given for this aspect in this study. However, observing the operation cycles of the quick freeze system show that there is excess

capacity from the 2-50 HP compressors. This system is also a brine circulated refrigeration system. Hence, considerations should be given to store chilled brine during off peak electrical demand periods.

- ii) The quick freeze system can also be used to chill production water during summer months. Since there is excess capacity the capital cost required for this change would be minimal.
- iii) The present mode of operation of the quick freeze system during winter months should be changed from cyclic mode to the use of one compressor after a start-up period. The surges involved in operating such large motors on a on-off cycle will lead to excessive maintenance.
- iv) Lowering the temperature of an existing 1000 gallon storage tank is recommended since this would decrease the heat loss from the tank and increase the efficiencies of the boilers.
- v) The use of an electrical hot water system to raise the water temperature to sterilization needs (82°C) from the storage tank temperature at 60°C . The quantity of this water is exceedingly small. As a result, the additional cost on electricity will be marginal. The flash type of heaters currently used

for the production of hot water for sterilization are noisy and involve considerable maintenance.

- vi) To utilize the waste heat from the condensers the present hot water system must be rearranged to include a shell and tube heat exchanger probably inside a storage tank to preheat storage water. With this arrangement the storage tank temperature would be lowered to 60°C.

2.6 Need for a Condenser Design Procedure

Waste heat recovery applied to the existing refrigeration system is feasible and economic but simplicity and a maintenance free exchanger is essential. Two feasible methods to satisfy these criteria are:

- i) Compressor outlet risers
- ii) Bayonet and/or U-type exchangers.

The compressor outlet risers can be wound with small diameter water tubes. For example the 40 kW compressor operating one of the deep freeze evaporators uses R-502. This refrigerant leaves the compressor at 88°C, that is with 44°C of superheat and it condenses at 43°C. The estimated flow is 0.3 kg/s and while condensing and cooling this flow rejects over 60 kW of heat. The existing pipe diameter of the outlet diameter is 38 mm and an arrangement shown in

Fig. 2.10 consisting 6.35 mm diameter tubing wound with a 25.4 mm pitch could reclaim 30 kW. This is 50 percent of the heat rejected. The length required to recover this amount of heat is 6 meters. This method is low cost and could be installed by the in-house personnel. Since only 50 percent of the heat is removed complete condensation would not take place. Therefore the roof top condensers would still be required. A small amount of condensate would be formed within the riser which could flood the compressor. Hence, adequate precautions must be taken to drain the condensate with a trap back into the condensate reservoir.

Bayonet or U-tube exchangers installed are shown in Fig. 2.11 would be advantageous providing extra storage as well as heat recovery. This type is easy to dismantle and clean. The inefficient hot water boilers could be shut down. The disadvantage in using this type of heat exchangers would be the cost and space requirements. Further they require pumping power to circulate the water through the shell to increase the water side heat transfer coefficient.

In both of the above mentioned systems the condensation of R-502 refrigerant vapor takes place within the tubes. Hence, the determination of the rate of heat transfer during in-tube condensation becomes necessary for an efficient design of a heat exchanger for the above purpose. Heat transfer in such an application depends on the heat transfer coefficient of the condensing vapor inside the tube and the

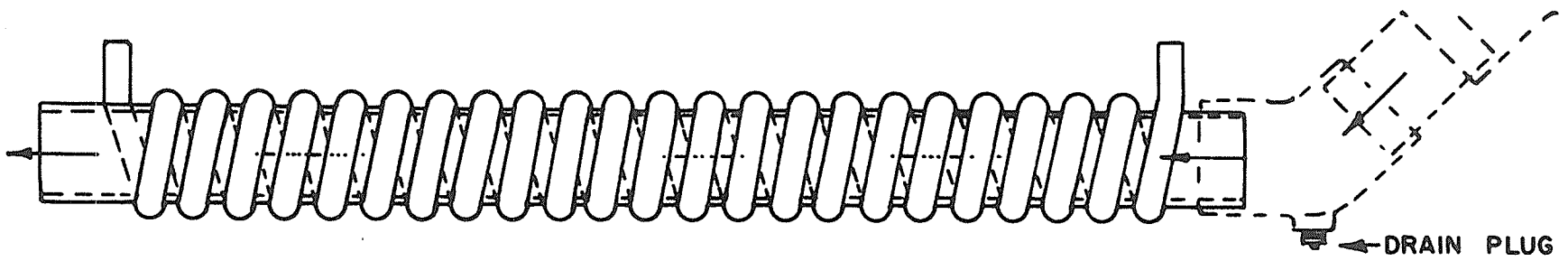


Fig. 2.10 Helical coil tube heat recovery unit

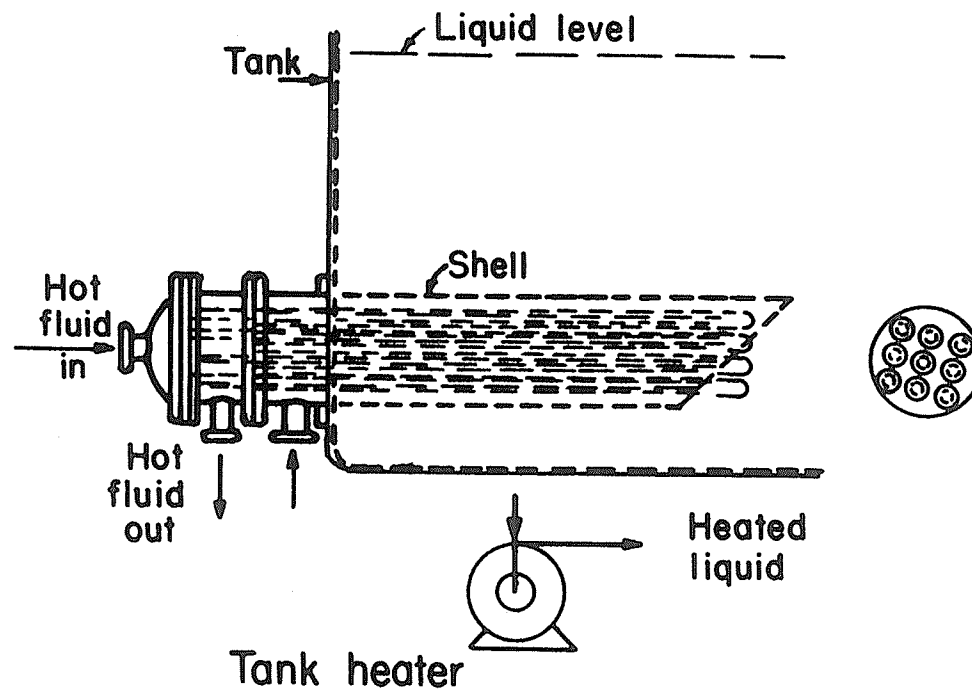


Fig. 2.11 Bayonet tube or U-tube tank heater

heat transfer coefficient of water outside the tube. There are methods to calculate the latter accurately. However, a procedure to determine the heat transfer correlation during in-tube condensation is not readily available.

Although there are number of correlations and design procedures in the literature which are applicable for the calculation of condensation heat transfer coefficients inside tubes, this subject has received less attention in text books and handbooks available for a practicing engineer. For example, ASHRAE Handbook 1985 fundamentals [2] devotes a brief portion for condensation inside horizontal tubes. The correlations given by ASHRAE [2] are of a particular nature valid only for limited applications. These are recommended for particular ranges of flow regimes but a method to determine the flow regimes is not given. That is no reliable design procedure exist for condensation of vapor inside tubes. As a result, this work was undertaken to evaluate some of the recent correlations available in the literature and develop a design procedure.

CHAPTER 3
REVIEW OF LITERATURE ON CONDENSATION HEAT
TRANSFER INSIDE TUBES

When a saturated vapor, flowing in a tube, is cooled by an exterior fluid two phase flow patterns develop. The development of flow patterns in the direction of flow during condensation is shown in Fig. 3.1. The hydrodynamics of two phase flow under adiabatic conditions are not well understood. Since the hydrodynamics of two phase flows involving heat transfer are more complicated due to the interdependence between thermal characteristics and local flow conditions, no single set of correlations can be used to predict the heat transfer rates for all two-phase flow systems. Therefore, the heat transfer correlations that exist in the literature have been categorized for specific thermal and hydrodynamic operating conditions. When these correlations are applied outside the range of applicability the deviations are of an unacceptable magnitude.

3.1 ASHRAE Recommended Correlations

There are three recommended correlations for horizontal in-tube condensation in the ASHRAE Handbook 1985 Fundamentals [2]. All three can be divided into two categories, (i) laminar flow model and (ii) turbulent flow model.

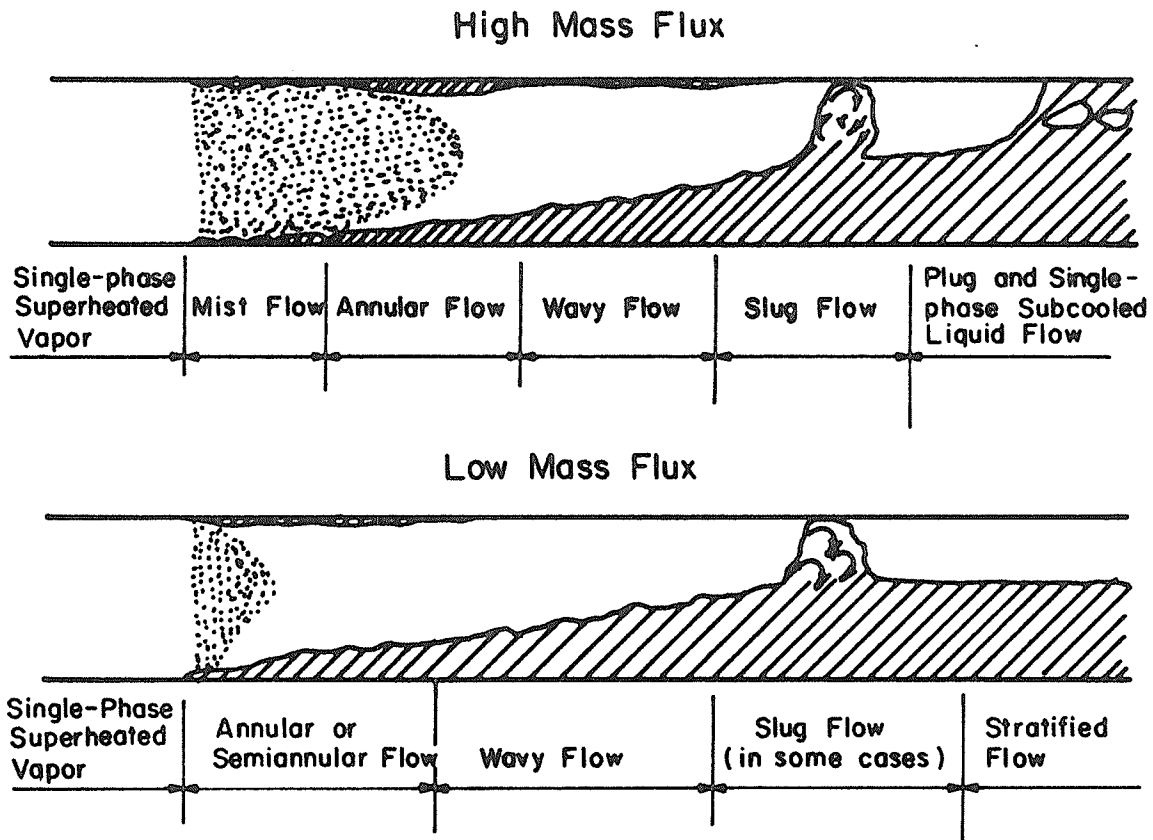


Fig. 3.1 Development of flow patterns in the direction of flow during condensation

3.1.1 Laminar Flow Model

Akers and Rosson [3] postulated three primary flow regions during condensation inside tubes. The three flow regions are semistratified flow, laminar annular flow, and turbulent annular flow. The semistratified flow regime is characterized by annular condensation and vertical flow of condensate due to gravity superimposed on stratified flow. A semi-empirical correlation was developed on the basis of laminar flow within the condensate liquid and linear temperature drop across the liquid film. Although the above two assumptions were the basic assumptions made by Nusselt [4], to develop the first mathematical expression for laminar liquid flow under the influence of gravity, Akers and Rosson [3] incorporated a vapor shear term into the correlation to account for the shear force resulting from the vapor-condensate interface inside the horizontal tube. The force influencing the liquid condensate flow inside a horizontal tube is the vapor shear force. Therefore, Akers and Rosson [3] considered three dimensionless groups, namely vapor Reynolds number (Re_v), Prandtl number of the liquid (Pr_L) and the thermal potential influencing the heat transfer mechanism. The Re_v describes the dynamic effects of the vapor on the liquid film and is given by,

$$Re_v = \frac{D G_v}{\mu_L} \left[\frac{\rho_L}{\rho_v} \right]^{1/2} \quad (3.1)$$

Where, D = tube diameter,
 G_V = vapor mass velocity based on total cross
 section of tube,
 μ_L = dynamic viscosity of the saturated liquid,
 ρ_L = density of liquid,
 ρ_V = density of vapor.

The influence of thermal properties of the condensing vapor on the heat transfer coefficient is given by the Pr_L and the third dimensionless group, the thermal potential, is defined by $h_{fg}/C_p \Delta T$. The data were obtained by condensing methanol and Freon-12 inside a 16 mm ID copper tube 305 mm in length. Based on the data so obtained the three dimensionless groups were correlated with Nusselt number (Nu). This correlation was limited to only laminar liquid film flow. The transition from laminar to turbulent flow in the liquid film was believed to occur at a Re_L of 5000. However, Kirkbride [5] while extending Nusselt's [4] theory for condensation on vertical tubes found turbulence to occur when the Reynolds number of the condensate flow (Re_L) exceeded 2000.

The local heat transfer relations developed by Akers and Rosson [3], for Re_L less than 5000 is given by,

$$Nu = 13.8 Pr_L^{1/3} \left[\frac{h_{fg}}{C_{pL} \Delta T} \right]^{1/6} Re_V^{0.2} \quad (3.2)$$

for Re_v from 1000 to 20,000 and

$$Nu = 0.1 Pr_L^{1/3} \left[\frac{h_{fg}}{C_{pL} \Delta T} \right]^{1/6} Re_v^{2/3}, \quad (3.3)$$

for values of Re_v from 20,000 to 100,000.

Where,

N_u = local Nusselt number,

h_{fg} = enthalpy of vapor relative to condensate film,
J/kg,

C_{pL} = specific heat of liquid at constant pressure,
J/(kg. K),

ΔT = temperature drop across the condensate film, °C.

These relationships were not recommended for use for values of Re_L in excess of 5000, where

$$Re_L = \frac{G(1-x)D}{\mu_L}$$

G = total mass velocity, and

x = vapor quality.

3.1.2 Turbulent Flow Models

When the Re_L is above 5000 and Re_v greater than 20,000 the data were not correlated by Equations 3.2 and 3.3. Hence, Akers et al. [6], based on the data obtained from condensing propane and Freon-12 inside a 16 mm ID 2.9 m

horizontal tube, recommended a correlation for the local Nusselt number of the form,

$$\text{Nu} = 0.026 \text{Pr}_L^{1/3} \left[\frac{DG_E}{\mu_L} \right]^{0.8}, \quad (3.4)$$

for $\text{Re}_E > 5 \times 10^4$ and

$$\text{Nu} = 5.03 \text{Pr}_L^{1/3} \left[\frac{DG_E}{\mu_L} \right]^{1/3}, \quad (3.5)$$

for $\text{Re}_E < 5 \times 10^4$.

$$\text{Where, } G_E = G_L + G_V \left[\frac{\rho_L}{\rho_V} \right]^{1/2}, \quad (3.6)$$

$$\text{and } \text{Re}_E = DG_E/\mu_L. \quad (3.7)$$

G_L and G_V are the average mass velocities per unit area ($\text{kg}/(\text{m}^2 \cdot \text{s})$) of both liquid and vapor respectively. When the vapor mass velocity is high, the flow could be considered as an annular ring of condensate surrounding a core of vapor. The resistance to heat transfer is caused by the liquid and therefore the flow characteristics of the condensate film should determine the heat transfer coefficient. The most important force determining the flow characteristics should result from the interaction between the vapor core and the liquid film. Therefore, Akers et al. [6] theoretically replaced the vapor core with a liquid, whose flow would yield the same value for the shear. Hence the equivalent mass velocity given in equation (3.6) is a sum of the condensate mass velocity and the equivalent liquid mass velocity that

would exert the same force on the condensate film as the vapor core.

The ASHRAE Handbook [2] gives the equivalent mass velocity as,

$$G_E = G_V \left[\frac{\rho_L}{\rho_V} \right] + G_L \quad (3.8)$$

ignoring the exponent on the density ratio given by Akers et al. [6]. A comparison made between Equations 3.6 and 3.8 shows Equation 3.8 to give a G_E two to five times greater than the value given by Equation 3.6. The equation recommended by ASHRAE [2] for turbulent annular flow, of the equations given by Akers et al. [6], is Equation 3.4. When G_E given by Equation 3.8 is used to determine the Nu number with Equations 3.4 and 3.5 extremely high values result. Hence, G_E must be determined by Equation 3.6 rather than Equation 3.8.

The correlation of Akers et al. [6] did not take into consideration the flow characteristics within the condensate film. Only the vapor-liquid interaction was considered. Altman et al. [7] developed a theoretical correlation based on an annular model analogy. The liquid annulus resisting the heat flow from the vapor core was studied in detail. The viscous sublayer and the turbulent boundary layer of the liquid annulus are two different components contributing to this resistance. In order to evaluate these two resistances the Prandtl-Nikuradse universal velocity distribution was

assumed for the condensate film. The effect of vapor shear stress at the vapor-liquid interface was also included. The correlation for the local heat transfer coefficient (h) is then given by,

$$h = 0.057 \left[\frac{C_{pL} k_L \rho_L}{\mu_L} \right]^{0.5} F^{0.5} \quad (3.9)$$

Where, h = local heat transfer coefficient, $W/(m^2 \cdot K)$

$$F = \Delta P_{TPF} \left[\frac{g_0 D}{4L} \right], \quad Pa. \quad (3.10)$$

Where ΔP_{TPF} = frictional two phase pressure drop given by

Forster and Zuber [8], Pa,

g_0 = gravitational constant,

k_L = thermal conductivity of the liquid,
 $W/(m \cdot K)$,

L = length of condenser, m.

This correlation was experimentally verified by condensing R-22 inside a 9mm ID 2.4 m copper tube. The agreement was within $\pm 10\%$ of the measured data. ASHRAE [2] recommends this correlation for condensing R-22 and other similar fluids.

3.2 Correlations Based on Theoretical Analysis

Nusselt [4] derived theoretical relations to predict the coefficient of heat transfer of a pure condensing vapor on a

colder surface in a pioneering paper in 1916. He assumed laminar flow to exist throughout the thickness of the continuous film which completely wets the surface. In his model the flow is assumed to be under the action of gravity alone, thus the action of the vapor velocity on the thickness is neglected. Nusselt [4] was able to derive theoretical relationships for the mean film coefficient on various condensing surfaces by making further assumptions. A constant temperature difference between the saturated vapor and tube wall at all points, and the entire resistance to heat flow in the condensate film was assumed. The application of this theory to condensation on horizontal tubes required integration over the surface covered by the condensing film. Nusselt [4] evaluated this by graphical methods. However, Abromowitz [9] prepared a table of functions to evaluate the integral. For an effective surface for condensation over an angle (ψ) of approximately 40° (refer Fig. 3.2) the mean heat transfer coefficient (h_m) outside the tube is given by,

$$h_m = 0.959 \left[\frac{L k_L^3 \rho_L (\rho_L - \rho_v) g}{W_T \mu_L} \right]^{1/3} \quad (3.11)$$

Where, g = acceleration due to gravity, m/s^2 and
 W_T = total fluid flow rate, kg/s .

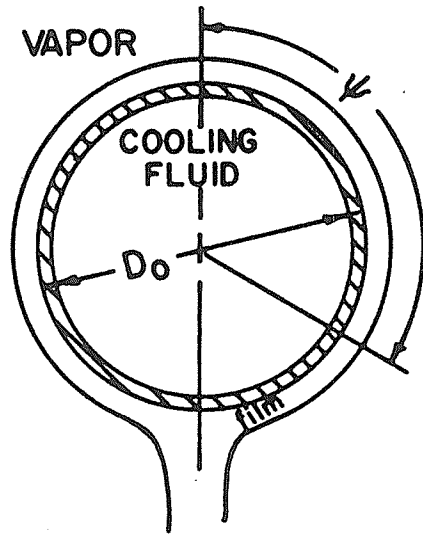
Although Equation 3.11 is developed for condensation outside the tubes, Kern [10] empirically modified it for condensation within tubes. He proposed an empirical substitution of $2W_T$ for W_T in Equation 3.11 to correct for the poor heat transfer resulting from the draining liquid, flowing into a stratified pool, during condensation within tubes. This modified equation for mean heat transfer coefficient within horizontal tubes is given by,

$$h_m = 0.761 \left[\frac{\bar{k}_L^3 \rho_L (\rho_L - \rho_V) g}{WT \mu_L} \right]^{1/3} \text{ W/m}^2\cdot\text{K} \quad (3.12)$$

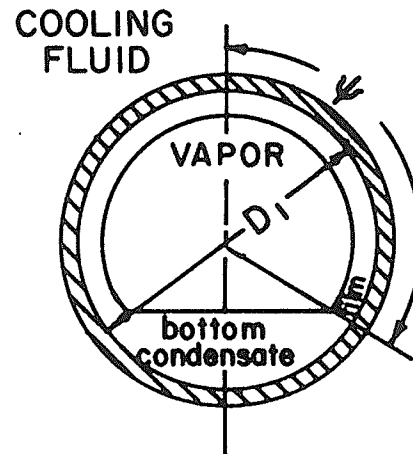
The condensation heat transfer coefficient within horizontal tubes during laminar condensate film flow was analyzed in great detail by Chaddock [11]. He assumed that the tube area covered by the condensing film was constant with length and could be represented by the mean film angle (Fig. 3.2.), ψ_m , where

$$\psi_m = \pi - \left[\frac{0.47 J L (\Delta T)^{3/4}}{D^{2.75}} \right]^{0.142} \quad (3.13)$$

$$\text{and } J = \left[\frac{\bar{k}_L^3 (\rho_L - \rho_V) g}{\mu_L \rho_L^3 h_{fg}^3} \right]^{1/4} \quad (3.14)$$



On a Horizontal Tube



Inside a Horizontal Tube

Fig. 3.2 Surface covered by the Condensing film over the film angle

The mean heat transfer coefficient is given by,

$$h_m = \frac{\psi_m}{\pi} \frac{\beta \Omega}{(D\Delta t)^{1/4}} \quad \text{W/m}^2\cdot\text{K.} \quad (3.15)$$

$$\text{Where, } \beta = (0.9036/\psi_m) \int_0^{\psi_m} (d\theta/S^{1/4}), \quad (3.16)$$

S = perimeter of the tube, m,

$d\theta$ = the infinitesimal film angle, and

$$\Omega = \left[\frac{k_L^3 \rho_L (\rho_L - \rho_V) g h_{fg}}{\mu_L} \right]^{1/4}. \quad (3.17)$$

The angular function β is the same function tabulated by Abramowitz [9].

All of the three correlations discussed in this section deal only the laminar flow of the condensate film with negligible vapor shear on the condensate vapor interface. A correlation to predict the rate of heat transfer, while the condensate layer was in turbulent flow, was derived by Carpenter and Colburn [12]. They hypothesized that the condensate film becomes turbulent at a Re_L around 240 in the presence of high vapor friction whereas the transition takes place around $Re_L = 2000$ in the absence of vapor friction. It was assumed that the major resistance to heat flow was from the laminar sublayer and the turbulent boundary above this sublayer offered negligible resistance. Based on the velocity distribution of the condensate boundary layer, approximated by the use of Von Karman Universal velocity

distribution, the thickness of the laminar sublayer was determined. From the experimental data, obtained by condensing steam, methanol, ethanol, toluene and trichloroethylene inside a vertical tube 12 mm ID and 2.4 m long, the condenser tube was divided into three sections. They observed that in the first short region the condensate layer was entirely laminar and therefore applied,

$$h = k_L \left[\frac{\rho_L F}{2 \mu_L \Gamma} \right]^{1/2} \quad (3.18)$$

Where, Γ = condensate rate of flow per unit periphery at any point,

$$F = F_f + F_m .$$

Where, F_f = force due to vapor friction and

F_m = force due to momentum change of the condensing vapor.

In the second region the condensate layer was turbulent and the transition occurred at Re_L greater than 250. In this region the local heat transfer coefficient is given by,

$$h = 0.043 \left[\frac{C_{pL} \rho_L k_L}{\mu_L} \right]^{1/2} F^{1/2} \quad \text{W/m}^2.\text{K.} \quad (3.19)$$

Where, $F = F_f + F_a + F_m$ and

$$F_a = \frac{\Gamma g}{10(F/\rho_L)^{1/2}} \quad \text{is the force due to gravity.}$$

The value F is the total drag force per unit surface of the laminar layer, and the other components contributing to this are vapor friction force (F_f), gravity force (F_a) and the force owing to momentum change of the condensing vapor (F_m).

Since the above correlations are laborious in design calculations, the following simplified average coefficient was given by Carpenter and Colburn [12].

$$h_m = 0.065 \left[\frac{C_{pL} k_L \rho_L f_v}{2 \mu_L \rho_v} \right]^{1/2} G_m \quad \text{W/m}^2 \cdot \text{K.} \quad (3.20)$$

Where, f_v = Fanning friction factor [13] and

$$G_m = \left[\frac{G_1^2 + G_1 G_2 + G_2^2}{3} \right]^{1/2} \quad (3.21)$$

Where G_1 is the value of G_v at the top of the tube and G_2 is the value at the bottom of the tube.

The effect of vapor shear stress on the rates of condensation at the liquid vapor interface is theoretically analyzed by Rohsenow et al. [14] [15]. The system considered is a vertical plate with pure saturated vapor condensing on a uniform temperature plate. The universal velocity distribution is applied in the turbulent film. The average heat transfer coefficient is given in a graphical form since the evaluation of the theoretical correlation is cumbersome for design purposes.

A method to predict local heat transfer coefficients inside horizontal tubes during annular and stratified flow of the condensate is given by Rosson and Myers [16]. The effect of liquid accumulating inside the pipe was considered. To predict the coefficient of heat transfer at the bottom of the tube, where condensate accumulates due to gravity, Von Karman's analogy is used. The local shear stress is assumed to be not too different from the average shear. Therefore, the Lockhart and Martinelli [17] method could be used to evaluate the shear stresses near the wall. The agreement yielded by this correlation is good, however, at high Re_L the experimental values are found to be lower than the predicted values. With low Re_L the reverse is found true. The reason given for these phenomena is that the Lockhart - Martinelli [17] correlation becomes unsuitable for use at low Re_L and for high waves occurring at high Re_L . During condensation heat transfer experiments low heat transfer coefficients are obtained near the exit end of the condenser. This is because by the time the vapor reaches the exit end of the condenser most of it would have condensed and as a result the liquid condensate fills partially the tube. This reduces the area available for condensation within the tube. Hence, the low heat transfer coefficient. In order to predict the low heat transfer coefficients encountered at the exit end of the condenser, they defined an angle at which an arithmetic average of the high and low coefficients of heat transfer

existed during stratified flow. This angle is a function of the ratio of gravitational force to viscous forces, multiplying this ratio by the Re_L results in Galileo number (Ga). From the parameters the angular location of the mean heat transfer coefficient is found.

The heat transfer coefficient at the top of the tube (h_o) is given by

$$h_o = 0.31 Re_v^{0.12} \left[\frac{k_L^3 h_{fg} \rho_L (\rho_L - \rho_v) g}{D \mu_L \Delta T} \right]^{1/4} \text{ W/m}^2 \cdot \text{K} \quad (3.22)$$

and at the bottom of the tube is given by

$$Nu = \frac{\phi_v (8 Re_L)^{1/2}}{5 + \frac{5}{Pr_L} \ln (5 Pr_L + 1)} \quad (3.23)$$

Where ϕ_v is Lockhart - Martinelli [17] pressure drop parameter defined by,

$$\phi_v = 1 + 1.09 X_{tt}^{0.039} \quad (3.24)$$

$$\text{Where, } X_{tt} = [(1-x)/x]^{0.9} [\rho_v/\rho_L]^{0.5} [\mu_L/\mu_v]^{0.1}, \quad (3.25)$$

Nu = Nusselt number at the bottom of the tube, and

X_{tt} = Lockhart - Martinelli [17] parameter.

The Galileo number (Ga) is defined as,

$$Ga = \frac{D^3 \rho_L (\rho_L - \rho_v) g}{\mu_L^2} \quad (3.26)$$

and the mean of h_o and h_π (obtained from Equation 3.23) are found at an angle defined by (refer Fig. 3.3),

$$\theta_m = 0.27 \pi \text{Re}_v^{0.1} \quad , \quad \text{if} \quad \frac{\text{Re}_v^{0.6} \text{Re}_L^{0.5}}{\text{Ga}} < 6.4 \times 10^{-5} \quad (3.27)$$

$$\text{and} \quad \theta_m = \frac{1.74 \times 10^{-5} \pi \text{Ga}}{(\text{Re}_v \text{Re}_L)^{0.5}} \quad , \quad \text{if} \quad \frac{\text{Re}_v^{0.6} \text{Re}_L^{0.5}}{\text{Ga}} > 6.4 \times 10^{-5}. \quad (3.28)$$

The mean coefficient of heat transfer at any axial location is given by,

$$h = h_\pi + (h_o - h_\pi) \frac{\theta_m}{\pi} \quad (3.29)$$

This correlation was experimentally tested by the authors against condensing methanol and acetone inside a 10 mm stainless steel condenser. The correlation agreed with the experimental data within $\pm 36\%$ at 90% confidence level. However, the agreement at the top of the tube was $\pm 27\%$ and at the bottom of the tube 41%, at the same confidence level.

The single phase Dittus-Boelter type heat transfer correlation was modified by Boyko and Kruzhilin [18] to develop a correlation for annular condensation. The correlation is developed on the basis of experiments conducted by condensing steam inside 8 mm and 17 mm ID tubes. The Boyko-Kruzhilin [18] correlation for the mean heat transfer coefficient for condensing a stream from quality x_1 to quality x_2 is given by,

LOCAL HEAT TRANSFER COEFFICIENT

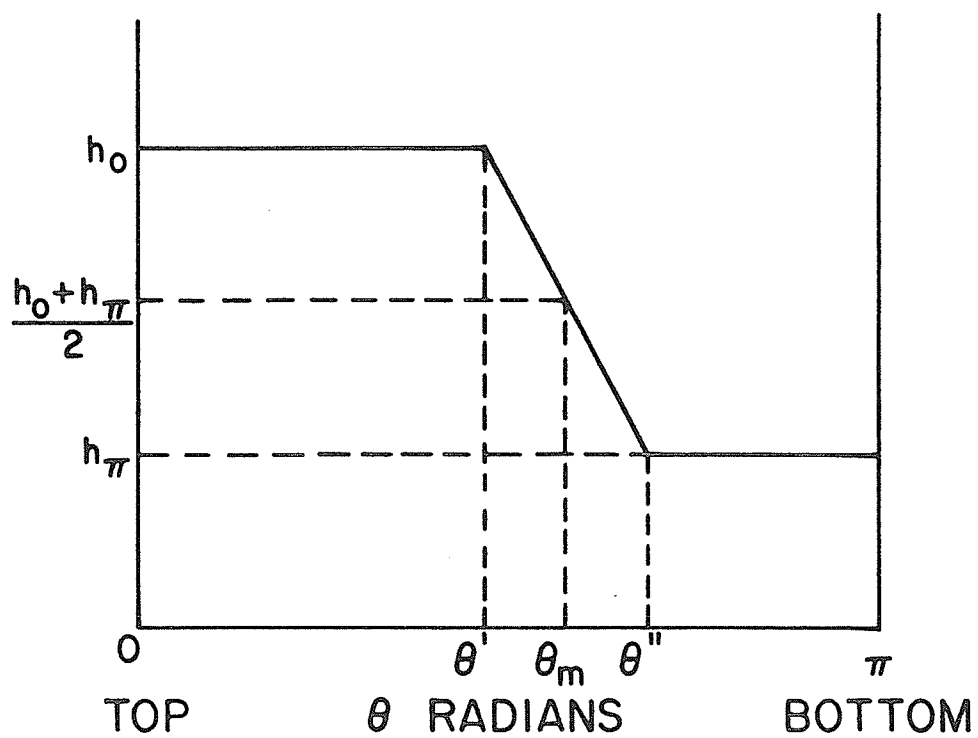


Fig. 3.3 Typical variation of h with the increase of film angle

$$\frac{h_m D}{k_L} = 0.024 \text{Re}_L^{0.8} \text{Pr}_L^{0.43} \left[\frac{\sqrt{(\rho/\rho_m)_1} + \sqrt{(\rho/\rho_m)_2}}{2} \right] \quad (3.30)$$

$$\text{Where, } (\rho/\rho_m)_1 = 1 + \left[\frac{\rho_L - \rho_V}{\rho_V} \right] x_1 \quad (3.31)$$

and for $(\rho/\rho_m)_2$ equation (3.31) is used with x_2 in place of x_1 .

The Carpenter-Colburn [12] approach to evaluate heat transfer coefficients based on the effect of vapor velocity and gravity on condensation is modified by Soliman et al. [19]. It is assumed that a liquid annular flow pattern persists over the major portion of the condensing length. Hence, an annular flow model is developed, assuming a turbulent vapor core and a turbulent liquid film, based on the momentum analogy. The effect of friction, momentum and gravity forces on the process of forced condensation and the wall shear stresses are studied. It is observed that the friction between the vapor and liquid film dominate the wall shear stress at high and intermediate qualities. The effect of momentum becomes increasingly important at high density ratio (ρ_L/ρ_V) and dominates in the low quality region in the absence of an axial gravitational field. The gravity contribution for vertical down flow under gravity is negligible at high quality, while it could dominate the wall shear stress at low quality. From published data the Carpenter-Colburn [12] equation for condensation is modified

based on the theoretical analysis made on the effect of friction, momentum and gravity. The local condensing heat transfer coefficient is given as,

$$\frac{h \mu_L}{k_L \rho_L^{1/2}} = 0.036 \text{Pr}_L^{0.65} \text{Fo}^{1/2} \quad (3.32)$$

$$\text{Where, } \text{Fo} = \text{F}_f + \text{F}_m \pm \text{F}_a, \quad (3.33)$$

$$\begin{aligned} \frac{\text{F}_f}{8W_T^2/\pi^2 \rho_V D^4} &= 0.045 \text{Re}_T^{-0.2} \left[x^{1.8} + 5.7 \left[\frac{\mu_L}{\mu_V} \right]^{0.0522} (1-x)^{0.47} x^{1.33} \right. \\ &\quad \left. \left[\frac{\rho_V}{\rho_L} \right]^{0.261} + 8.11 \left[\frac{\mu_L}{\mu_V} \right]^{0.105} (1-x)^{0.94} x^{0.86} \left[\frac{\rho_V}{\rho_L} \right]^{0.522} \right], \quad (3.34) \end{aligned}$$

$$\begin{aligned} \frac{\text{F}_m}{8W_T^2/\pi^2 \rho_V D^4} &= 0.5 \left[\frac{D}{dz} \frac{dx}{dz} \right] \left[2(1-x)(\rho_V/\rho_L)^{2/3} + \left[\frac{1}{x} - 3 + 2x \right] \right. \\ &\quad \left. (\rho_V/\rho_L)^{4/3} + (2x-1-\delta x)(\rho_V/\rho_L)^{1/3} + (2\delta - \delta/x - \delta x) \right. \\ &\quad \left. (\rho_V/\rho_L)^{5/3} + 2(1-x-\delta + \delta x)(\rho_V/\rho_L) \right], \quad (3.35) \end{aligned}$$

$$\frac{\text{F}_a}{8W_T^2/\pi^2 \rho_V D^4} = 0.5 \text{Fr}_T^{-1} \left[1 - \left[1 + \left[\frac{1-x}{x} \left[\frac{\rho_V}{\rho_L} \right]^{2/3} - 1 \right] \right] \right], \quad (3.36)$$

$$\text{Fr}_T = 16 W_T^2/\pi^2 D^5 a (\rho_L - \rho_V) \rho_V, \quad (3.37)$$

$$\text{Re}_T = 4W_T/\pi D \mu_V, \quad (3.38)$$

$$D \frac{dx}{dz} = -D/L \quad (\text{for a quality change from 0 to 1}), \quad (3.39)$$

$$a = g \sin \theta, \quad (3.40)$$

s = circumference of tube, m,

θ = angle of vapor flow vector with the horizontal, and

γ = constant relating interfacial liquid velocity to the average velocity throughout the condensate film and may be taken as 1.25 for a turbulent film and 2 for a laminar film.

The fluid properties for the above equations are taken at saturation temperature.

A modification to the approach given by Soliman et al. [19] is proposed, based on the heat and momentum analogy suggested by Rohsenow et al. [14] for vertical plates, by Bae et al. [20]. This theory followed an annular flow model where a momentum balance is made on an element. As a result, the static pressure gradient is found to be a sum of gradients due to friction, gravity and momentum. To determine the heat transfer coefficient it is assumed that the Karman momentum heat transfer analogy is applicable in the liquid layer. The heat transfer coefficient is given by,

$$\frac{hD}{k_L} = \frac{\rho_L C_{pL} D u_\tau}{k_L F_2} \quad (3.41)$$

Where,
$$u_\tau = \frac{g_o \tau_o}{\rho_L}^{1/2}, \quad (3.42)$$

τ_o = wall shear stress, and

$$F_2 = \delta^+ Pr \quad \text{for } 0 < \delta^+ < 5, \quad (3.43)$$

$$F_2 = 5 Pr + 5 \ln \left[1 + Pr \left[\frac{\delta^+}{5} + 1 \right] \right] \quad \text{for } 5 < \delta^+ < 30, \quad (3.44)$$

$$F_2 = 5 \text{ Pr} + 5 \ln (1 + 5 \text{ Pr}) + \frac{2.5}{\left[1 + \frac{10M}{\text{Pr} \delta^+}\right]^{1/2}}$$

$$\ln \left[\frac{2M-1 + \left[1 + \frac{10M}{\text{Pr} \delta^+}\right]^{1/2} \frac{60}{\delta^+} M - 1 - \left[1 + \frac{10M}{\text{Pr} \delta^+}\right]^{1/2}}{2M-1 - \left[1 + \frac{10M}{\text{Pr} \delta^+}\right]^{1/2} \frac{60}{\delta^+} M - 1 + \left[1 + \frac{10M}{\text{Pr} \delta^+}\right]^{1/2}} \right] \text{ for } \delta^+ > 30. \quad (3.45)$$

$$\text{Here, } M = \frac{F_o \delta^+ \nu}{\tau_o u_t}, \quad (3.46)$$

Where ν = kinematic viscosity of the liquid, m^2/s ,

$$F_o = - \left[\frac{dP}{dZ} \right] + \frac{a}{g_o} \rho_L - \frac{G^2}{g_o \rho_v} \left[\frac{dx}{dZ} \right] \left[\frac{1}{1-\alpha} \left[\frac{\rho_v}{\rho_L} \right]^{1/3} - \frac{(1-x)(2-\beta)}{(1-\alpha)^2} \left[\frac{\rho_v}{\rho_L} \right] \right], \text{ and} \quad (3.47)$$

z = axial distance from condensation starting point, m .

By trial and error the non dimensional film thickness (δ^+) is obtained by,

$$\text{Re}_L = 2(\delta^+)^2 \quad \text{for } \delta^+ < 5, \quad (3.48)$$

$$\text{Re}_L = 50 - 32.2 \delta^+ + 20 \delta^+ \ln \delta^+ \quad \text{for } 5 < \delta^+ < 30, \quad (3.49)$$

$$\text{Re}_L = -256 + 12 \delta^+ + 10 \delta^+ \ln \delta^+ \quad \text{for } \delta^+ > 30 \text{ and} \quad (3.50)$$

$$\alpha = \frac{1}{1 + \left[\frac{1-x}{x} \right] \left[\frac{\rho_v}{\rho_L} \right]^{2/3}} \quad (3.51)$$

The components of the pressure gradients are obtained by,

$$\left[\frac{dP}{dz} \right]_f \frac{g_o D}{G^2 / \rho_v} = -0.09 \frac{GD}{\mu_v}^{-0.2} \left[x^{1.8} + 5.7 \left[\frac{\mu_L}{\mu_v} \right]^{0.05} (1-x)^{0.47} x^{1.33} \right. \\ \left. \left[\frac{\rho_v}{\rho_L} \right]^{0.261} + 8.11 \left[\frac{\mu_L}{\mu_v} \right]^{0.105} (1-x)^{0.94} x^{0.86} \left[\frac{\rho_v}{\rho_L} \right]^{0.522} \right], \quad (3.52)$$

$$\left[\frac{dP}{dz} \right]_a = \frac{g \sin \theta}{g_o} \left[a \rho_v + (1-a) \rho_L \right] \quad \text{and} \quad (3.53)$$

$$\left[\frac{dP}{dz} \right]_m \frac{g_o D}{G^2 / \rho_v} = -D \left[\frac{dx}{dz} \right] \left[2x + (1-2x) \left[\frac{\rho_v}{\rho_L} \right]^{1/3} + (1-2x) \left[\frac{\rho_v}{\rho_L} \right]^{2/3} \right. \\ \left. - 2(1-x) \left[\frac{\rho_v}{\rho_L} \right] \right]. \quad (3.54)$$

$$\text{Hence,} \quad \left[\frac{dP}{dz} \right] = \left[\frac{dP}{dz} \right]_f + \left[\frac{dP}{dz} \right]_a + \left[\frac{dP}{dz} \right]_m \quad (3.55)$$

Where θ = angle of inclination and also

$$\left[\frac{dP}{dz} \right]_f = -\zeta_o \frac{S}{A_z} \quad (3.56)$$

Where A_z is the cross sectional area and S is the perimeter.

This equation was tested against data obtained by condensing R-12 and R-22 inside 12.5 mm ID 3.7 m long smooth nickel tube. Their data, as well as the data of Akers and

Rosson [3], Altman et al. [7] and Chen [21], agreed within $\pm 10\%$ of the experimental values.

A correlation developed by Abis [22] based on annular film model was verified experimentally by Azer et al. [23] [24]. In all the models described so far the mathematical difficulties were mainly encountered while predicting the thickness of the liquid film. To keep the model simple, the dimensionless temperature drop (t_δ) (which is the result of evaluating the film thickness) across the condensate film is empirically correlated by a simple expression,

$$t_\delta = 3.88 \text{Pr}_L^{0.663} (4.67 - x). \quad (3.57)$$

The heat transfer correlation recommended for annular flow condensation is given by,

$$\text{Nu} = 0.039 \frac{x^{0.9}}{4.67 - x} \left[\frac{\mu_V}{\mu_L} \right] \left[\frac{\rho_L}{\rho_V} \right]^{0.5} \phi_V \text{Pr}_L^{0.337} \text{Re}_V^{0.9}, \quad (3.58)$$

Where, $\text{Re}_V = GD/\mu_V$.

The empirical correlation for the film thickness was obtained by condensing R-12 inside 13 mm ID and 2.4 m long yellow brass tube.

The correlation developed by Traviss et al. [25] is based on a turbulent annular flow model. The velocity distribution in the turbulent liquid film is predicted by Von Karman's universal velocity distribution. The analysis is

similar to the analysis presented by Bae et al. [20], however, by relating the liquid Reynolds number with the normalized film thickness (δ^+) empirically, a simple easy to use equation to evaluate δ^+ is obtained.

The local Nusselt number is given by,

$$\text{Nu} = F(X_{tt}) \frac{\text{Pr}_L \text{Re}_L^{0.9}}{F_2} \quad \text{for } F(X_{tt}) < 2 \quad (3.59)$$

$$\text{and } \text{Nu} = [F(X_{tt})]^{1.15} \frac{\text{Pr}_L \text{Re}_L^{0.9}}{F_2} \quad \text{for } F(X_{tt}) > 2. \quad (3.60)$$

$$\text{Where, } F(X_{tt}) = 0.15[X_{tt}^{-1} + 2.85 X_{tt}^{-0.476}] \quad (3.61)$$

$$\text{and } F_2 = 0.707 \text{Pr}_L \text{Re}_L^{0.5} \quad \text{for } \text{Re}_L < 50, \quad (3.62)$$

$$F_2 = 5 \text{Pr}_L + 5 \ln [1 + \text{Pr}_L(0.09636 \text{Re}_L^{0.585-1})] \\ \text{for } 50 < \text{Re}_L < 1125, \quad (3.63)$$

$$F_2 = 5 \text{Pr}_L + 5 \ln [1+5 \text{Pr}_L]+2.5 \ln[0.00313 \\ \text{Re}_L^{0.812}] \quad \text{for } \text{Re}_L > 1125, \quad (3.64)$$

and X_{tt} is the Martinelli [17] parameter given by Equation 3.25. This correlation was verified by condensing R-12 and R-22 in a copper 8 mm ID 4.4 m horizontal test section. As a result of this verification an empirical correction to the theoretically obtained correlation (Equation 3.59) is made by developing the exponent for $F(X_{tt})$ given in Equation 3.60.

On the basis of a theoretical analysis made by Jaster and Kosky [26], to establish a valid criterion for the flow

transition from the initial annular regime to the final stratified regime, a heat transfer correlation for the transition zone is recommended. A correlation of the transition between annular and stratified flow is made in terms of the stress ratio (F_S) where,

$$F_S = \frac{\text{axial shear force}}{\text{Gravitational body force}} = \frac{\tau_o}{\rho_L g \delta} \\ = \frac{(1 + X_{tt}^{2/N})^{3N/2} \rho_L x^3 G^3 f_{v1}^{3/2}}{2 \sqrt{2} (\rho_v / \rho_L)^{3/2} \mu_L \delta^+ g}, \quad (3.65)$$

$$\delta^+ = \frac{Re_L}{2} \quad \text{if } Re_L \leq 1250, \quad (3.66)$$

$$\delta^+ = 0.0504 Re_L^{0.875} \quad \text{if } Re_L > 1250, \quad (3.67)$$

$$f_{v1} = \frac{0.079}{Re_v^{0.25}} \quad (3.68)$$

$$\tau_o = \frac{\phi_g^2 f_{v1} x^2 G^2}{2 \rho_v} \quad (3.69)$$

$$\phi_g = (1 + X_{tt}^{2/N})^{N/2} \quad \text{and} \quad (3.70)$$

$N =$ a constant between 4 and 5.13.

Experimental observations showed that when F_S was greater than 29 the flow was annular, when between 29 and 5 the flow was in transition and below 5 flow was in a stratified regime.

With these transitional criteria the Nusselt number for annular regime (Nu_{an}) is given as,

$$Nu_{an} = \frac{1}{T^+} \frac{\rho_L D C_{pL} u_*}{k_L} \quad . \quad (3.71)$$

$$\text{Where, } T^+ = \delta^+ \left[\frac{5}{\delta^+} \right]^{H(\delta^+-5)} \left[\text{Pr} + H(\delta^+-5) \ln \left[1 + \text{Pr} \left[\frac{\delta^+}{5} - 1 \right] \right] \right. \\ \left. \left[\frac{5}{\delta^+/5-1} \right]^{H(\delta^+-30)} + H(\delta^+-30) \ln(\delta^+/30) \right] \quad (3.72)$$

in which $H(\delta^+-C)$ is the heaviside unit function defined by,

$$\begin{aligned} H(\delta^+-C) &= 0 & \text{if } \delta^+ < C \\ &= 1 & \text{if } \delta^+ \geq C, \end{aligned} \quad (3.73)$$

Where C is a numerical constant with different values as given in Equation 3.72, and

$$u_* = (\tau_0/\rho_L)^{1/2} \quad . \quad (3.74)$$

The Nusselt number for stratified flow (Nu_{st}) regime is given by,

$$Nu_{st} = 0.725 \left[\frac{\rho_L (\rho_L - \rho_V) h_{fg} g D^3 \alpha^3}{k_L \mu_L \Delta T} \right]^{1/4} \quad (3.75)$$

$$\text{and } \alpha = \frac{1}{1 + \left[\frac{1-x}{x} \right] \left[\frac{\rho_v}{\rho_L} \right]^{2/3}} \quad (3.76)$$

In the transition zone the Nusselt number (Nu_{tr}) is given by,

$$Nu_{tr} = Nu_{an} + \left[\frac{F_s - 29}{24} \right] \left[Nu_{an} - Nu_{st} \right] \quad (3.77)$$

3.3 Correlations Based on Empirical Methods

A dimensionless equation was developed by Cavallini and Zecchin [27]. The dimensionless groups were based on the parameters involved in the annular flow models, similar to models developed by Bae et al. [20] and Traviss et al. [25]. Seven independent dimensionless groups were identified. A statistical correlation (regression analysis) was made with the data obtained by Geodykoontz and Brown [28], Bae et al. [20], Traviss et al. [25], Altman et al. [7] and Cavillini and Zecchin [29]. The following equation was obtained,

$$Nu = 0.038 \left[\frac{\rho_L}{\rho_v} \right]^{0.098} \left[\frac{\mu_v}{\mu_L} \right]^{0.054} \left[\frac{GD}{\mu_L} \right]^{0.84} \left[\frac{C_{pL}(T_v - T_o)}{h_{fg}} \right]^{0.057} \\ \left[1+x \left[\frac{\sqrt{\rho_L} - 1}{\sqrt{\rho_v}} \right] \right]^{0.69} Pr_L^{0.35} \left[\frac{G \cdot \rho_v}{\sqrt{g \sin \theta \cdot D}} \right]^{-0.01} \quad (3.78)$$

Where T_v = vapor temperature and
 T_o = wall temperature.

A close inspection of Equation 3.78 shows that the first, second, fourth and the last groups have negligible influence on the Nu number. Hence,

$$\text{Nu} = 0.0344 \text{Re}^{0.83} (1+x (\sqrt{\rho_L/\rho_V} - 1)^{0.82} \text{Pr}_L^{0.35}) \quad (3.79)$$

A theoretical analysis yielded a correlation of the form,

$$\text{Nu} = 0.05 \text{Re}_e^{0.8} \text{Pr}_L^{0.33} \quad (3.80)$$

$$\text{Where } \text{Re}_e = \text{Re}_v \left[\frac{\mu_v}{\mu_L} \right] \left[\frac{\rho_L}{\rho_v} \right]^{0.5} + \text{Re}_L \quad (3.81)$$

Equation 3.80 correlated the data base within $\pm 30\%$.

An empirical correlation was developed by Shah [30] based on his work on boiling heat transfer and verified by other published data is given below. The deviation from the experimental values was within $\pm 15\%$.

$$\frac{h}{\bar{h}_1} = 1 + 3.8/Z_C^{0.95} \quad (3.82)$$

$$\text{Where } Z_C = (1/x - 1)^{0.8} \text{Pr}^{0.4} \quad (3.83)$$

Pr = reduced pressure, and

$$h_1 = h_L (1-x)^{0.8} \quad (3.84)$$

The single phase heat transfer coefficient (h_L) assumes all the mass to be flowing as liquid and is calculated by the Dittus-Boelter equation,

$$h_L = 0.023 \left[\frac{GD}{\mu_L} \right]^{0.8} Pr_L^{0.4} \frac{k_L}{D} \quad (3.85)$$

Experimental data obtained by Tandon et al. [31], using condensing R-12 and R-22 inside a 10 mm ID tube, were used to modify Akers and Rosson's [3] correlation given by equations (3.2) and (3.3). Tandon et al. [31] found that three correlations recommended by Akers and Rosson [3] could be reduced to two. Further, they found that these correlations to be independent of the liquid Reynold number. These modified correlations are given by,

$$Nu = 0.084 Pr_L^{1/3} \left[\frac{h_{fg}}{C_{pL} \Delta T} \right]^{1/6} Re_v^{2/3} \quad \text{for } Re_v > 3 \times 10^4 \quad \text{and} \quad (3.86)$$

$$Nu = 23.1 Pr_L^{1/3} \left[\frac{h_{fg}}{C_{pL} \Delta T} \right]^{1/6} Re_v^{1/8} \quad \text{for } Re_v < 3 \times 10^4. \quad (3.87)$$

Equations (3.2) and (3.3) were developed on a laminar flow model, however, Tandon et al. [31] found that with a change in the numerical coefficients of the two Akers and Rosson's [3] equations discussed above the entire condensation data in the condenser agreed within $\pm 20\%$. The Akers et al. [6] correlations for annular flow (equation (3.4) and (3.5)) were

not required to correlate the experimental data. Hence, the number of correlating equations has been reduced to two and the limiting value of Re_v for the two laminar film correlations is shifted from 2×10^4 (as given by Akers and Rosson [3]) to 3×10^4 .

All theoretical and empirical correlations considered were models applicable to annular flow, stratified flow or for the transition zone between annular and stratified flows. These correlations when applied for mist flow regime, which is characterized by high entrainment and breakdown of a continuous liquid film, results in wide discrepancies between measurements and predictions. Hence, Soliman [32] developed a correlation based on published data for condensation within the mist regime. The underlying assumption of this correlation is that the vapor phase and the bulk of the liquid phase are flowing in a form of homogeneous mixture. This assumption is supported by visual observations made by a number of authors. The liquid phase is found in droplet form during the flow regime, as a result, the single phase turbulent flow correlation for heat transfer is used, which is as follows:

$$Nu = C Re^{0.875} Pr^{1/3} \quad (3.88)$$

The above correlation results from momentum and heat transfer analysis. In order to obtain a suitable Reynolds number to represent the homogeneous mixture (Re_m) of vapor and liquid droplets, it is defined as,

$$Re_m = GD/\mu_m \quad (3.89)$$

$$\text{Where, } 1/\mu_m = x/\mu_v + (1-x)/\mu_L \quad (3.90)$$

The final form of the equation was determined empirically. The Nusselt number for mist flow is given by,

$$Nu = 0.00345 Re_m^{0.9} \left[\frac{\mu_v h_{fg}}{k_v \Delta T} \right]^{1/3}, \text{ for } We > 35. \quad (3.91)$$

Where, We = Weber number

$$We = 0.85 Re_v^{0.79} \left[\frac{\mu_v}{\rho_v \sigma D} \right]^{0.3} \left[\frac{\mu_v}{\mu_L} \right]^2 \left[\frac{\rho_L}{\rho_v} \right]^{0.084} \left[\frac{x_{tt}}{\phi_v^{2.55}} \right]^{0.157} \text{ for } Re_L > 1250, \quad (3.92)$$

$$\text{and } We = 2.45 \frac{Re_v^{0.64}}{\phi_v^{0.4}} \left[\frac{\mu_v}{\rho_v \sigma D} \right]^{0.3} \text{ for } Re_L \leq 1250 \quad (3.93)$$

Where σ = surface tension, N/m.

This correlation was best suited for We greater than 35. The

empirical constants were determined based on five data sets using steam, R-113 and R-12 as condensing fluids and is only applicable for the mist flow regime.

The review of literature on condensation heat transfer revealed that each correlation is unique to one flow regime. Therefore, it is important that such correlations be applied only to cases falling into that regime. This implies that the designer should first determine the flow regime existing at each point along the condenser and choose an appropriate correlation. Consequently, the designer requires reliable criteria to establish the flow regimes under a given condition. The following chapter briefly discusses few flow regime criteria.

CHAPTER 4

DEVELOPMENT OF DESIGN PROCEDURE

There is complete agreement among research workers, engaged in condensation heat transfer, that the determination of flow regimes must be part of the selection of a heat transfer model. Hence, from a designer's point of view, the understanding of the hydrodynamic behaviour of two-phase flow is important and necessary for achieving improved design of equipment in which such flows occur.

4.1 Flow Regime Concept

Several extensive research projects dealing with two-phase, two component (gas-liquid), adiabatic flow are reported in the literature. These investigations result in information about flow patterns, phase distributions, and pressure drops associated with the flow. However, the study of two-phase, one component flows with heat transfer has been thoroughly researched but not methodically documented. This type of flow includes both boiling and condensation cases. When heat transfer is associated with the flow it causes phase changes and changes in phase distribution along the flow passage. Consequently, the flow pattern never becomes fully developed and it changes continuously in the direction of flow.

The term flow pattern describes the different configurations which appear during two phase flow. The type of flow pattern existing at a certain location within a tube depends on mass flow rates of the two phases, physical and transport properties, and tube diameter and orientation. During adiabatic gas-liquid flows the flow pattern does not change between the inlet and outlet of the duct, while for diabatic flows the pattern changes continuously in the direction of the flow due to the interdependence of heat transfer and local flow conditions.

To determine the flow patterns existing under a given design condition there are a number of two-phase diabatic flow maps available in the literature. In order to select a simple, accurate and easy to use flow map a brief survey of these maps is included.

The graphical representation of flow patterns using a coordinate system is called a flow map. For example a flow map developed by Baker [33] is given in Fig. 4.1. In developing such flow maps flow pattern observations are plotted on the flow map. Transition lines between different areas are then drawn arbitrarily. These lines represent a transition zone rather than an abrupt change of flow patterns.

In 1954 Baker [33] developed a flow map for adiabatic two-phase flows in horizontal tubes. He used data produced by investigators which covers a wide range of tube diameters

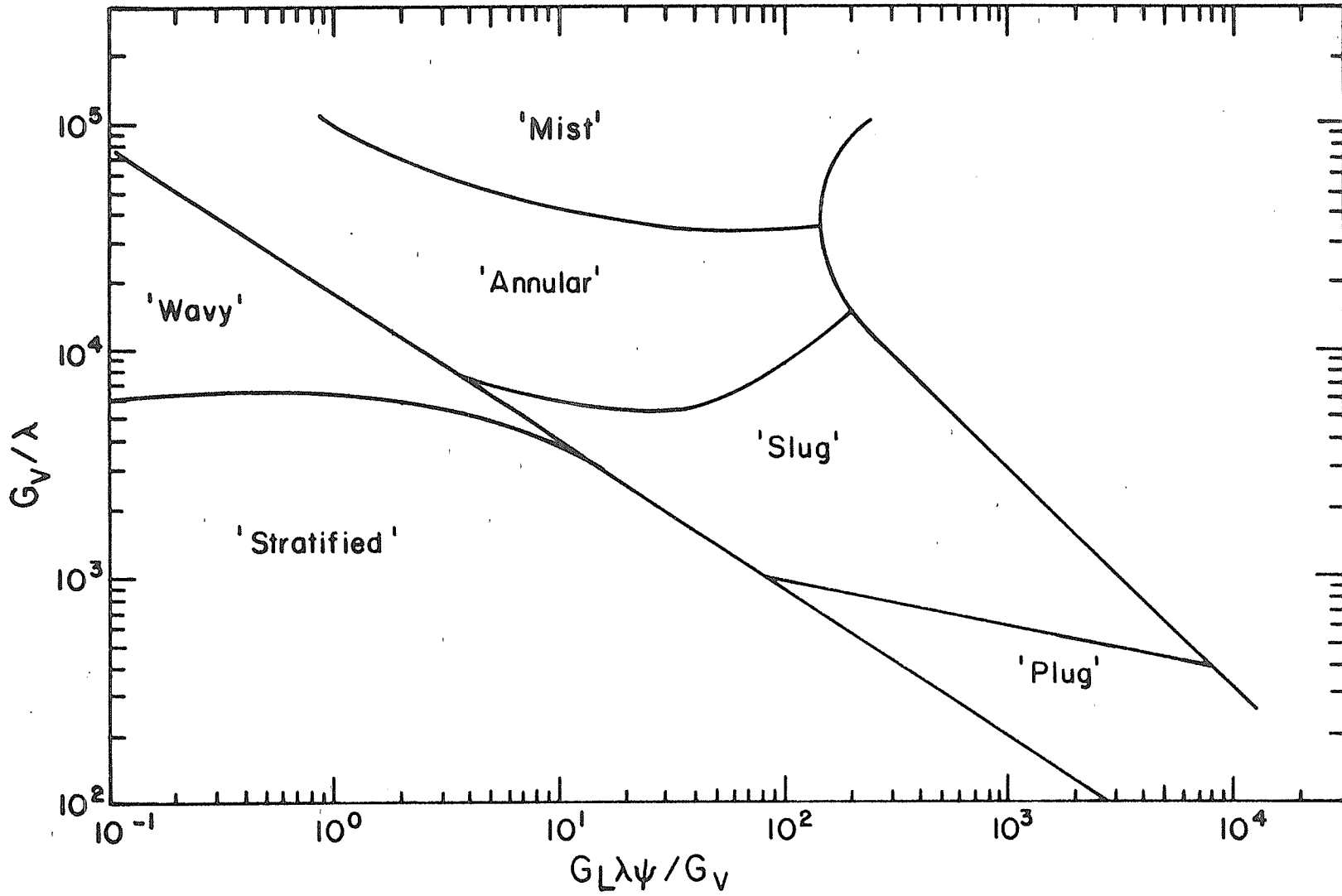


Fig. 4.1 Typical flow map developed by Baker [33]

and gas-liquid combinations in preparing a flow map using coordinates which are functions of the superficial mass velocities G_V and G_L . He used the following correlating factors to account for the physical properties of the flowing mixture.

$$\psi = \frac{\sigma_{\text{water}}}{\sigma} \left[\mu_L \left[\frac{\rho_{\text{water}}}{\rho_L} \right]^2 \right]^{1/3} \quad (4.1)$$

$$\lambda = [(\rho_V / \rho_{\text{air}}) (\rho_L / \rho_{\text{water}})]^{1/2} \quad (4.2)$$

There are several drawbacks with this map (i.e. the numerical constants in the correlating factors ψ and λ add nothing but make calculations difficult) which have been pointed out by others, but it has gained acceptance because of the wide base of experimental data covered especially in adiabatic flows. Isbin [34] found Baker's [33] map reasonably accurate if used for a steam-water mixture at high pressures. Scott [35] modified Baker's [33] map by converting the line boundaries into zones. This modified Baker's map was found by Traviss and Rohsenow [36] to agree well with condensation flow regimes observed in small diameter tubes. The same research workers found that condensation data developed by Soliman and Azer [37] agreed with the modified Baker's map when certain flow regimes were regrouped.

Flow regime parameters developed by Quandt [38] were based on order of magnitude analysis for adiabatic flows. He

postulated that two-phase configurations of each flow regime is dominated by the fundamental forces influencing flow regimes. The fundamental forces are: pressure gradient, gravitational acceleration and interfacial surface tension. The transition of flow from one configuration to the other was related to numerical values of the dimensionless Froude (Fr) and Weber (We) numbers. Fr is the ratio of inertia force to gravity forces whereas We is the ratio of inertia to surface tension forces.

After comparing the boundaries of observed flow patterns with derived analytical criteria, Quandt [38] observed that, bubble, dispersed (mist) and annular flow patterns were in fact subclasses of a pressure gradient controlled flow. The flow patterns identified as slug, wave, stratified and falling film were subclasses of a gravity controlled phenomena. Consequently, he devised three major flow regimes in his map; namely dispersed, annular and wavy.

The flow map, developed by Baker [33] for adiabatic flow, was found to be inadequate by Soliman and Azer [37] to predict the flow patterns during condensation. As a result, they developed a new flow map using Froude number

$$Fr = (V_V + V_L)^2 / gD \quad (4.3)$$

with gas volumetric ratio (R)

$$R = Q_V / (Q_V + Q_L) \quad (4.4)$$

as coordinates.

Where,

V_V = superficial vapor velocity,

V_L = superficial liquid velocity,

Q_V = Vapor volume flow rate and

Q_L = liquid volume flow rate.

The determination of flow regimes to predict condensing heat transfer coefficients inside horizontal tubes was given further consideration by Breber et al [39]. They found that the theoretically obtained parameters proposed by Taitel and Dukler [40] were a good characterization of the condensation flow regimes. A transitional criterion to determine whether the flow is shear controlled (annular flow) or gravity controlled (wavy flow) was used. Therefore, the map developed by Taitel and Dukler [40] used the ratio of shear force to gravity force (K) as ordinate and Martinelli [17] parameter (X_{tt} Equation 3.61) as abscissa. The parameter j_g^* , the dimensionless gas velocity defined by Wallis [41], was used to relate the ratio of shear force to gravity force.

$$j_g^* = \frac{Gx}{[\rho_V(\rho_L - \rho_V)Dg]^{1/2}}$$

which can also be expressed as

$$j_g^* = \left[\frac{G}{[\rho_V(\rho_L - \rho_V)Dg]^{1/2}} \right] \left[\frac{k_p}{X_{tt}^{1.11} + k_p} \right] \quad (4.5)$$

Where, G = Total mass velocity and

$$k_p = (\rho_v/\rho_L)^{0.555} (\mu_L/\mu_v)^{0.111} \quad (4.6)$$

The ordinate of the map is defined by,

$$K = (j_g^*)(Re_L)^{1/2} \quad (4.7)$$

Simple, easy to use, and reasonably accurate transition criteria were proposed by Soliman [42] [43]. Criteria was developed from the Fr and a modified We . It was hypothesized that the transition from annular flow to wavy flow occurred at a constant Fr irrespective of the tube diameter or the type of condensing fluid. Soliman [42] showed that the results when correlated by these parameters predicted the transition more consistently and accurately than the correlations proposed by Weisman et al. [44], Taitel and Dukler [40] and Mandhane et al. [45]. Soliman [43] also observed that the inertia force of the gaseous phase was dominant in maintaining mist flow, while the major stabilizing forces, inducing the liquid film to form, were the surface tension and liquid viscous forces. The transition from mist flow to annular was theorized to occur when the stabilizing forces exceeded the destabilizing effect of the inertia forces. Similarly, the annular to wavy flow transition, inside horizontal tubes, was observed to occur when the gravity forces exceeded the inertia forces. Hence, the regime of flow under a given set of flow conditions is obtained from the following relationships.

i) Mist to Annular:

The We is obtained from Equations 3.92 or 3.93 for the flow under consideration, The transition from mist to annular flow occurs between a We of 30 to 20. For We's greater than 30 the flow is mist and for We less than 20 the flow is annular.

ii) Annular to Wavy:

The Fr is obtained from the following relationship:

$$Fr = 0.024 \left[\frac{G(1-x)D}{\mu_L} \right]^{1.6} \left[\frac{\mu_L^2}{gD^3 \rho_L^2} \right]^{0.5} \left[\frac{\phi_v}{X_{tt}} \right]^{1.5} \text{ for } Re_L \leq 1250 \text{ and} \quad (4.8)$$

$$Fr = 1.28 \left[\frac{G(1-x)D}{\mu_L} \right]^{1.04} \left[\frac{\mu_L^2}{gD^3 \rho_L^2} \right]^{0.5} \left[\frac{\phi_v}{X_{tt}} \right]^{1.5} \text{ for } Re_L > 1250 . \quad (4.9)$$

Where $\phi_v = 1 + 1.09 X_{tt}^{0.039}$.

It was found that the transition from annular to wavy flow occurred at Fr of approximately seven. When Fr is lower than seven the flow was wavy.

From the foregone discussion it is clear that two phase flow transition criteria for diabatic flows are arbitrary.

There are no defined criteria to determine transitions from one flow regime to another. Nevertheless criteria based on fundamental physical phenomena are gaining attention. Therefore, based on the range of variables encountered, and on the ease of applying, this study was performed using Soliman's [42] [43] transitional criteria. The heat transfer correlations available from the literature review (Chapter 3) are based on three main flow patterns, namely,

- i) mist or dispersed flow (example Soliman's [32] correlation),
- ii) annular flow models (example Traviss et al. [25], Akers and Rosson [3], etc.) and
- iii) wavy or stratified flow models (example Rosson and Myers [16]).

Hence, it is logical to divide the flow patterns in the same manner. Soliman's [42] [43] transitional criteria offer a straight forward method to demarcate these three flow regimes. Whereas the other transitional criteria like Baker's [33] require a map in order to determine the flow regimes.

4.2 Creation of a Heat Transfer Data Base

A number of workers (Shah [30], Bell [46] and others) have cautioned against the use of correlations developed for halocarbon refrigerants to predict steam condensation and vice versa. This is because the thermal properties of

halocarbon compounds differ greatly from steam. However, there are few correlations which have been tested with both fluids and are found to be equally applicable to halocarbon and steam condensation.

For convenience, condensation correlations suitable for practical day to day engineering design should be applicable to both groups of fluids. Hence, a data base was chosen to represent aqueous and halocarbon fluids.

The data base selected for this study is given in Table 4.1. It is comprised of four sets of data published in the literature. Two of the data sets used steam as test fluid and the remaining two used Freon-12. The data set No. 3 is mostly mist and data set No. 4 is mostly annular flow. Set No. 1 covers mist and annular flow data equally. The second data set consists of only annular flow but because the condenser tube was oriented vertically for the data sets 1 and 2, the flow regimes were either mist or annular. Therefore, only the mist flow to annular flow transition criteria was applied to the first two data sets (1 and 2). Data sets 3 and 4 were developed during horizontal in-tube condensation. Hence, both, mist to annular and annular to wavy, transition criteria were used. Because all three flow regimes are represented, it is expected to simulate the situations encountered in an actual application. However, it must be emphasized that this data base does not cover the entire range of parameters likely to be encountered in all

TABLE 4.1
HEAT TRANSFER DATA BASE

Data Set No.	Inside Tube Dia. mm	Tube Orientation	Condensing Fluid	Saturation Temperature °C	Mass Flux, G kg/m ² .s	Quality	Modified Weber Number	Froude Number	liquid Prandtl Number	T Wall °C	Source
1.	7.4	V	Steam	85.8-121.9	88.1-456.1	0.99-0.011	78.6-3.68	--	1.3-2.3	69.7-6.3	Goodykoontz & Dorsch [47]
2.	15.9	V	Steam	108.9-134.4	21.6- 74.5	0.99-0.06	19.36-2.68	--	1.26-1.6	64.6-12.3	Goodykoontz & Dorsch [48]
3.	8.0	H	R-12	25.7-58.3	263.8-1533.5	0.944-0.068	89.88-5.98	234-0.99	3.0-3.3	11.3-2.8	Traviss [49]
4.	12.7	H	R-12	32.7-54.6	135.7-446.6	0.97-0.22	45.44-15.0	71-3.82	3.1-3.2	30.8-6.3	Azer, Abis, & Swearingen [23]

applications. As such, the results obtained limit the applicability to the range of parameters specified in the data base. Since the number of data points available in the wavy flow regime is limited the correlations selected for this regime requires additional verification.

Data sets 1, 2 and 3 provided measured saturation temperatures whereas data set 4 provided vapor temperatures at different locations along the condenser. Therefore, an arithmetic average of these temperatures was used as the saturation temperature for calculations. All data sets consisted of a number of runs with local measurements (inner wall temperature, coolant temperature, static pressure, etc.) made axially along the condenser. Along with the point measurements, calculated values such as quality, heat flow rate, local heat transfer coefficient, temperature drop across the liquid film, etc. were also given.

4.3 Assessment of Correlations with the Data Base

A total of 96 test runs were available from the four data sets given in Table 4.1. Over 600 data points were obtained from the 96 published test runs which formed the data base. With the saturation temperatures given for each run (except data set 4 where an average vapor temperature was used) the thermophysical and transport properties of Freon-12 were obtained from ASHRAE Handbook of Fundamentals [2]. Similarly the steam properties were obtained from the ASME

steam tables [50].

Seven correlations were selected for the assessment from the eighteen correlations discussed in Chapter 3. Laminar flow of liquids is seldom encountered (Bell [46] and Carpenter [12]) in the majority of industrial applications since high mass flow rates are normally used. Therefore, all laminar flow models (Nusselt [4], Kern [10], Chaddock [11] and Akers and Rosson [3]) were not selected for the assessment. All correlations, except those recommended by ASHRAE [2] and, Rosson and Myers [16], as reviewed by Bell [46] in a similar assessment were not included. Rosson and Myers [16] correlation was included because of its special theoretical treatment of the wavy flow regime. All other correlations applicable to the wavy flow regime were either correlations developed for a laminar flow model (Jaster and Kosky [26]) or empirical modifications of an annular flow model (Kern [10]) subsequently extended for wavy flow regimes. The Altman et al. [7] correlation, although recommended by ASHRAE [2] for Freon-22, was not included because of its narrow data base. Similarly correlations recommended by Rohsenow [14], Soliman et al. [19], Bae et al. [20], Jaster and Kosky [26] and Cavallini and Zecchin [27] were not included due to their narrow data base support. Hence, the following seven correlations were selected for the assessment:

- i) Soliman's [32] Equation 3.91,

- ii) Tandon et al. [31] Equations 3.86 and 3.87,
- iii) Shah's [30] Equation 3.82,
- iv) Traviss et al. [25] Equations 3.59 and 3.60,
- v) Azer et al. [23] Equation 3.58,
- vi) Rosson and Myers [16] Equation 3.29 and
- vii) Akers et al. [6] Equations 3.4 and 3.5.

A computer program in BASIC language was developed to calculate the transitional criteria (given by Equations 3.92, 3.93, 4.8 and 4.9) and the heat transfer coefficients predicted by the above mentioned correlations with the fluid properties, quality, and the temperature drop across the film as inputs.

Data points yielding a modified We greater than 30 were categorized as mist flow and there were 285 points within this regime among the total of the 616 data points evaluated. All data points with a modified We below 30 and a Fr greater than or equal to seven, for horizontal condensers, were considered to be in annular flow regime. In case of vertical tube condensation all data points with a We below 30 were considered to be in the annular flow regime. There were 312 data points falling within the annular flow regime in both horizontal (43) and vertical (269) tube condensation. The rest of the points, 18 in number, belonged to the wavy flow regime. Table 4.2 gives the percentages and the actual number (given within parenthesis) of calculated heat transfer

TABLE 4.2
 NUMBER OF CALCULATED HEAT TRANSFER COEFFICIENTS FALLING WITHIN $\pm 30\%$
 OF THE HEAT TRANSFER COEFFICIENT FOUND EXPERIMENTALLY

Serial No.	Correlation by	Data Set No. 1 & 2 Steam Condensing Inside Vertical Tube		Data Set No. 3 R-12 Condensing Inside Horizontal Tube			Data Set No. 4 R-12 Condensing Inside Horizontal Tube		
		Mist Flow Regime 100% (162)*	Annular Flow Regime 100% (269)	Mist Flow Regime 100% (61)	Annual Flow Regime 100% (22)	Wavy Flow Regime 100% (12)	Mist Flow Regime 100% (62)	Annular Flow Regime 100% (21)	Wavy Flow Regime 100% (6)
1	Soliman [32]	48.2 (78)	27.5 (74)	93.4 (57)	86.4 (19)	0 (0)	61.3 (38)	81 (17)	67 (4)
2	Tandon et al. [31]	77.8 (126)	61 (165)	1.6 (1)	18 (4)	50 (6)	48.4 (30)	48 (10)	17 (1)
3	Shah [30]	70.4 (114)	55 (149)	75.4 (46)	86.4 (19)	67 (8)	50 (31)	62 (13)	67 (4)
4	Traviss et al. [25]	1.2 (2)	11 (30)	98.4 (60)	91 (20)	67 (8)	32.3 (20)	43 (9)	0 (0)
5	Azer et al. [23]	0 (0)	22 (59)	90.2 (55)	64 (14)	0 (0)	45.1 (28)	62 (13)	83 (5)
6	Akers et al. [6]	64.2 (104)	48 (129)	0 (0)	36 (8)	100 (12)	48.4 (30)	52 (11)	83 (5)
7	Rosson and Myers [16]	11.7 (19)	13.8 (37)	0 (0)	4.6 (1)	42 (5)	30.7 (19)	52 (11)	67 (4)

* Figures within parenthesis indicate the actual number of data points.

coefficients falling within $\pm 30\%$ of the heat transfer coefficient found experimentally.

As a first step in assessing the correlations, the predicted heat transfer coefficients were checked as follows.

The calculated heat transfer coefficients using Traviss et al. [25] correlation were checked against his own data. Table 4.3 compares Traviss et al. [25] correlation with his own data set [49] for all three flow regimes.

Table 4.3

Comparison of Traviss et al. [25] Correlation With
Traviss's [49] Data

Flow Regime	Number of Calculated Heat Transfer Coefficients Falling Within $\pm 30\%$ of the Experimental Value		Total Number of Data Points
Mist	60	(98.4%)	61
Annular	20	(91%)	22
Wavy	8	(67%)	12
Overall	88	(92.6%)	95

Approximately 92% of the heat transfer coefficients calculated using Traviss et al. [25] formula agreed within $\pm 30\%$ of the experimentally determined heat transfer coefficients. This is in agreement with the results reported

by Traviss et al. [25]. A similar comparison was made with Azer et al. [23] correlation. Table 4.4 compares Azer et al. [23] correlation with his own data. Only 51% of the calculated heat transfer coefficients agree with the experimental values (within $\pm 30\%$). A similar observation was made by Tandon et al. [31] where Azer et al. [23] correlation failed to predict their own data. The reason given by Tandon et al. [31] for this failure was the property values used by Azer et al. [23]. Tandon et al. [31] indicated that the property values used in calculation were obtained from ASHRAE Handbook of Fundamentals 1967.

Table 4.4
Comparison of Azer et al. [23] Correlation With
Azer's [23] Data

Flow Regime	Number of Calculated Heat Transfer Coefficients Falling Within $\pm 30\%$ of the Experimental Value		Total Number of Data Points
Mist	28	(41.5%)	62
Annular	13	(62%)	21
Wavy	5	(83%)	6
Overall	46	(51.7%)	89

The analysis of the present work was based on ASHRAE Handbook of Fundamentals 1985 [2]. The property values given in 1967

issue of ASHRAE Handbook Fundamentals were revised in 1977 issue of ASHRAE Handbook of Fundamentals. The same revised property values are reported in 1985 issue of ASHRAE Handbook of Fundamentals used for this study. A comparison was made between the 1967 and 1977 property values. Table 4.5 shows the percentage deviations of dynamic viscosity of Freon-12 between 1967 and the revised 1977 ASHRAE values.

For Freon-12 the ratio of liquid to vapor dynamic viscosity deviates up to 50% at temperatures normally encountered in condensers (90°C). There were no significant change of other property values (specific heat, thermal conductivity, density, enthalpy and entropy) between those reported in 1977 and the values contained in the 1967 ASHRAE Handbook of Fundamental. The data points given in Azer et al. [23] publication were recalculated with the dynamic viscosity values reported in ASHRAE Handbook of Fundamentals 1967. Table 4.6 shows that approximately 76% of the calculated data points to be within $\pm 30\%$ of the heat transfer coefficient determined experimentally.

Hence, Azer et al.'s [23] correlation requires modification using the revised dynamic viscosity values.

TABLE 4.5
 COMPARISON OF THERMOPHYSICAL PROPERTIES OF R-12 REPORTED IN
 1967 AND 1977 ASHRAE HANDBOOKS

Temp- erature F	μ_L 1977 lb/ft.hr	μ_L^* 1967 lb/ft.hr	% Deviation	μ_V 1977 lb/ft.hr	μ_V^* 1967 lb/ft.hr	% Deviation	% Deviation [μ_L/μ_V] 1977 [μ_L/μ_V] 1967
-40	0.99	1.024	3.3	--	0.0257	--	--
-20	0.866	0.898	3.6	0.0249	0.0264	6.0	2.3
0	0.767	0.811	5.4	0.0265	0.0274	3.4	-2.2
20	0.687	0.746	7.9	0.0279	0.0281	0.7	-11.3
40	0.62	0.692	10.5	0.0291	0.0288	-1.0	-14.2
60	0.564	0.651	13.4	0.0301	0.0298	-1.0	-14.2
80	0.517	0.617	16.3	0.0311	0.0310	-0.3	-17.8
100	0.477	0.586	18.6	0.0324	0.0312	-3.7	-21.6
120	0.441	0.562	21.5	0.0339	0.0320	-5.7	-26.0
140	0.409	0.538	23.9	0.0359	0.0327	-8.9	-30.8
160	0.307	0.518	40.8	0.0384	0.0334	-13.0	-40.7
180	0.329	0.501	34.4	0.0417	0.0339	-18.7	-46.6
200	0.273	0.484	43.6	0.0458	0.0346	-24.5	-57.4

* Values reported in centipoise

An analysis conducted on the data revealed that if the correlation is modified as follows:

$$\text{Nu} = 0.032 \frac{x^{0.9}}{4.67 - x} \left[\frac{\mu_V}{\mu_L} \right] \left[\frac{\rho_L}{\rho_V} \right]^{0.5} \phi_V \text{Pr}_L^{0.337} \text{Re}_V^{0.9} \quad (4.10)$$

Table 4.6

Comparison of Azer et al. [23] correlation using μ values Reported in ASHRAE Handbook of Fundamentals 1967 with the Data of Azer et al. [23].

Flow Regime	Number of Calculated Heat Transfer Coefficients Falling Within +30% of the Experimental Value		Total Number of Data Points
Mist	46	(74.2%)	62
Annular	18	(85.7%)	21
Wavy	4	(66.6%)	6
Overall	68	(76.4%)	89

the accuracy could be restored back to the accuracy claimed by using 1967 ASHRAE property values. Fig. 4.2 shows the modified correlation with the original correlation using 1967 and 1977 ASHRAE property values for Run No. 6 of Azer et al. [23] data.

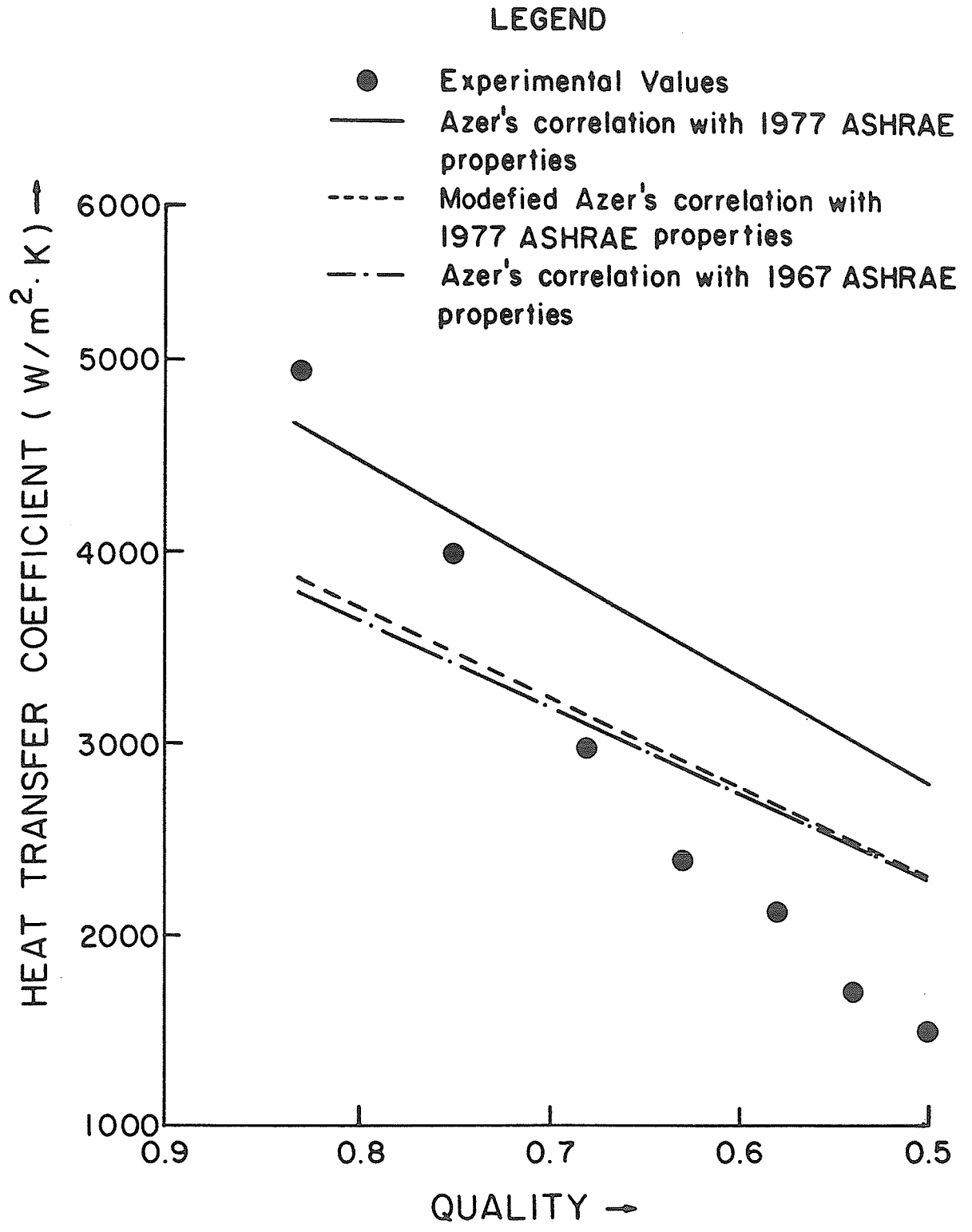


Fig. 4.2 Comparison of Azer et al. [23] correlation with his data Run No. 6 using 1967 and 1977 ASHRAE transport property values

Tandon et al. [31] used Azer et al. [23] data to verify their correlation. Table 4.7 shows the analysis of the present work.

Table 4.7
Comparison of Tandon et al. [31] Correlation with
Azer et al. [23] Data

Flow Regime	Number of Calculated Heat Transfer Coefficients Falling Within +30% of the Experimental Value	Total Number of Data Points
Mist	30 (48.4%)	62
Annular	10 (48%)	21
Wavy	1 (17%)	6
Overall	41 (46%)	89

Tandon et al. [31] correlation agreed with 46% of the data points of Azer et al. [23]. This is in good agreement with his results.

4.4 Selection of Correlations

The selection of correlation for the three flow regimes defined by Soliman's [42] [43] correlation is made on the basis of the percentage of experimental data points that fall within $\pm 30\%$ of each of the seven correlations selected for this study. That is, if the experimentally determined condensation heat transfer coefficients agree within $\pm 30\%$ of the correlating formulae it was deemed satisfactory. Table 4.8 gives the number of data points predicting the

TABLE 4.8

COMPARISON OF CORRELATIONS WITHIN THE THREE FLOW REGIMES

Serial No.	Correlation	Number of calculated heat transfer coefficients falling within +30% of the experimental heat transfer coefficients (reported as a percentage of the data points within a flow regime).		
		Mist Flow Regime 100% (285)*	Annular Flow Regime 100% (312)	Wavy Flow Regime 100% (18)
1	Soliman [32]	61 (173)	35 (110)	22 (4)
2	Tandon <u>et al.</u> [31]	55 (157)	57 (179)	39 (7)
3	Shah [30]	67 (191)	58 (181)	67 (12)
4	Traviss <u>et al.</u> [25]	29 (82)	19 (59)	44 (8)
5	Azer <u>et al.</u> [23]	29 (83)	28 (86)	28 (5)
6	Akers <u>et al.</u> [6]	47 (134)	47 (148)	94 (17)
7	Rosson and Myers [16]	13 (38)	16 (49)	50 (9)

* Figures within the parenthesis indicate the actual number of data points.

condensation correlation, within the limits of accuracy stipulated above, for all seven correlations.

4.4.1 Mist Flow Regime

The mist flow regime is characterized by very high heat transfer coefficients. In this regime high vapor mass velocities interrupt the continuity of the liquid condensate film and therefore the effective heat transfer coefficient is increased. Since the condensation mechanism within the regime deviates considerably from the annular model, correlations based on this models do not predict what is happening in this regime. This is shown clearly by Figs. 4.3 to 4.9. Except Soliman's [32] and Shah's [30] correlation, all other correlations can not be used within this regime. However, correlations developed on the basis of a particular data set predicted satisfactory experimental results even in the mist flow regime of the same data set. For example, Traviss et al. [25] correlation (Fig. 4.3) covers approximately 98% of the experimental points, within the mist flow regime of his data set. Fig. 4.3 shows that Traviss et al. [25] correlation to be less accurate in predicting other data sets.

Akers et al. [6], Rosson and Myer's [16] and Tandon et al. [31] correlations generally predicted lower than the experimental heat transfer coefficient within this regime. The accuracy of Tandon et al. [31] and Akers et al. [6]

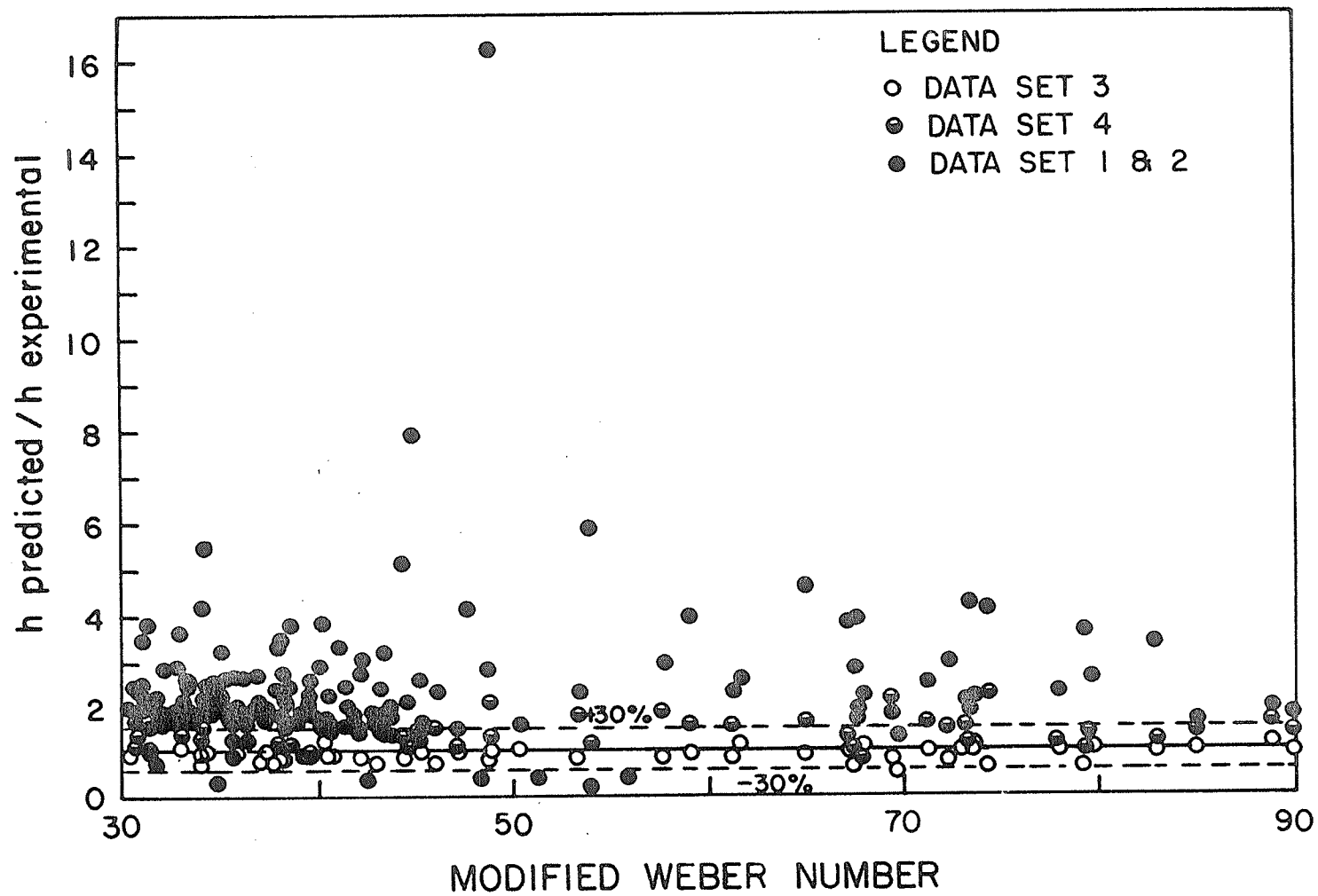


Fig. 4.3 Comparison of mist flow data with Traviss et al. [25] correlation

correlation improve slightly for steam below a modified We of about 40. Both of these correlations produce almost identical results within mist flow regime.

The accuracy of Azer et al. [23] correlation is low (Fig. 4.4) within the mist flow regime. The correlation was developed on the basis of an annular flow model and therefore in high quality regions the experimental values are lower than the correlation would predict. This fact can be clearly seen in Fig. 4.2 where the curve fits are low for experimental values at qualities above 0.68. Azer et al. [23] correlation gives one and a half to three times higher heat transfer coefficients for steam. Hence, this correlation is inappropriate for steam in the mist flow regime.

Within the mist flow regime 67% of the data points are correlated (within $\pm 30\%$) by Shah's [30] formula (Table 4.8), whereas 61% of the experimental points are within $\pm 30\%$ of Soliman's [32] correlation. However, comparing Figs. 4.5 and 4.6 show that Soliman's [32] correlation improves the accuracy at high modified We's. Therefore the number of data points, within the limits of accuracy, were determined again for modified We's greater than 40. When the data points above 40 were considered on a modified We scale (Table 4.9) the accuracy of Soliman's [32] correlation improved (78%) whereas Shah's [30] correlation dropped (68%).

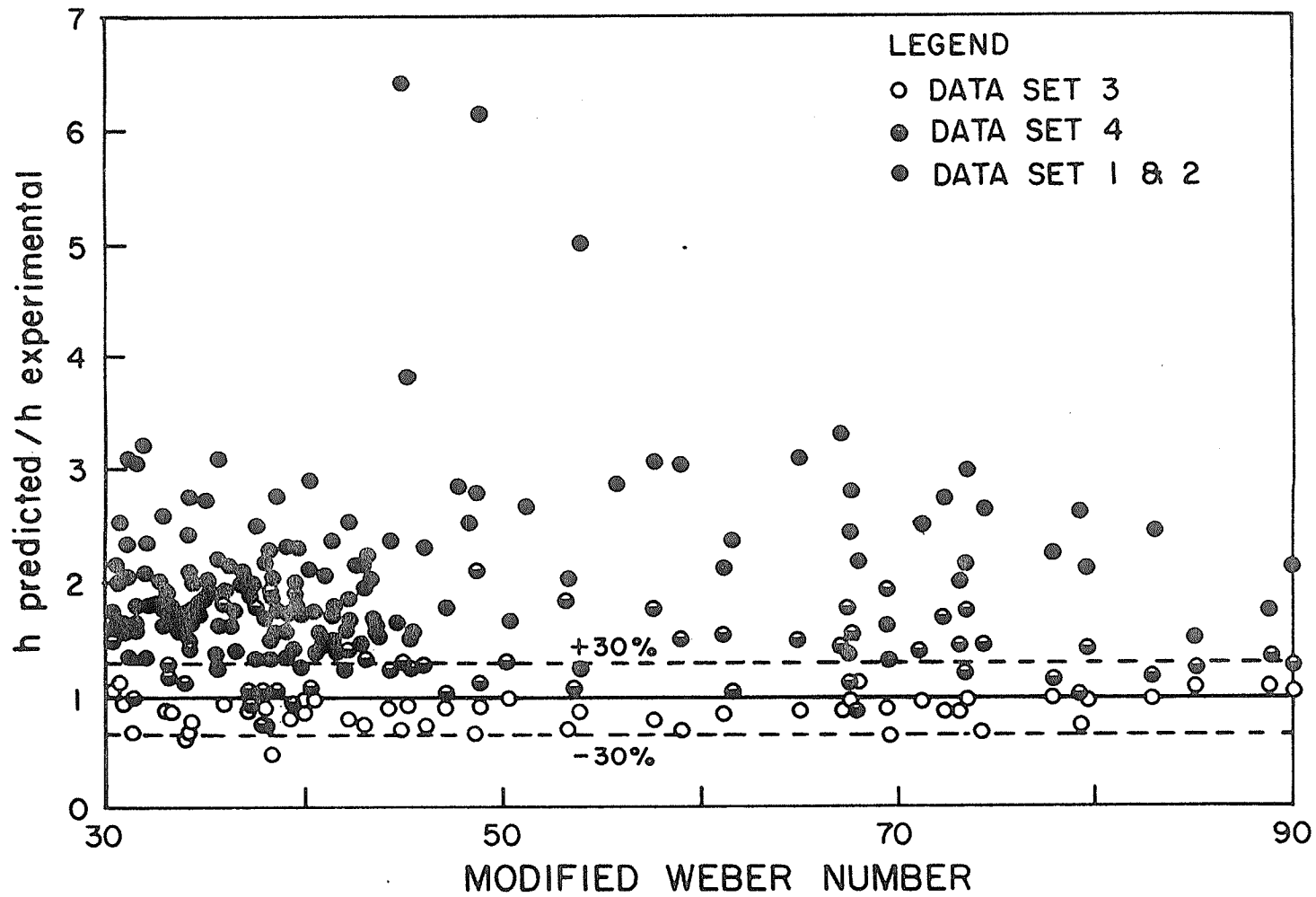


Fig. 4.4 Comparison of mist flow data with Azer et al. [23] correlation

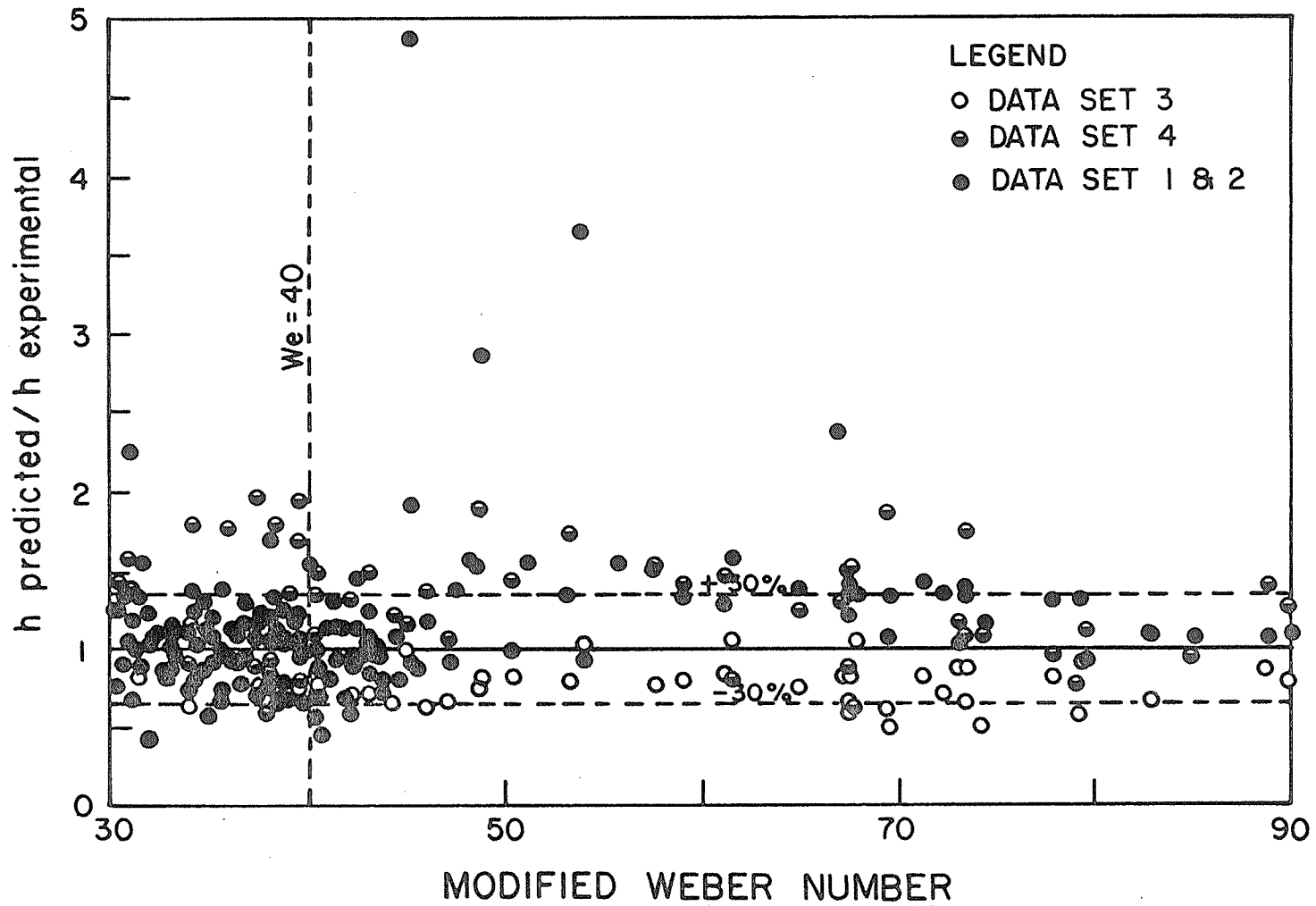


Fig. 4.5 Comparison of mist flow data with Shah's [30] correlation

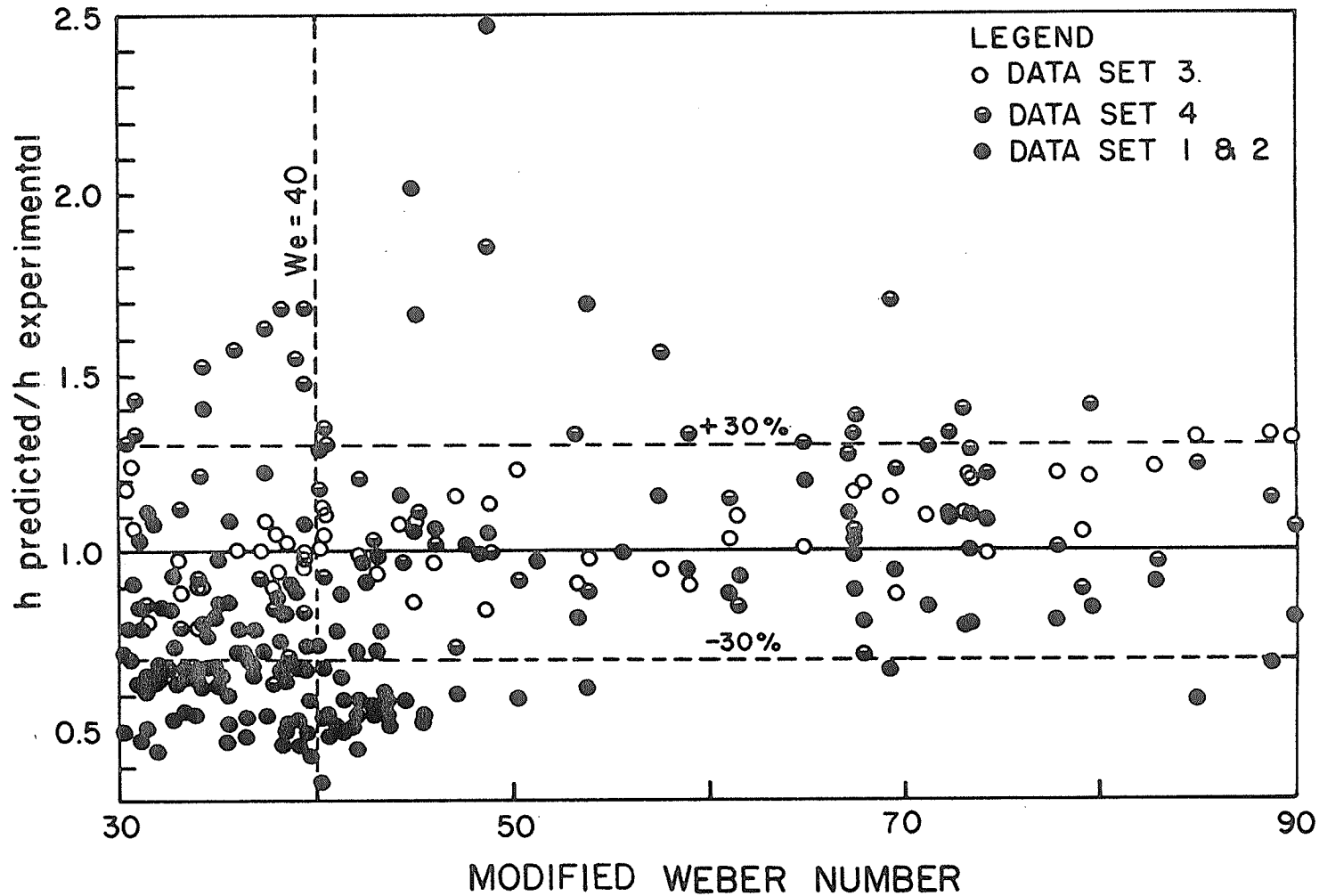


Fig. 4.6 Comparison of mist flow data with Soliman's [32] correlation

Table 4.9

Comparison of Soliman's [32] Correlation With Shah's [30]
Correlation for Flows with a We Greater Than 40

Data Set No.		Percentages of points within $\pm 30\%$ of Experimental Value	
		Soliman's [32]	Shah's [30]
1 and 2	100% (76)	71 (54)	66 (50)
3	100% (41)	93 (38)	73 (30)
4	100% (26)	73 (19)	65 (17)
Overall	100% (143)	78 (111)	68 (97)

Soliman's [32] correlation provides acceptable results for both steam (71%) and Freon-12 (85%) condensation, compared to 66 and 70% for Shah's [30] correlation for the steam and Freon-12 respectively. This implies that Soliman's [32] correlation is more generally acceptable.

Soliman's [32] correlation was selected for use in the mist flow regime defined by the modified We greater than 40 for non-aqueous and aqueous fluids. This correlation is not appropriate for use below a modified We of 40.

In reviewing the literature it was stated that Traviss et al. [25] used an empirical exponent on the factor $F(X_{tt})$

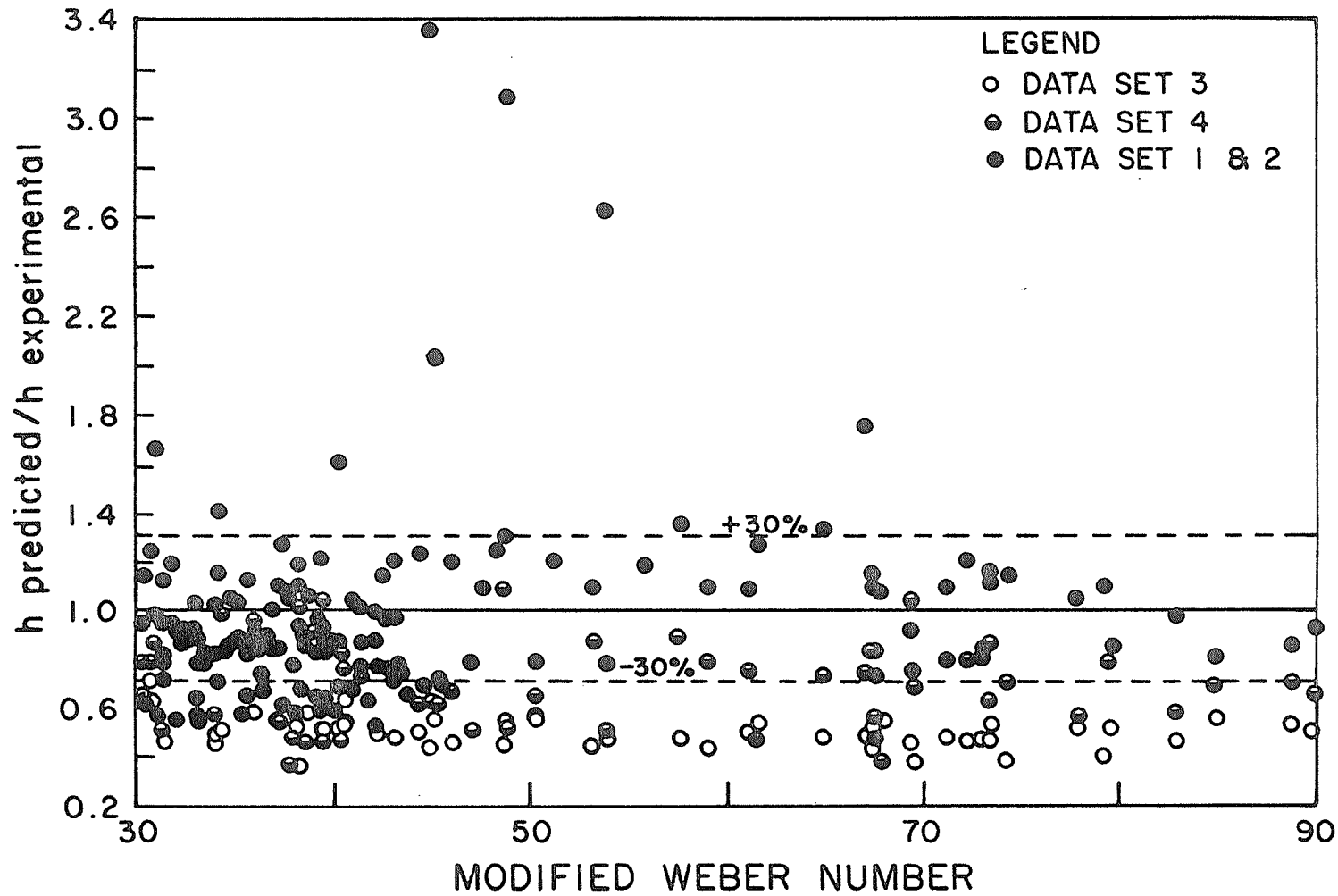


Fig. 4.7 Comparison of mist flow data with Tandon et al. [31] correlation

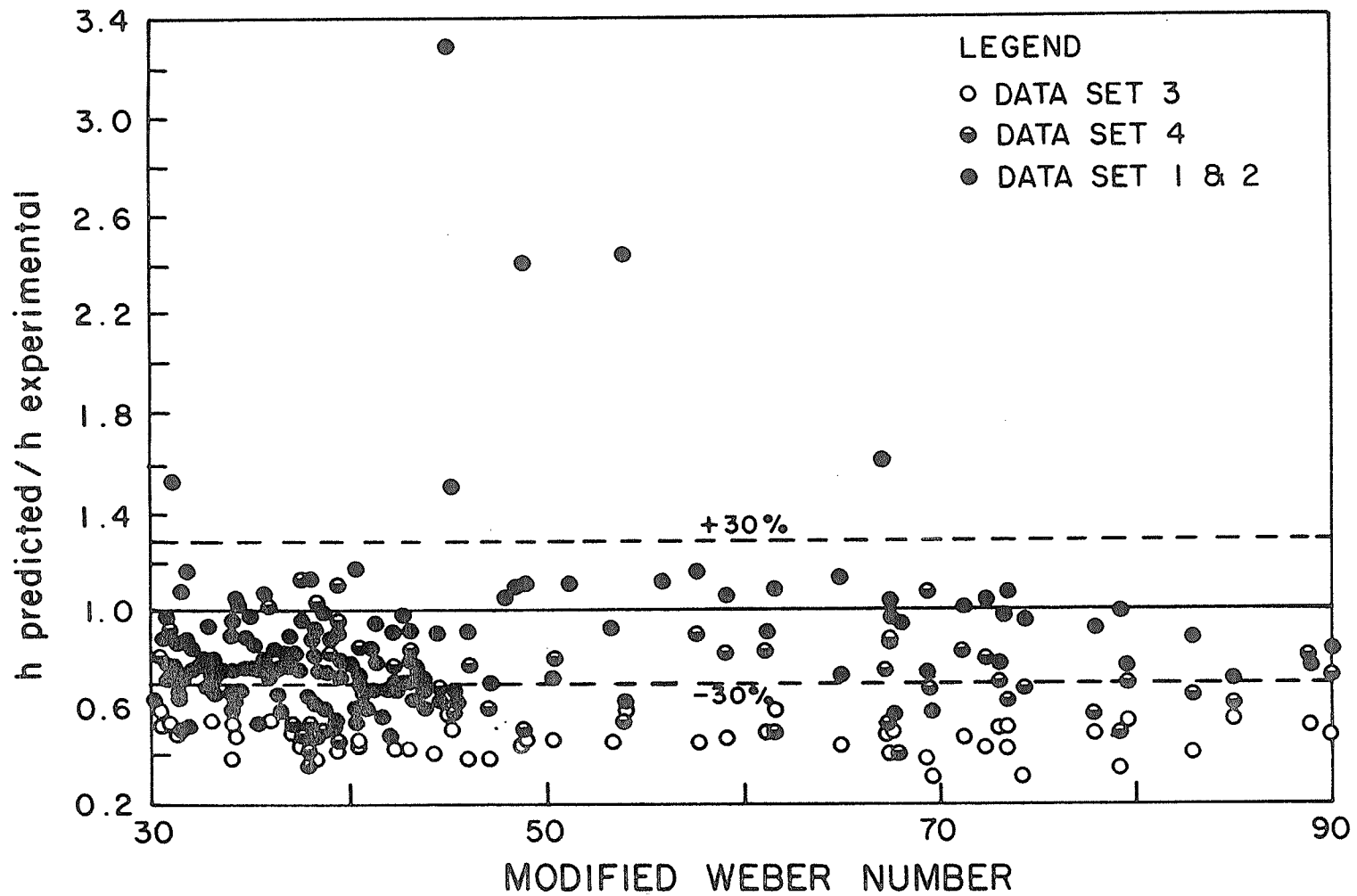


Fig. 4.8 Comparison of mist flow data with Akers et al. [6] correlation

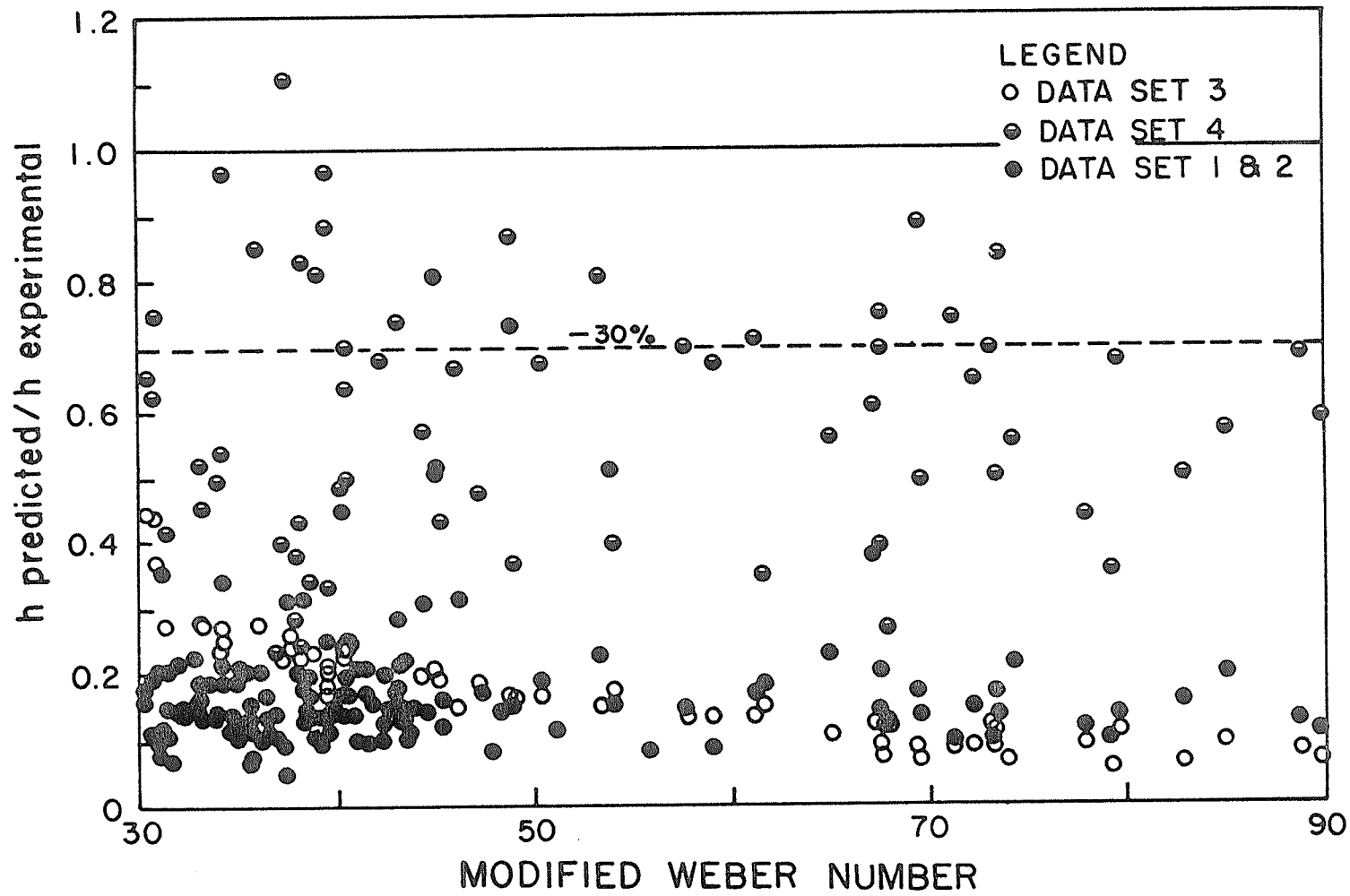


Fig. 4.9 Comparison of mist flow data with Rosson and Myers [16] correlation

to correct a group of his data set. When Equation 3.59 was used the experimental data points with a $F(X_{tt})$ value greater than two were found to be above the correlating line. Therefore, Traviss et al. [25] suggested that Equation 3.60 be used instead when $F(X_{tt})$ is greater than two. In the mist flow regime, out of a total of 285 data points 226 (79%) had a $F(X_{tt})$ greater than two. Hence, Traviss et al.'s [25] correlation requires an empirical correction in the mist flow regime, where any correlation developed on the basis of an annular flow model is bound to be inaccurate.

4.4.2 Annular Flow Regime

The annular flow data in Table 4.2 consists of experiments conducted under two different condenser tube orientation, vertical and horizontal. In the vertical tubes, stratification of condensate due to the effect of gravity does not occur, the application of the Fr is inappropriate. Therefore, the annular to wavy transitional criteria was applied only for the R-12 data. In the vertical tubes at the end of the tube, when condensation is complete, the liquid may fill the tube and produce slug or plug flow. Since this type of flow is likely to occur only in a relatively short length of the condenser this was not considered.

Since the data points with a modified We greater than 40 are being considered by Soliman's [32] correlation in the mist flow regime, data points with a modified We less than 40

must now be included in the annular flow data in order to preserve the continuity of the local heat transfer coefficient along the axial length of the condenser. Therefore, for the data points between 30 and 40 in the modified We scale were added to the annular flow data points given in Table 4.8. As a result, the number of data points in the annular flow regime, with a modified We less than 40 and a Fr greater than seven (only in case of horizontal flows), increased to 454. The selection of a suitable heat transfer correlation is based on the above defined, regrouped data set.

The correlations of Tandon et al. [31] (Fig. 4.10), Akers et al. [6] (Fig. 4.11) and Rosson and Myers [16] (Fig. 4.12) show a similarity within the annular and wavy flow regimes during condensation inside horizontal tubes. The experimentally determined coefficients of heat transfer are consistently higher than all three correlations. Hence the use of ASHRAE [2] recommended Akers et al. [6] correlation results in a conservative design. Among all seven correlations Akers et al. [6] correlation is acceptable for Fr less than seven. The flow under such conditions is wavy.

The condensation heat transfer coefficients predicted by Shah's [30] (Fig. 4.13) and Traviss et al. [25] (Fig. 4.14) correlations for horizontal flow condensers are comparable. The accuracy is consistent throughout the range of Fr.

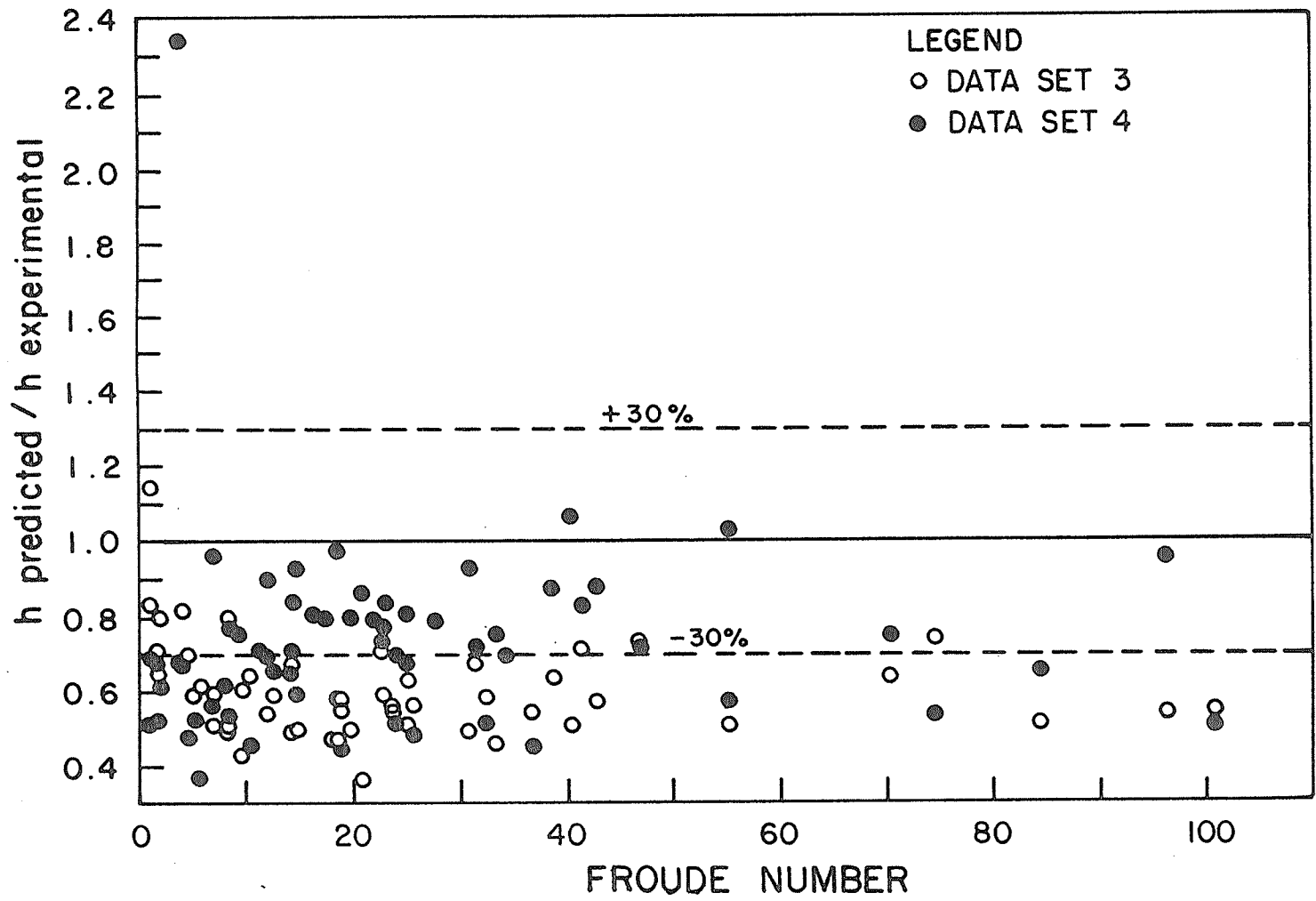


Fig. 4.10 Comparison of annular and wavy flow data (for Condensation inside horizontal tubes) with Tandon et al. [31] correlation

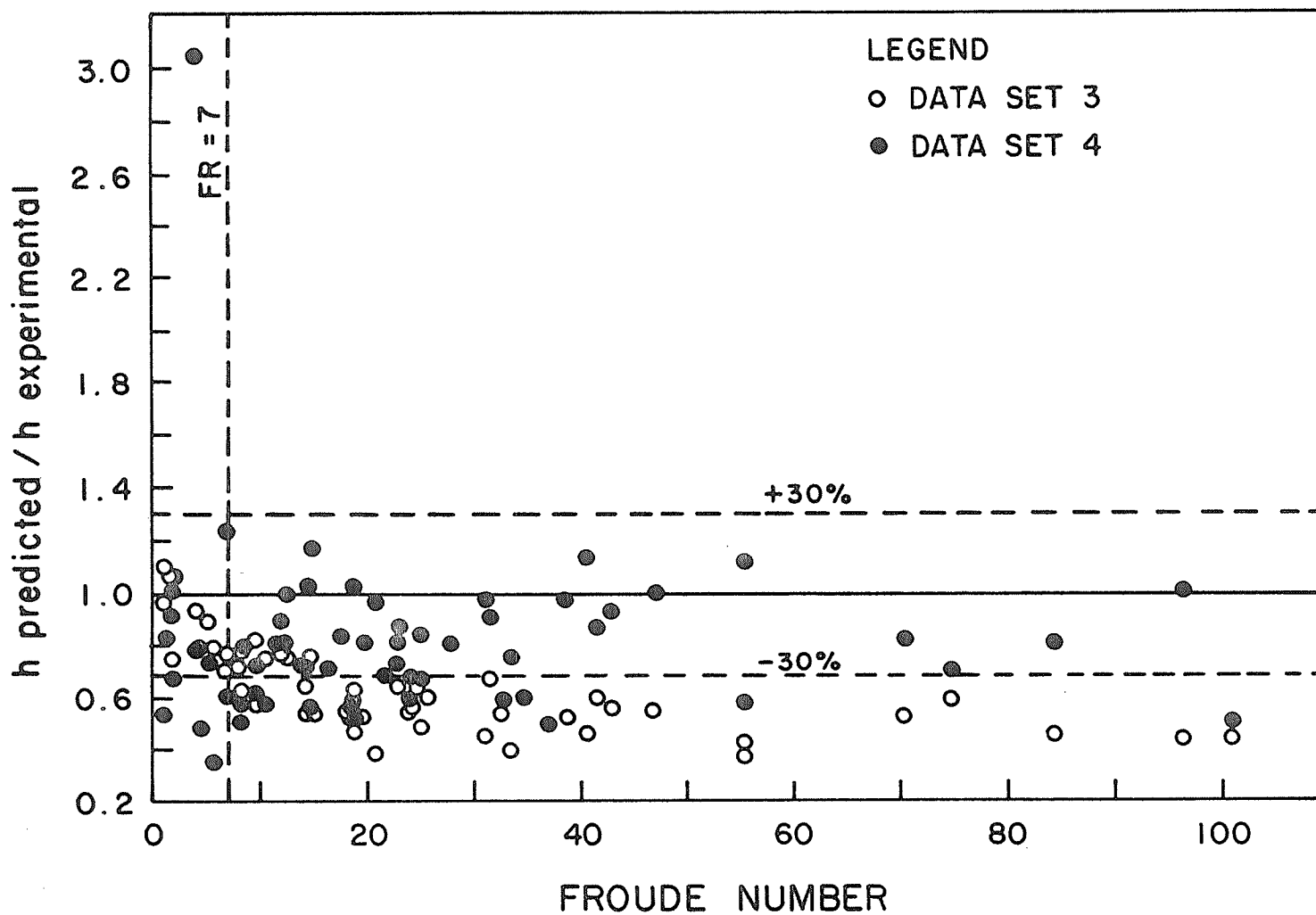


Fig. 4.11 Comparison of annular and wavy flow data (for condensation inside horizontal tubes) with Akers et al. [6] correlation

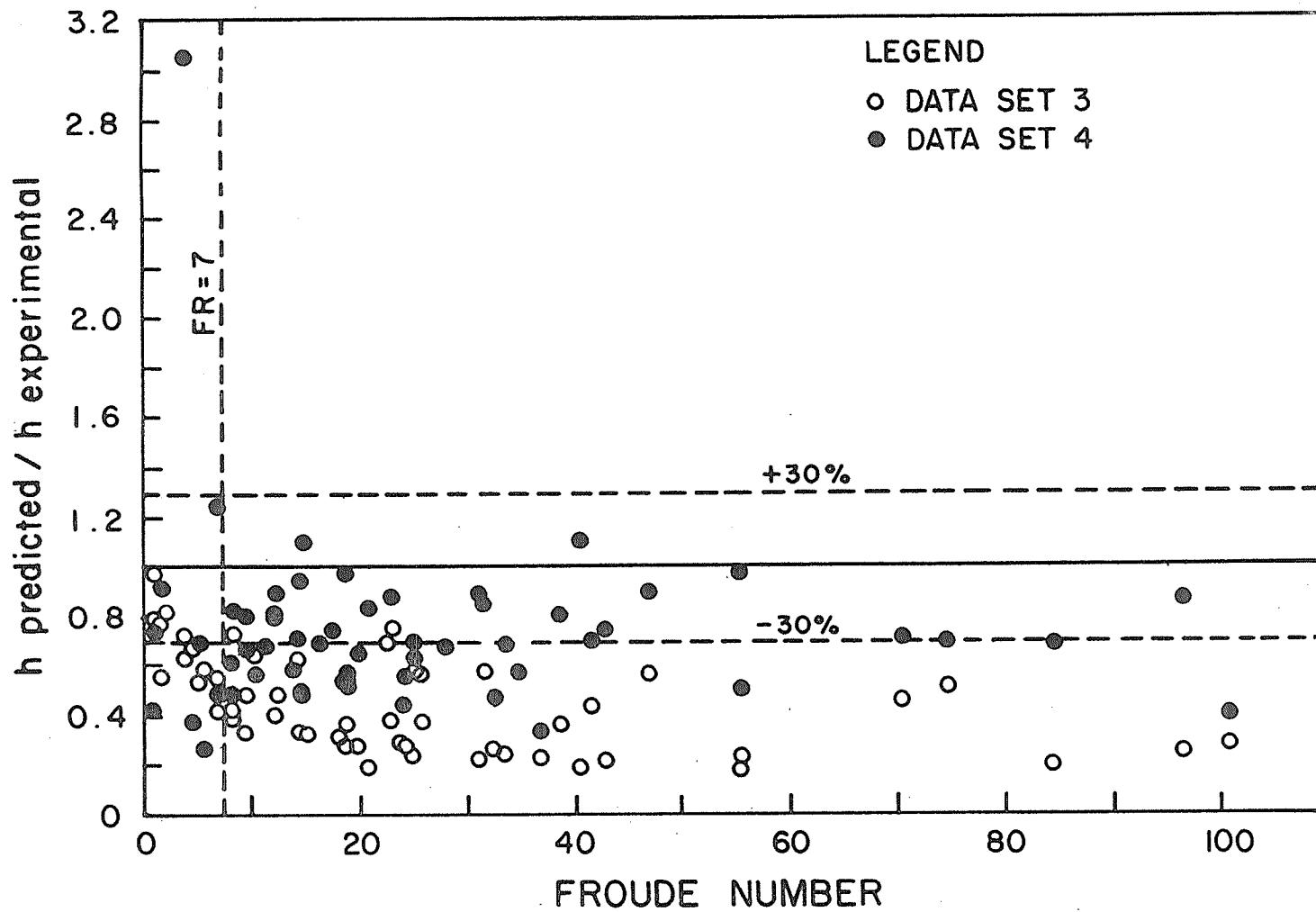


Fig. 4.12 Comparison of annular and wavy flow data (for condensation inside horizontal tubes) with Rosson and Myers [16] correlation

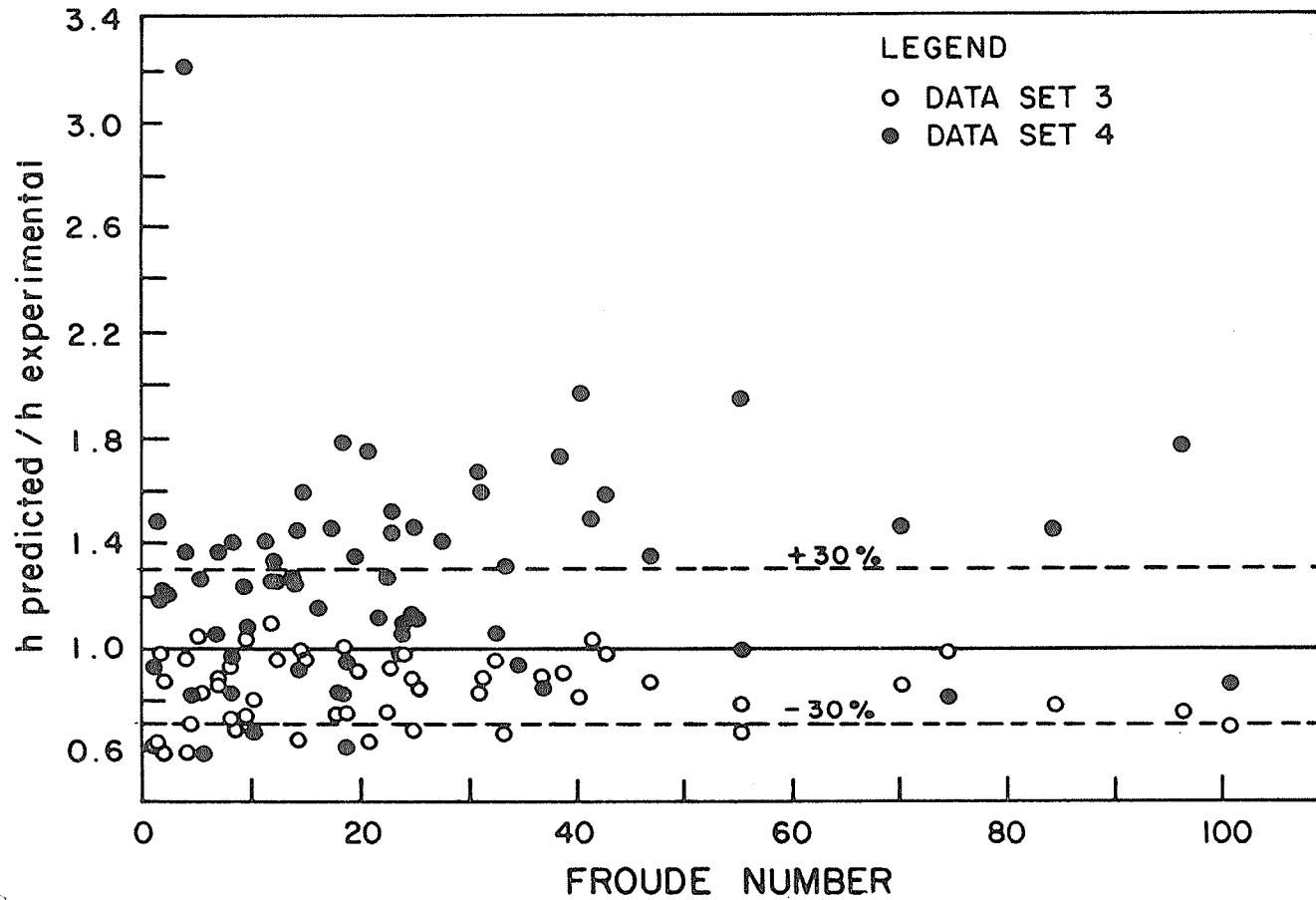


Fig. 4.13 Comparison of annular and wavy flow data (for condensation inside horizontal tubes) with Shah's [30] correlation

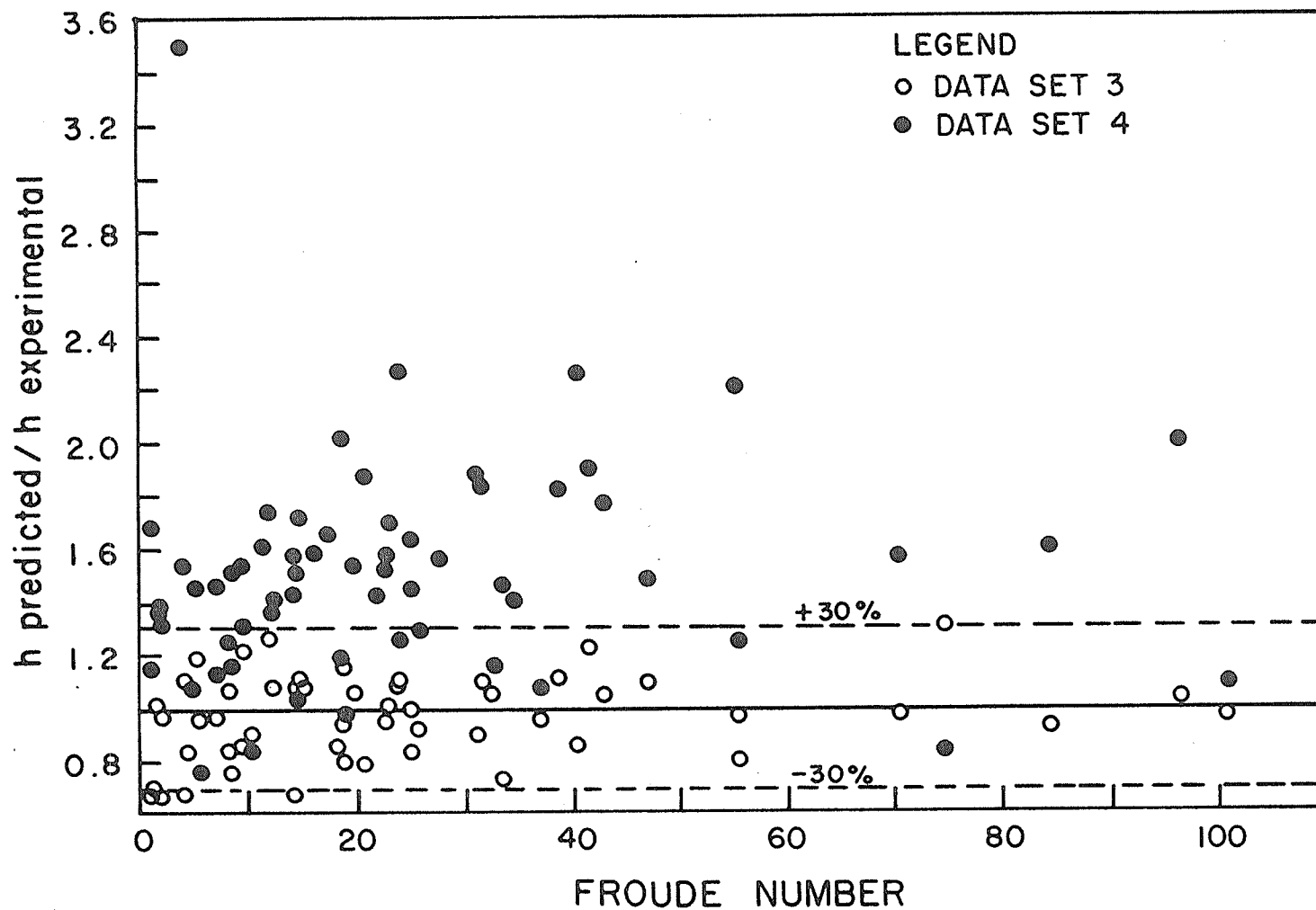


Fig. 4.14 Comparison of annular and wavy flow data (for condensation inside horizontal tubes) with Traviss et al. [25] correlation

However, Traviss et al. [25] correlation is good for Traviss's [49] data covering 89%, that is 48 data points out of a total of 54 points are covered accurately.

Soliman's [32] correlation (Fig. 4.15) and Azer et al. [23] correlation (Fig. 4.16) gave very low values when Fr is lower than about 10 for condensation inside horizontal tubes. Soliman's [32] correlation predicted consistently low heat transfer coefficients during condensation inside vertical tubes (Fig. 4.17). Therefore, it is not advisable to use this correlation for annular or wavy flow regimes in a horizontal condenser and for annular flow regimes in a vertical condenser.

During condensation in a vertical tube Tandon et al. [31] and Shah's [30] correlations provide accurate results. Figs. 4.18 to 4.23 show that steam data are difficult to cover accurately. Since the deviations from the experimental heat transfer coefficients are 7 to 17 times as high for individual data points at qualities below 0.3 thus the correlations are inconclusive in this range. Hence, all data points falling within $\pm 30\%$ were counted and conclusions based on this criteria. A comparison of Fig. 4.17 and Fig. 4.18 to 4.23 show that the maximum deviations given by Soliman's [32] correlation Fig. 4.17 is appreciably lower than other correlations.

A comparison between Tandon et al. [31] and Shah's [30] correlations is shown in Table 4.10.

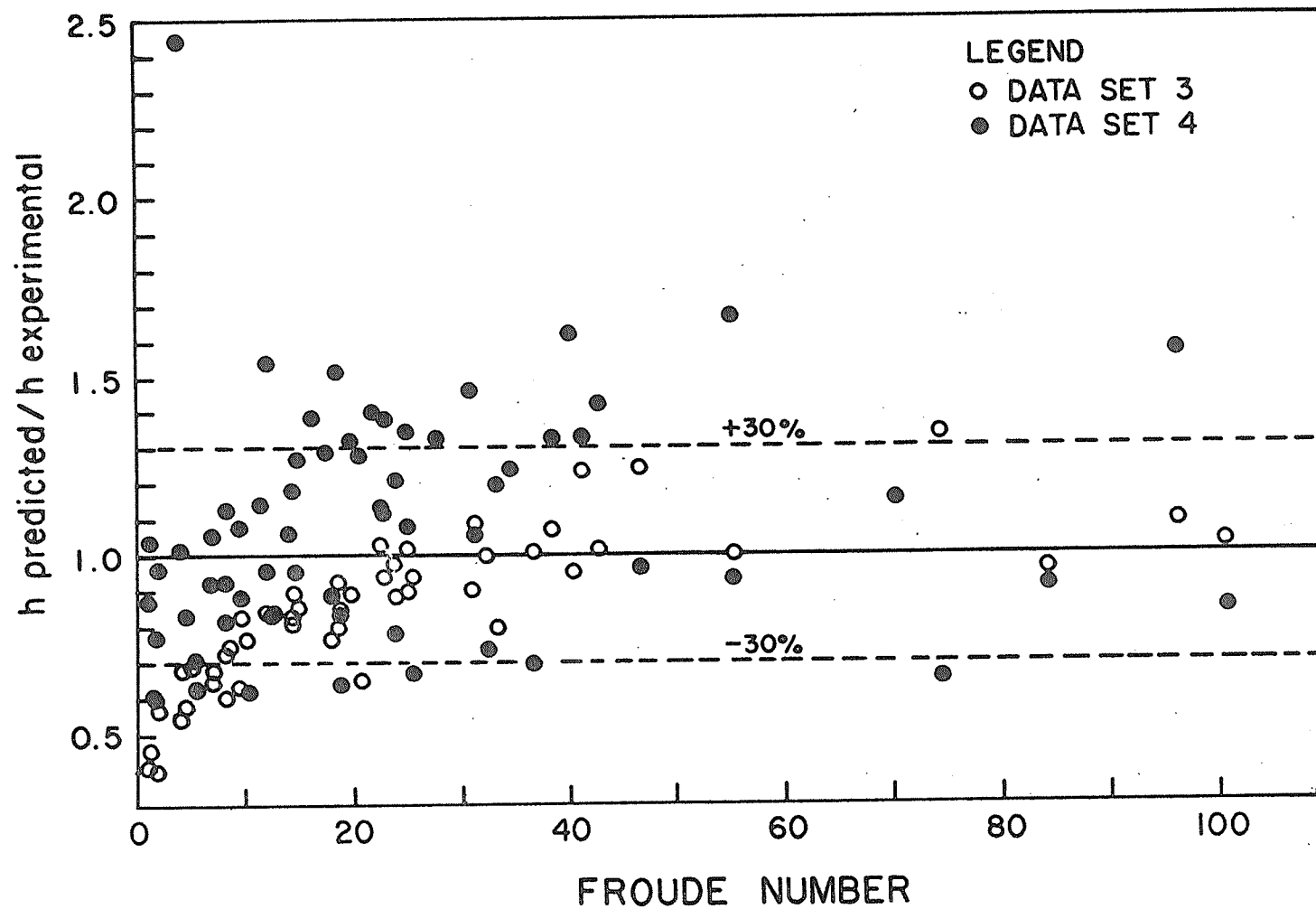


Fig. 4.15 Comparison of annular and wavy flow data (for condensation inside horizontal tubes) with Soliman's [32] correlation

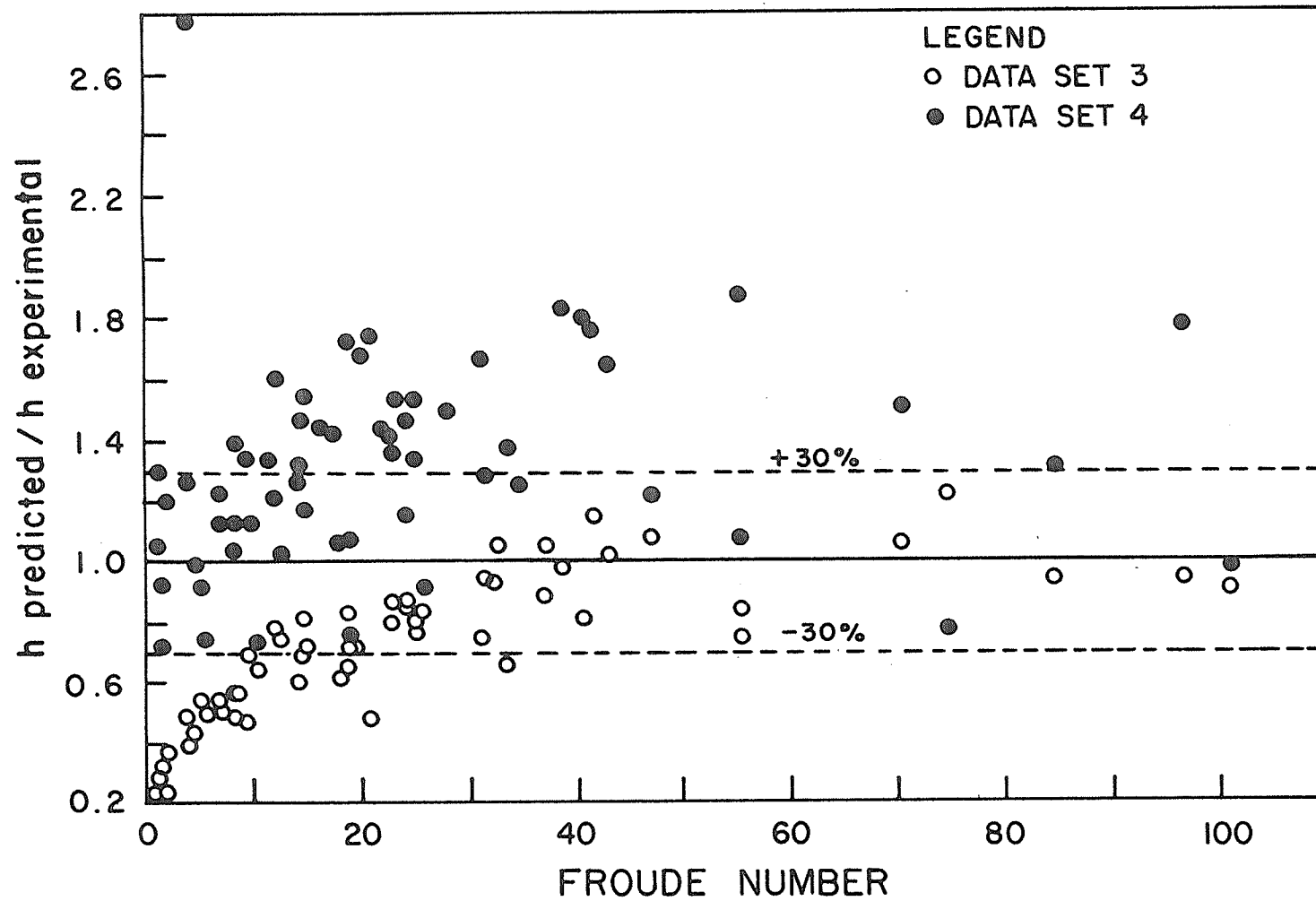


Fig. 4.16 Comparison of annular and wavy flow data (for condensation inside horizontal tubes) with Azer et al. [23] correlation

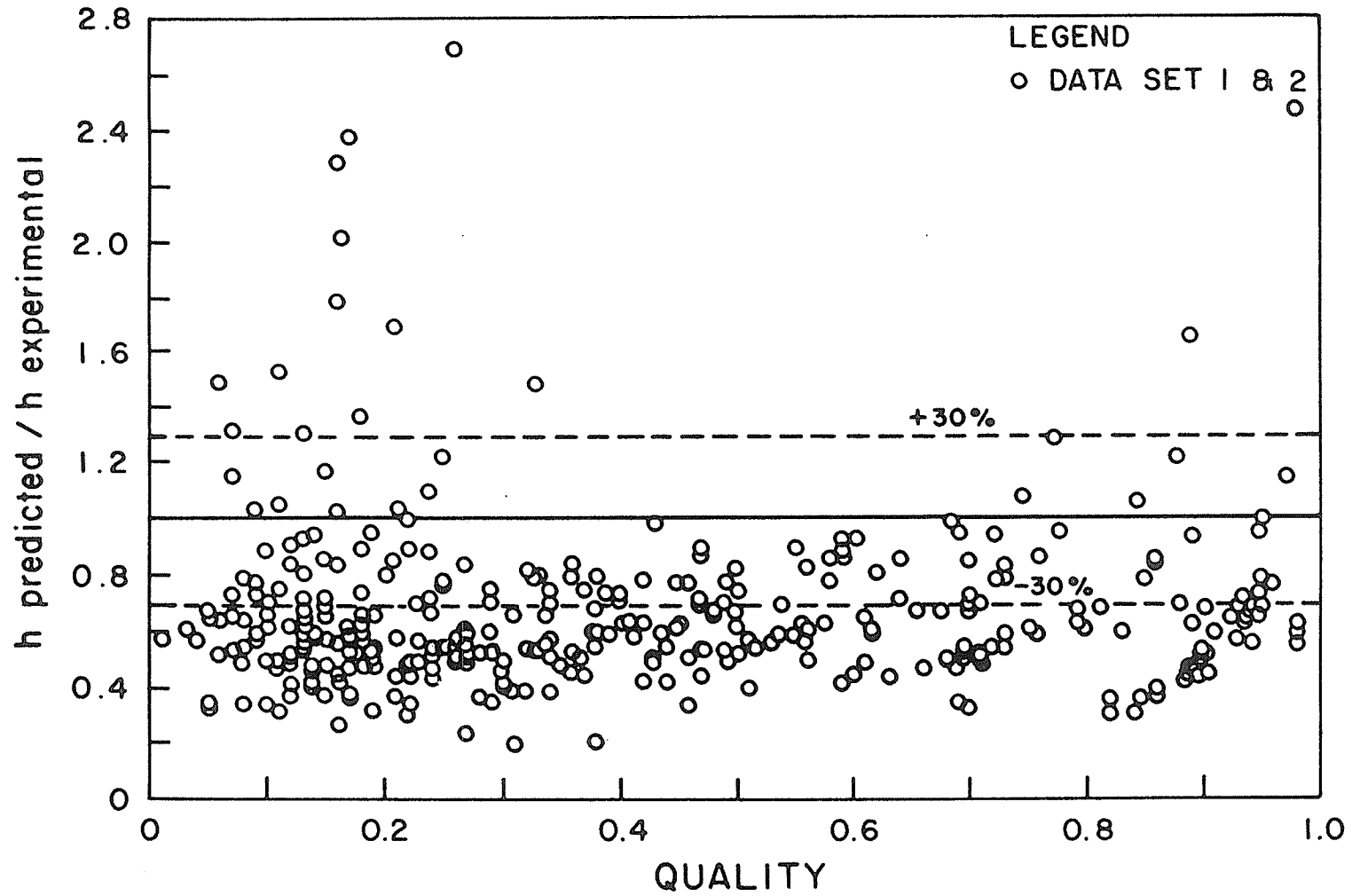


Fig. 4.17 Comparison of annular flow data (for condensation inside vertical tubes) with Soliman's [32] correlation

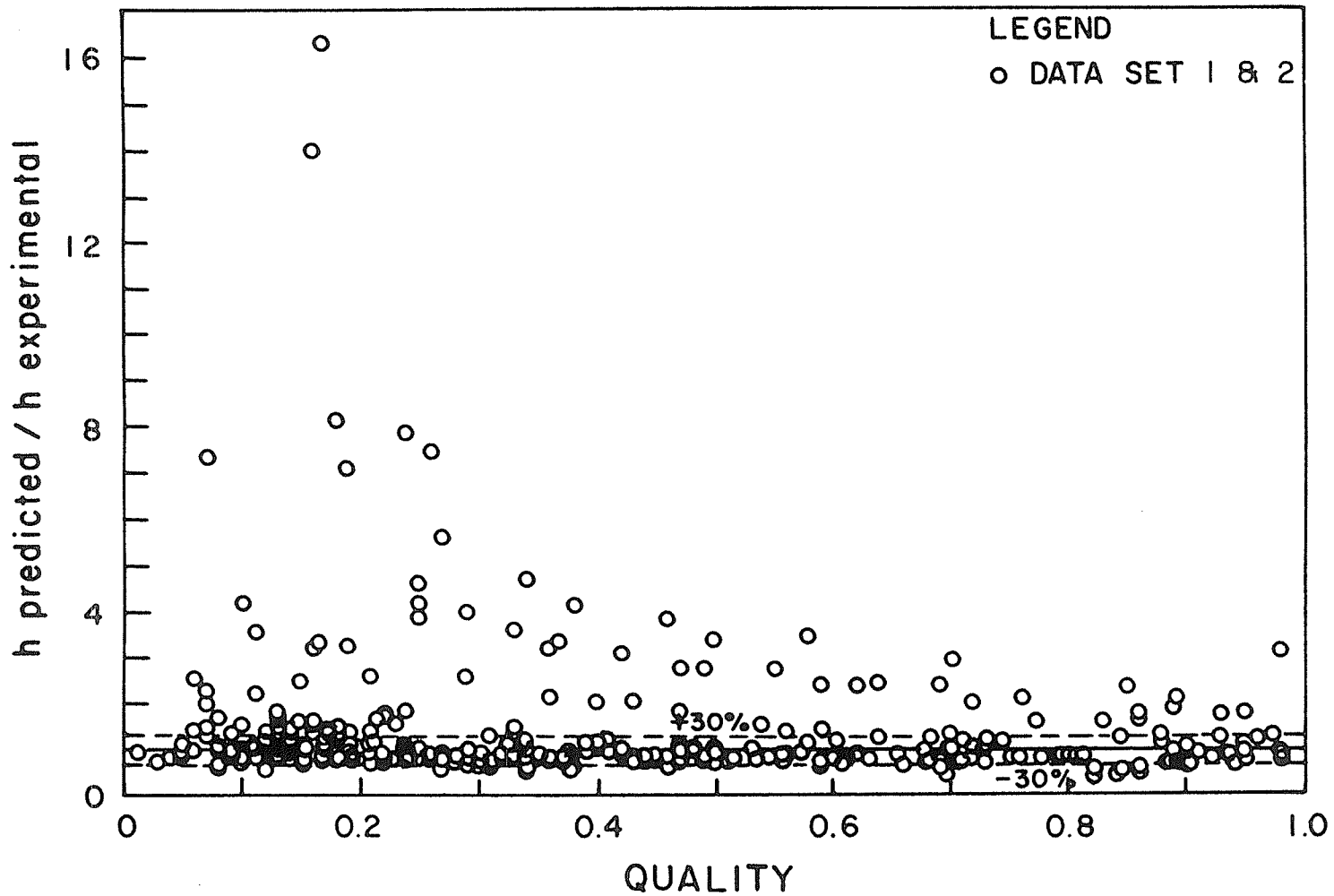


Fig. 4.18 Comparison of annular flow data (for condensation inside vertical tubes) with Tandon et al. [31] correlation

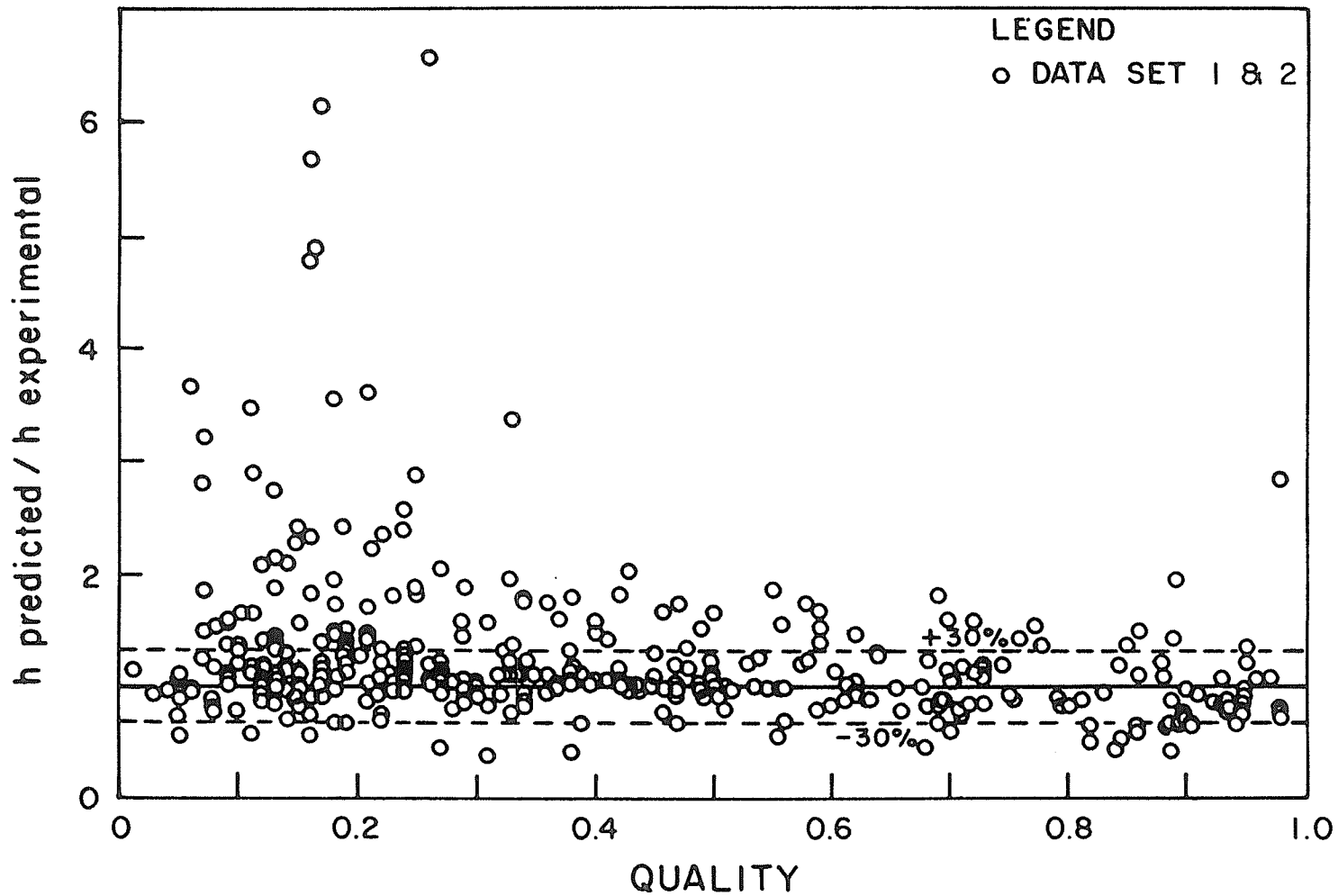


Fig. 4.19 Comparison of annular flow data (for condensation inside vertical tubes) with Shah's [30] correlation

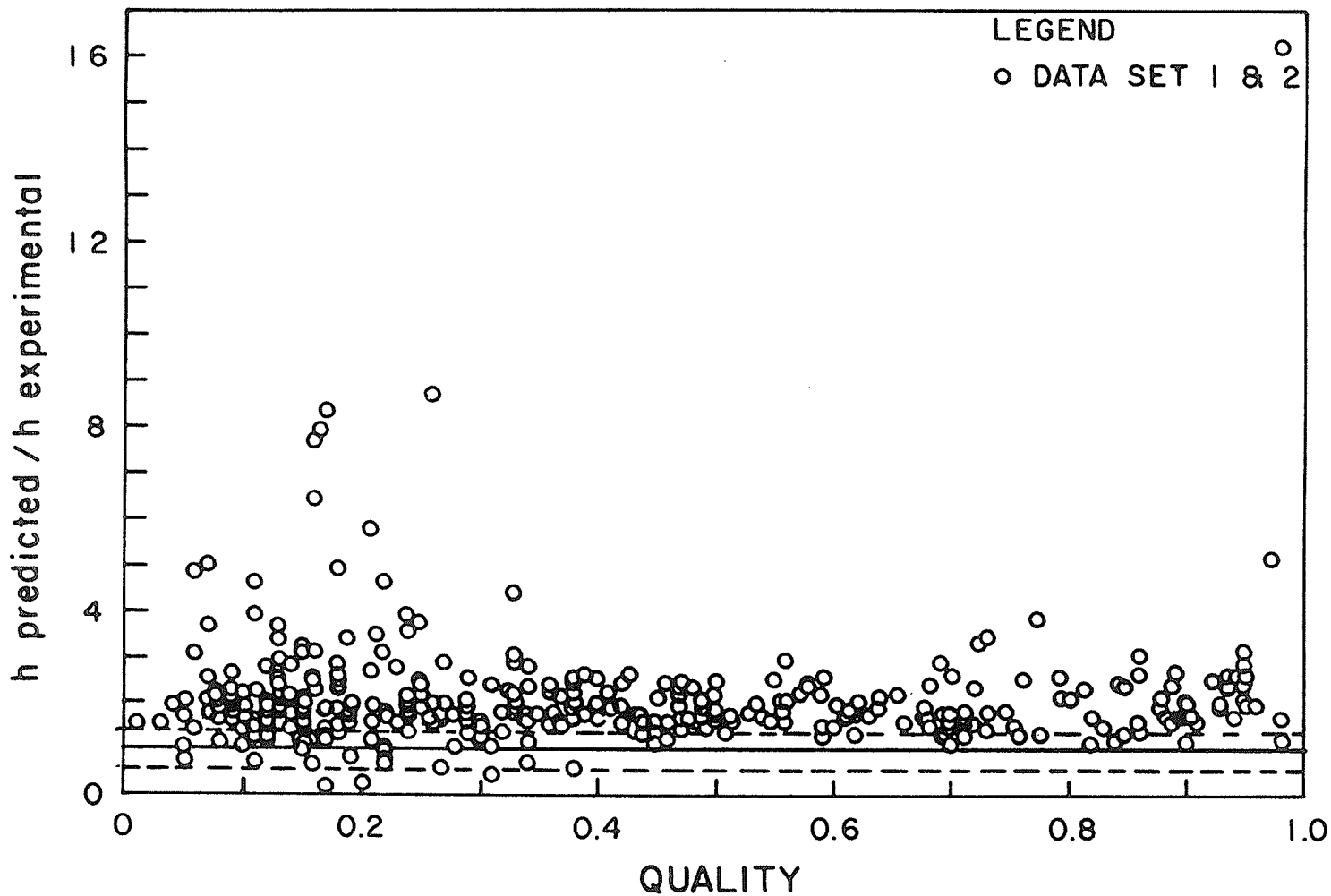


Fig. 4.20 Comparison of annular flow data (for condensation inside vertical tubes) with Traviss et al. [25] correlation

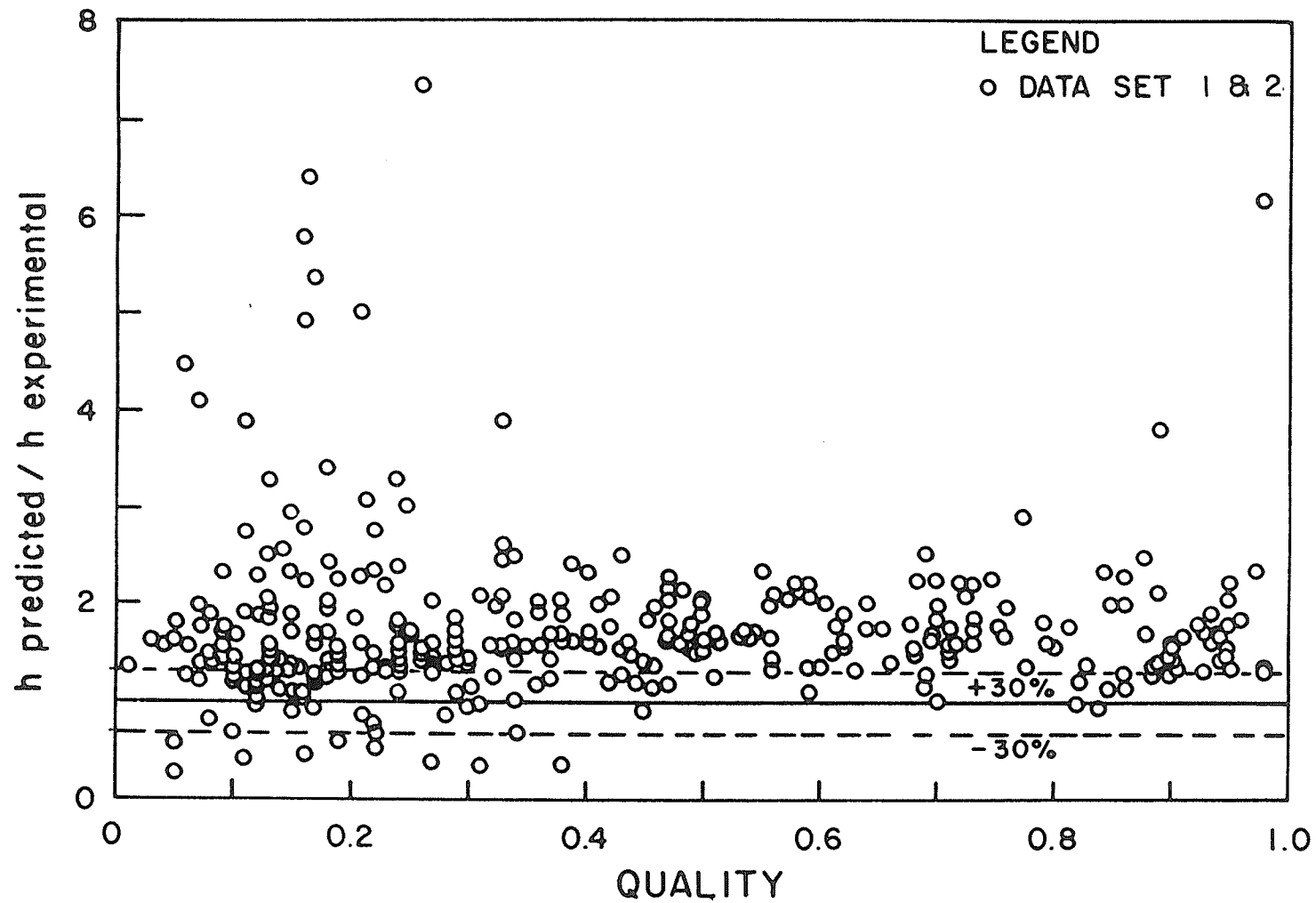


Fig. 4.21 Comparison of annular flow data (for condensation inside vertical tubes) with Azer et al. [23] correlation

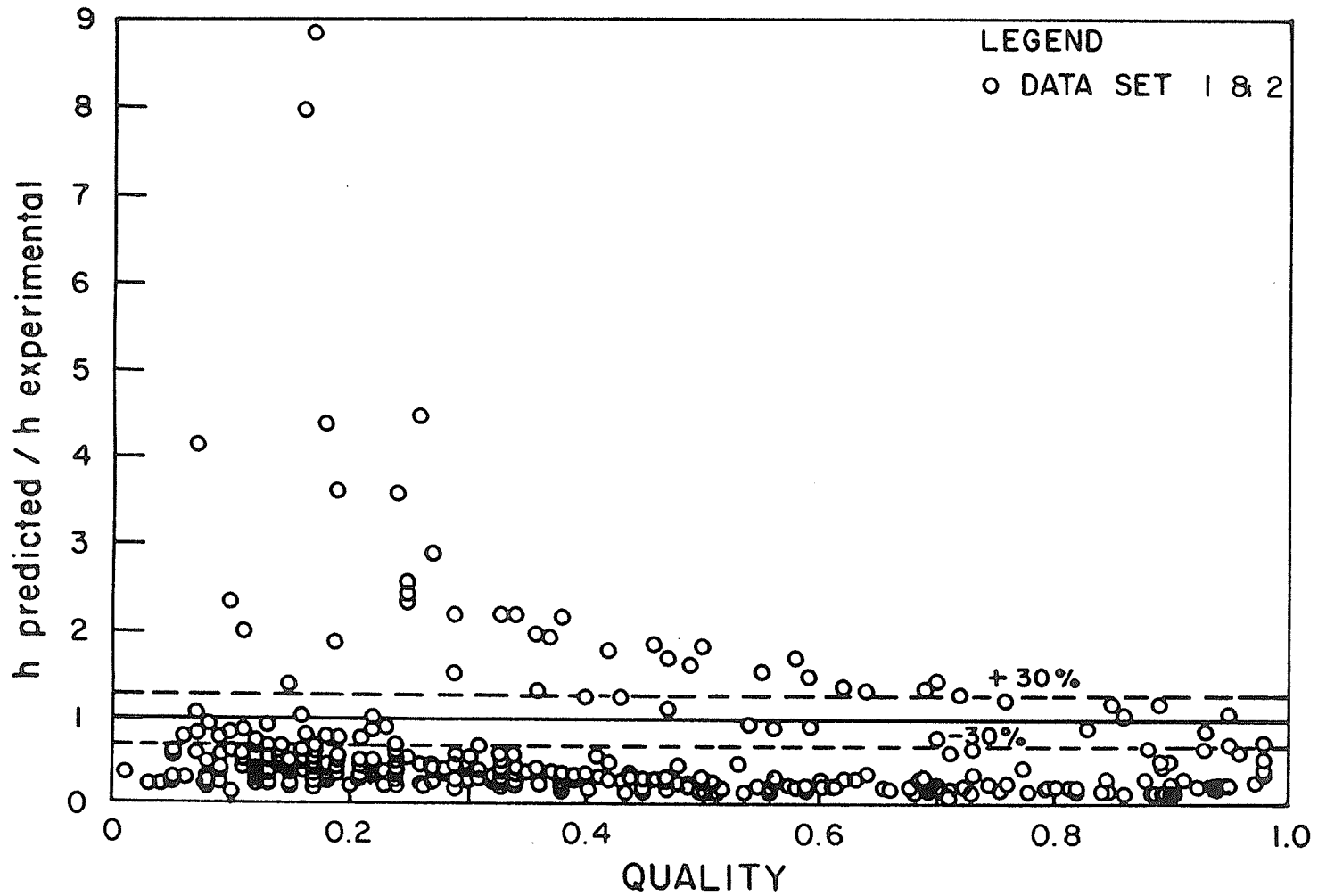


Fig. 4.22 Comparison of annular flow data (for condensation inside vertical tubes) with Akers et al. [6] correlation

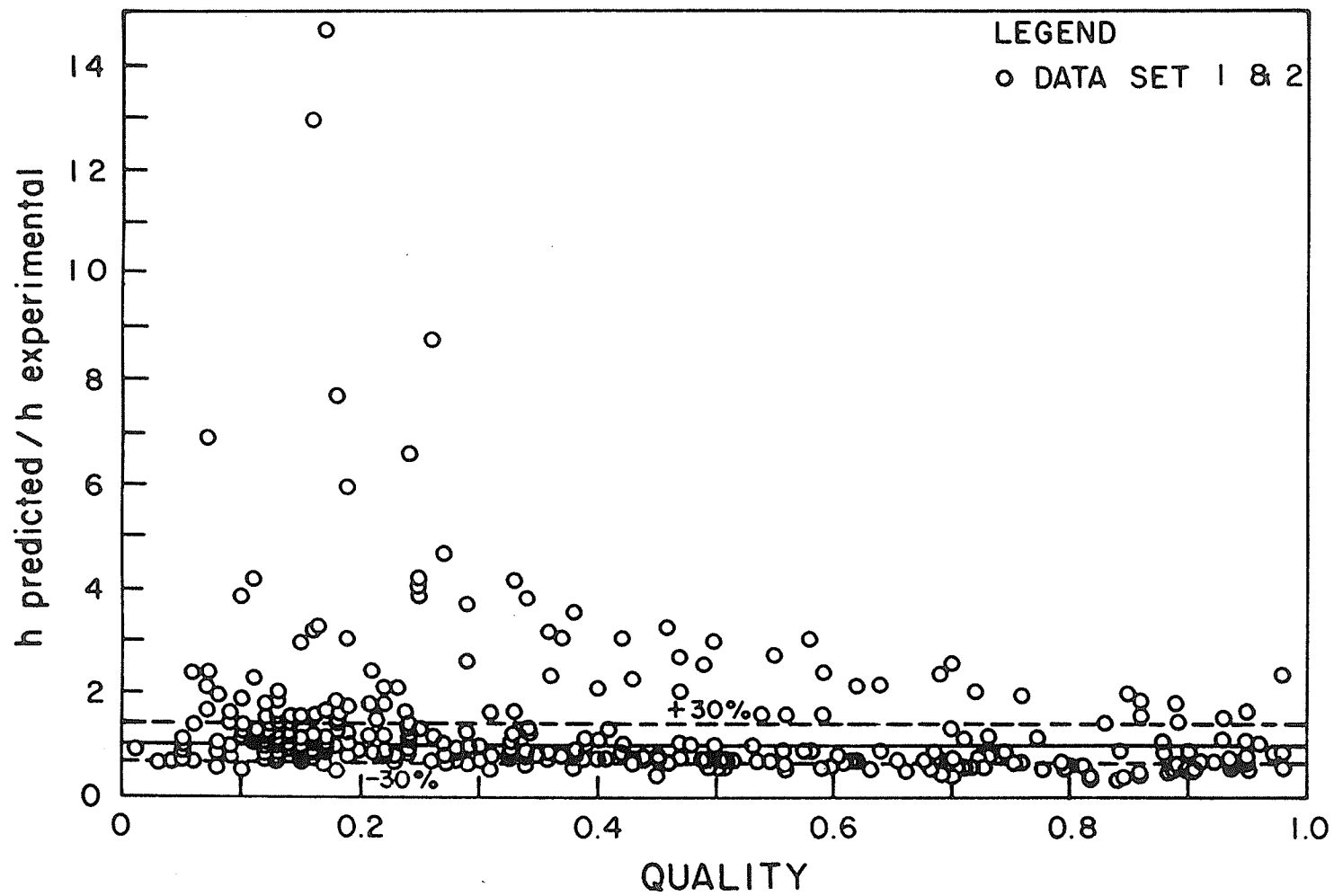


Fig. 4.23 Comparison of annular flow data (for condensation inside vertical tubes) with Rosson and Myers [16] correlation

Table 4.10
 Comparison of Shah's [30] Correlation With Tandon
et al. [31] Correlation for Flows With A
 We Less Than 40

Data Set No.		Percentages of points within $\pm 30\%$ of Experimental Value	
		Tandon <u>et al.</u> [31]	Shah's [30]
1 and 2	100% (355)	65 (230)	60 (213)
3	100% (42)	10 (4)	83 (35)
4	100% (57)	35 (20)	81 (46)
Overall	100% (454)	56 (254)	65 (294)

Shah's [30] correlation predicts 65% of the data points, during the horizontal and vertical flow, compared to 56% by Tandon et al. [31] correlation. Since a general correlation for different conditions is desirable, the overall performance in both vertical and horizontal tubes is used to evaluate the performance of the seven correlations. Hence, based on the performance, shown in Table 4.10, Shah's [30] correlation was selected for use within the annular flow regime. The flow is defined by the modified We less than 40, for vertical and horizontal condensation in tube, and Fr higher than seven, for horizontal flows.

4.4.3 Wavy Flow Regime

Flow with condensation inside horizontal tubes was considered to be wavy for all data with a Fr less than seven. Ninety-four percent of the data were correlated by Akers et al. [6] formula followed by Shah's [30] which correlated only 67%. A comparison between the experimental and predicted values of the condensation heat transfer coefficients is given in Fig. 4.24. An attempt was made to study the effect of shifting the Fr to 10 on the accuracy of the correlations. The accuracy for all correlations dropped significantly. Hence, the present criteria of a Fr of seven is considered to be adequate.

The number of data points available within this flow regime in the available data base were limited. Hence, caution must be exercised before confidence can be placed on the conclusions drawn from this study. Within the limitations of the number of data points, Akers et al. [6] correlation is found suitable for this regime. Fig. 4.25 shows that this correlation is in good agreement with the wavy flow data.

4.4.4 General

With the Freon-12 data specific correlations show improved accuracy. For example, within Traviss's [49] data range Traviss et al. [25] correlation cover 92% of the data. Similarly within Azer et al. [23] data range the modified correlation of Azer et al. [23] (given by Equation 4.10)

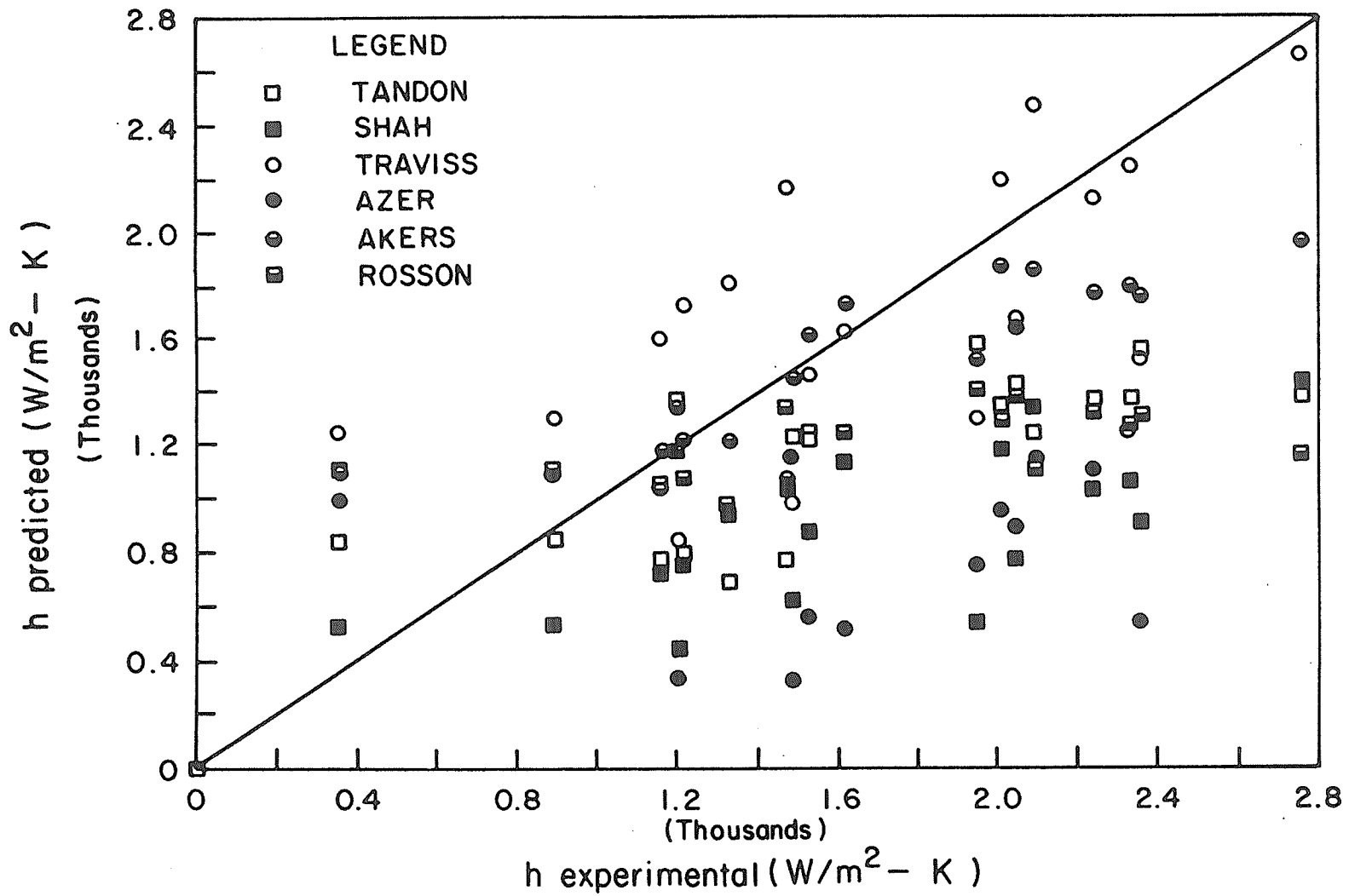


Fig. 4.24 Comparison of Akers et al. [6] correlation with Shah's [30] correlation in the wavy flow regime

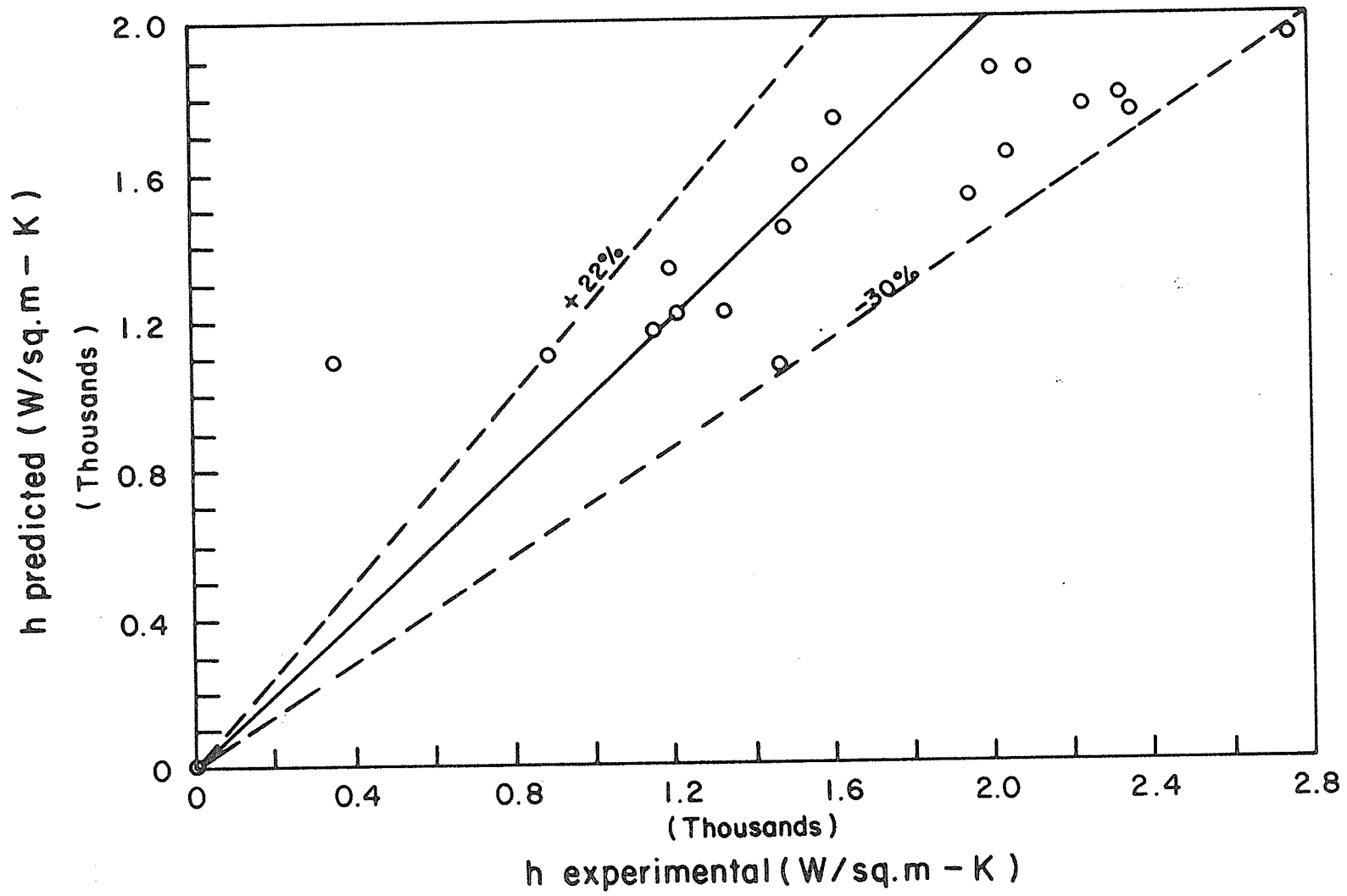


Fig. 4.25 Comparison of Akers et al. [6] correlation with wavy flow data

covers 76% of the data within $\pm 30\%$. Therefore, if improvements are required such correlations could be used, irrespective of the flow regimes, if the mass flow rates of R-12, the tube diameter of the condenser and the condensing temperatures are similar to those that have been used in generating the above mentioned data sets. These ranges of parameters are given in Table 4.1.

4.5 Development of a Design Procedure Based on the Theory of Successive Summation

Once a method to evaluate the local heat transfer coefficient is available the next step in the development of a design procedure to calculate the length of the heat exchanger required to condense a given mass flow of vapor.

Design methods available for condensers may be broadly classified into two categories. These are equilibrium methods and the successive summation method which is also called a differential method.

In the equilibrium methods, no attempt is made to describe the process on the vapor side mass transfer. The bulk of vapor and liquid condensate at any plane normal to the flow are assumed to be at equilibrium that is at the saturation temperature. The method is suited to the situation in which vapor and condensate do not become separated (like in mist flow).

In the second method, the calculation of local heat and

mass transfer rates are combined with differential mass and energy balances, which describe the down stream development of the vapor and coolant temperatures and vapor composition through the condenser. Design is accomplished by integration of these differential equations.

The classical method of calculating the overall heat transfer coefficient for an exchanger is to integrate the basic differential given by:

$$dq = U (T_v - T_w) dA. \quad (4.11)$$

After integrating over the heat transfer area

$$\begin{aligned} q &= UA (\Delta T_v - \Delta T_w) / \ln(\Delta T_v / \Delta T_w) \\ &= UA \Delta T_{LM}. \end{aligned} \quad (4.12)$$

results, where ΔT_{LM} is the log mean temperature difference. The application of this method becomes unsuitable when the condensation heat transfer coefficient inside the tube is calculated by three different methods depending on the local conditions prevailing along the length of the condenser. Log mean temperature method is well suited for situations where mean heat transfer coefficients are used. Therefore, a successive summation method is used for the development of the design procedure.

In the successive summation method the differential

equations are developed by the classical approach of defining steady state heat balance across an infinitesimal section ΔL of the heat exchanger (Fig. 4.26). The rate of change of temperature with distance (dT/dL) in the coolant stream varies along the condensing length of the exchanger, but because the elemental section ΔL is small the temperature within the infinitesimal section can be considered constant across this section. Similarly in the desuperheating section of the exchanger both vapor as well as coolant stream temperatures vary.

In order to calculate the rate of heat transfer within a differential element the heat transfer coefficients on the shell side and the tube side, the thermal conductivity of the condenser tube material and thickness, and any resistances due to fouling must be known. The shell side heat transfer coefficient is obtained by Dittus-Boelter equation for single phase flows. This equation is used for the cooling medium, which is generally water. For the super heated vapor Equation 3.85 is used until the super heat is removed. The single phase heat transfer equation is given by,

$$h = 0.32 Re_w^{0.61} Pr_w^{0.31} \frac{k_w}{D} \quad (4.13)$$

Where, h = single phase heat transfer coefficient,
 $W/m^2.K,$

Re_w = Reynold's number of the single phase flow,

Pr_w = Prandtl number of the fluid,

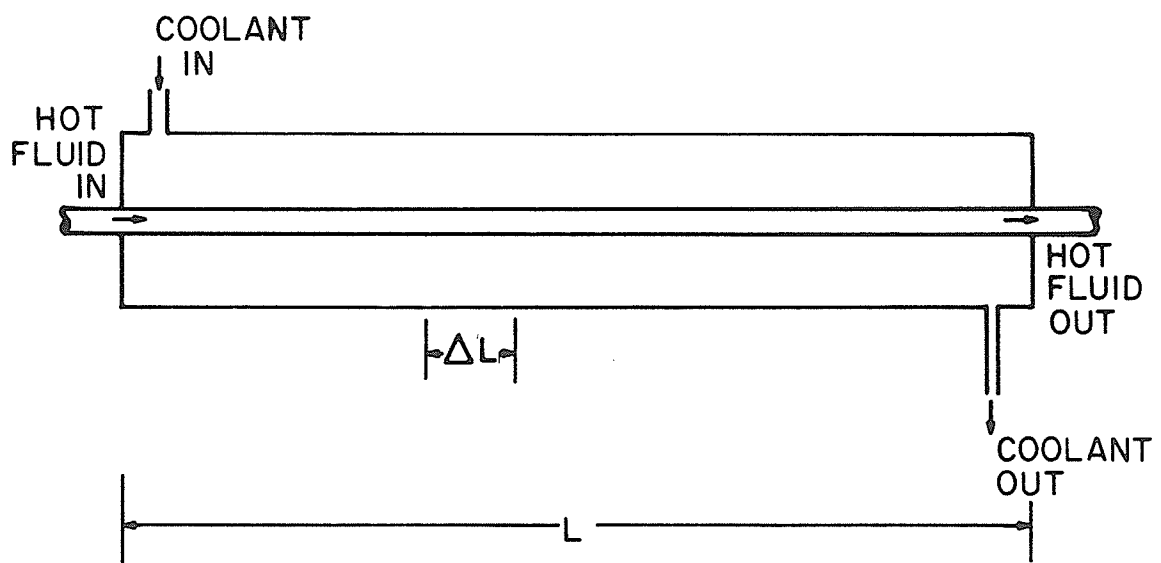


Fig. 4.26 A counter flow heat exchanger

D = diameter of the tube, m and

k_w = thermal conductivity of the fluid, w/m K

The overall heat transfer coefficient (U_i) for the differential element based on the inside differential area of the tube is obtained by,

$$\frac{1}{U_i} = \frac{1}{h_i} + \frac{1}{h_s(D_0/D_i)} + \frac{(D_0 - D_i)D_i}{k_T(D_0 + D_i)} \quad (4.14)$$

Where,

h_i = tube side heat transfer coefficient,

h_s = shell side heat transfer coefficient,

D_i = internal diameter of the tube,

D_0 = outside diameter of the tube and

k_T = thermal conductivity of the tube material.

In the desuperheating area of the condenser the rate of heat transfer by N tubes within the differential length is then given by,

$$\Delta q = \pi D^2 (\Delta L) U_i (T_v - T_w) N \quad (4.15)$$

where, ΔL = infinitesimal length of condenser,

T_v = vapor temperature and

T_w = coolant temperature.

Until the vapor temperature becomes equal to the saturation temperature, the down stream vapor and water temperatures are determined, from the rate of heat transfer (q) using the following equations.

$$T_{v2} = T_{v1} - \frac{q}{m_v C_{pv}} \quad (4.16)$$

$$T_{w2} = T_{w1} - \frac{q}{m_w C_{pw}} \quad (4.17)$$

Where,

T_{v2} = vapor temperature at the infinitesimal section immediately next to the current section,

T_{v1} = the vapor temperature of the current section of the condenser,

T_{w2} = coolant temperature in the adjoining section of the condenser,

T_{w1} = coolant temperature in the current infinitesimal section,

m_v = mass flow rate of vapor,

m_w = mass flow rate of coolant,

C_{pv} = specific heat of the vapor and

C_{pw} = specific heat of the coolant.

Once the vapor temperature is below the saturation temperature of the condensing vapor the length of heat exchanger required (ΔL) to condense each infinitesimal decrement of quality is evaluated as follows,

$$\Delta L = \frac{\dot{m}_v h_{fg} \Delta x}{D_i U_i (T_v - T_w) N} \quad (4.18)$$

Where,

Δx = infinitesimal change in quality and

T_v = saturated vapor temperature.

For the next infinitesimal area the quality is decreased by a suitable quantity as

$$x_2 = x_1 - \Delta x \quad (4.19)$$

until the quality is almost negligible at the end of condensation. The algorithm of the design procedure is given in APPENDIX B. The computer listing is also included in APPENDIX C. The final condenser length is obtained by summing all the infinitesimal lengths required to cool and condense the vapor.

CHAPTER 5

APPLICATION TO FIELD STUDY

The application of the design procedure developed in Chapter 4 is the design of a suitable condenser for the refrigeration system discussed in the FIELD STUDY (Chapter 2). Hence, the computer program given in APPENDIX C was used to design a condenser for the refrigeration system of the poultry plant.

Among the six subdivisions of the refrigeration system in the Dunn-Rite Products Ltd. poultry processing plant the deep freeze system was selected for the design purposes. This unit is operated by two 28 kW compressors using R-502 as refrigerant. It was estimated that the refrigerant leaves the compressors at 93°C (Figure 1.1) and condenses at 43°C . The estimated flow of refrigerant was 0.5 kg/s and in cooling and condensing this flow the total heat rejected was over 60 kW.

A shell and tube heat exchanger was selected for use. Various shell diameter and tube arrangements were tried. When the shell diameter is large the shell side heat transfer coefficient drops significantly and therefore the high heat transfer coefficients available on the tube side is not fully utilized. As a result the length of the condenser tubes required increases several fold.

A combination of 152 mm diameter shell with 40 tubes of 12.7 mm dia. arranged in a triangular 19.05 mm pitch offered a high shell side heat transfer coefficient. In order to provide a cross flow to assist in producing a high shell side heat transfer coefficient a tube bank baffle spacing of 0.6 m was provided.

Process water for the plant's use is obtained from the city water supply. During the winter months the water temperature average approximately 5°C. The total hot water requirement for production and domestic use on an average day is about 58 m³/day. This for an eight hour working day gives 7.25 m³/hr. Since there are number of compressor units of higher capacity the total water flow rate was split in two. Therefore, the water mass flow rate through one of the heat exchangers is 1 kg/s.

The total length of tubing required to condense the refrigerant completely is 3.4 m. Since this tube length is supplied as a U-tube the length of the condenser is 1.7 m. The outlet temperature of water is 22°C.

A heat recovery unit of the above dimensions is able to recover about 69 kW. The total heat rejected through both of the 28 kW compressors is 69.15 kW. Hence, the entire vapor mass of the refrigerant is condensed in the heat exchanger. By rounding off the condenser heat exchanger length to 2 m an excess capacity of approximately 18% which should allow for discrepancies in correlations and fouling.

The amount of heat recovered is worth approximately \$18/day. This is obtained converting the gas equivalent of the reclaimed heat generated by one of the hot water boilers at 52% overall efficiency and gas at \$5.24/GJ. The estimated annual savings in gas bill is then \$3,600. With a 10% interest for borrowed money compounded annually and a 10 year life for the water cooled heat exchanger gives present worth of economic investment on the equipment at approximately \$22,000. Hence, any investment less than this amount for the installation (including the cost of the extra refrigerant for retrofitting) and equipment would be cost effective, neglecting the cost of maintenance required for the equipment. The maintenance cost is marginal in such equipment requiring only a periodic cleaning of the water side of the exchanger for possible salt deposition. In a food industry high quality water is used and as a result the salt content is low. Hence, salt deposition and fouling on the shell side is expected to be an insignificant problem.

CHAPTER 6

CONCLUSIONS AND RECOMMENDATIONS

6.1 Conclusions

A number of conclusions were drawn from the results of the present investigation. For clarity these are presented in three groups and are described in order.

Regarding the industrial energy survey, the following conclusions may be drawn:

1. The recovery of waste heat energy from the condenser of industrial refrigerators is economically feasible. The rejected heat is available at approximately 43°C, a suitable temperature for water preheating.
2. The food industry, by virtue of its large low temperature process water requirements, derives significant economic benefits by recovering waste heat from refrigeration equipment and the use of water cooled condensers should be considered for such installations.

An extensive literature search provided seven correlations which were isolated and compared with a data base covering experimental data on condensation inside

vertical and horizontal tubes. The conclusions drawn from this search were as follows:

1. Hydrodynamic flow regimes must be identified with suitable transition criteria before a particular condensation heat transfer correlation is applied. This observation agrees with the observations made by Bell [46] and Breber et al. [39].
2. Soliman's [32] correlation is an appropriate correlation for the mist flow regime defined by a modified Weber number (Equations 3.92 and 3.93) greater than or equal to 40. This correlation is suitable for condensers using steam and R-12 as condensing fluids.
3. The mist flow regime is followed by an annular flow regime, which is defined by flows with a modified Weber number less than 40 for all flows except in case of condensation inside horizontal tubes where the flow must also be with a Froude number higher than seven, Shah's [30] correlation is recommended. This correlation is also found suitable for aqueous and non-aqueous (R-12) condensation inside tubes.
4. Then the wavy flow regime follows which is correlated by Akers et al. [6] formula, however, the number of data points available within this regime in the data base is small compared to the other two flow regimes. Akers et al. [6] correlation has a wide data base support in the

literature and was considered adequate within wavy flow regime.

5. Condensation heat transfer models, correlated on the basis of an experimental data set, predicted more accurately within the range of parameters covered by that experiment.
6. The modified Azer et al. [23] correlation (Equation 4.10) is suitable for more accurate predictions within the annular flow regime for parameters defined by data set No. 4. Similarly Traviss et al. [25] correlation is suitable for accurate predictions within the range of parameters defined by data set No. 3.

On the basis of the design procedure developed, the following conclusions are made:

1. For condensers with condensation occurring inside the tubes the design must provide for the different flow regimes. That is a section of the condenser must be designed for each flow regime rather than using a single data correlation for the entire length of the condenser without any regard to flow transitions.
2. Successive summation method of heat exchanger design provides a suitable algorithm for incorporating the concept of flow transitions and the associated change in the applicable heat transfer correlations.

6.2 Recommendations

This investigation , like many others in the literature, has been able to answer only a limited number of questions. However, the study has led to further questions and ideas. These ideas and questions require research efforts to increase our perception of the mechanisms involved in condensation of saturated vapors inside horizontal tubes.

1. In order to increase the generality of the correlations, selected for use in a particular flow regime, the analysis described in Chapter 4 must be repeated with as many data sets as possible. Such data sets must include different fluids, mass flow rates and tube diameters.
2. Since the present study has not been able to incorporate all condensation heat transfer correlations available to date, an effort to verify condensation correlations available in other parts of the World must be made.
3. The application of specific condensation heat transfer correlations for each flow regimes gives rise to abrupt changes in the predicted heat transfer coefficients in the transition zone. Research effort is required to ensure a smooth transition of heat transfer coefficients at the transition zones where two different correlations meet.
4. New data are required in large diameter pipes (25 mm and above) which are lacking in the literature.

REFERENCES

1. Young, F.L., and Wohlenberg, W.J., "Condensation of Saturated Freon-12 Vapor on a Bank of Horizontal Tubes", Transactions of the ASME, Vol. 64, 1942, pp. 787-794.
2. ASHRAE Handbook of Fundamentals (1985).
3. Akers, W.W., and Rosson, H.F., "Condensation Inside a Horizontal Tube", Chem. Eng. Symp. Ser., No. 30, Vol. 56, 1960, pp. 145-149.
4. Nusselt, W., "Die Oberflächenkondensation des Wasserdampfes", Zeitschrift des Vereines deutscher Ingenieure, Vol. 60, 1916, pp. 541-546 and 569-575.
5. Kirkbride, C.G., "Heat Transfer by Condensing Vapor on Vertical Tubes", Trans. American Institute of Chemical Engineers, Vol. 30, 1933-1934, pp. 170-186.
6. Akers, W.W., Deans, H.A., and Crosser, O.K., "Condensing Heat Transfer Within Horizontal Tubes", Chem. Eng. Symp. Ser., No.29, Vol. 55, 1959, pp. 171-176.
7. Altman, M., Staub, F.W., and Norris, R.H., "Local Heat Transfer and Pressure Drop for Refrigerant - 22 Condensing in Horizontal Tubes", Chem. Eng. Symp. Ser., No. 30, Vol. 56, 1960, pp. 151-159.
8. Forster, H.K., and Zuber, N., "Dynamics of Vapor Bubbles and Boiling Heat Transfer", AIChE Journal, Vol. 1, No. 4, 1955, pp. 531-535.
9. Abromowitz, M., "Tables of Functions", Journal of Research, Nat. Bur. of Stds., Vol. 47, 1951, p. 288.
10. Kern, D.Q., "Process Heat Transfer", McGraw-Hill, New York, 1950, pp. 265-270.
11. Chaddock, J.B., "Film Condensation of Vapor in a Horizontal Tube", Refrigeration Engineering, Vol. 65, April, 1957, pp. 36-95.
12. Carpenter, E.F., and Colburn, A.P., "The Effect of Vapor Velocity on Condensation Inside Tubes", General Discussion on Heat Transfer, ASME, July 1951, pp. 20-26.
13. Bergelin, O.P., Kegel, P.K., Carpenter, F.G. and Gazley, C. Jr., "Co-Current Gas Liquid Flow. II. Flow in Vertical Tubes", Heat Transfer and Fluid Mechanics Institute, ASME, 1949.

14. Rohsenow, W.M., Webber, J.H., and Ling, A.T., "Effect of vapor velocity on Laminar and Turbulent - Film Condensation", Transactions of the ASME, Vol. 78, November, 1956, pp. 1637-1643.
15. Rohsenow, W.M., "Heat Transfer and Temperature Distribution in Laminar-Film Condensation", Transactions of the ASME, Vol. 78, November 1956, pp. 1645-1648.
16. Rosson, H.F., and Myers, J.A., "Point Values of Condensing Film Coefficients Inside a Horizontal Pipe", Chem. Eng. Prog. Symp. Ser., No. 59, Vol. 61, 1965, pp. 190-199.
17. Lockhart, R.W., and Martinelli, R.C., "Proposed Correlation of Data for Isothermal Two-Phase Two-Component Flow in Pipes", Chem. Eng. Prog., Vol. 45, No. 1, 1949, pp. 39-48.
18. Boyko, L.D., and Kruzhillin, G.N., "Heat Transfer and Hydraulic Resistance During Condensation of Steam in a Horizontal Tube and in a Bundle of Tubes", Int. J. Heat Mass Transfer, Vol. 10, 1967, pp. 361-373.
19. Soliman, M., Schuster, J.R., and Berenson, P.J., "A General Heat Transfer Correlation for Annular Flow Condensation", ASME Journal of Heat Transfer, Vol. 90, May, 1968, pp. 267-276.
20. Bae, S., Maulbetsch, J.S., and Rohsenow, W.M., "Refrigerant Forced - Convection Condensation Inside Horizontal Tubes", ASHRAE Transactions, Vol. 77, Part II, 1971, pp. 104-113.
21. Chen, C.J. "Condensing Heat Transfer in Horizontal Tube", M.S. Thesis, Dept. of Mechanical Engineering, Kansas State University, 1962.
22. Abis, L.V., "Forced Convection Condensation Inside Horizontal Tubes", Ph.D. Thesis, Dept. of Mechanical Engineering, Kansas State University, October 1969.
23. Azer, N.Z., Abis, L.V., and Swearingen, T.B., "Local Heat Transfer Coefficients During Forced Convection Condensation Inside Horizontal Tubes", ASHRAE Transactions, Vol. 77, Part I, 1971, pp. 182-201.
24. Azer, N.Z., Abis, L.V., and Soliman, H.M., "Local Heat Transfer Coefficients During Annular Flow Condensation", ASHRAE Transactions, Vol. 78, Part II, 1972, pp. 135-143.

25. Traviss, D.P., Rohsenow, W.M., and Baron, A.B., "Forced Convection Condensation Inside Tubes: A Heat Transfer Equation for Condenser Design", ASHRAE Transactions, Vol. 79, Part I, 1973, pp. 157-165.
26. Jaster, H., and Kosky, P.G., "Condensation Heat Transfer in a Mixed Flow Regime", Int. J. Heat Mass Transfer, Vol. 19, 1976, pp. 95-99.
27. Cavallini, A., and Zecchin, R., "Heat Transfer and Pressure Drop in Forced Convection Condensation Inside Tubes", in Heat and Mass Transfer in Refrigeration Systems and in Air-Conditioning, Bulletin of the International Institute of Refrigeration, 1972, pp. 139-148.
28. Goodykoontz, J.H., and Brown, W.F., "Local Heat Transfer and Pressure Distributions for Freon-113 Condensing in Downward Flow in a Vertical Tube", NASA Technical Note TN D-3952, May, 1967.
29. Cavallini, A. and Zecchin, R., "Scambio Termico Nella Condensazione ad Alta Velocita di Fluidi Organici Entro Tubi", La Termotecnica, Vol. XXVI, No. 4, 1972.
30. Shah, M.M., "A General Correlation for Heat Transfer During Film Condensation Inside Pipes", Int. J. Heat Mass Transfer, Vol. 22, 1979, pp. 547-556.
31. Tandon, T.N., Varma, H.K., and Gupta, C.P., "An Experimental Investigation of Forced-Convection Condensation During Annular Flow Inside a Horizontal Tube", ASHRAE Transactions, Vol. 91, Part IA, 1985, pp. 343-355.
32. Soliman, H.M., "The Mist-Annular Transition During Condensation and its Influence on the Heat Transfer Mechanism", Int. J. Multiphase Flow, Vol. 12, No. 2, 1986, pp. 277-288.
33. Baker, O., "Simultaneous Flow of Oil and Gas", Oil and Gas Journal, Vol. 53, 1954, pp. 185-195.
34. Isbin, H.S., et al., Preprint No. 147, Nuclear Engineering and Science Conference, Chicago, Illinois, 1958.
35. Scott, D.S., "Properties of Co-Current Gas-Liquid Flow", Advances in Chem. Eng., Vol. 4, 1963.

36. Traviss, D.P., and Rohsenow, W.M., "Flow Regimes in Horizontal Two-Phase Flow with Condensation", ASHRAE Transactions, Vol. 79, 1973, pp. 31-39.
37. Soliman, H.M., and Azer, N.Z., "Flow Patterns During Condensation Inside a Horizontal Tube", ASHRAE Transactions, Vol. 77, 1971, pp. 210-224.
38. Quandt, E., "Analysis of Gas-Liquid Flow Patterns", Chem. Eng. Prog. Symp. Ser., Vol. 61, No. 57, 1965, pp. 128-135.
39. Breber, G., Palen, J.W., and Taborek, J., "Prediction of Horizontal Tubeside Condensation of Pure Components Using Flow Regime Criteria", ASME Journal of Heat Transfer, Vol. 102, August, 1980, pp. 471-476.
40. Taitel, Y., and Dukler, A.E., "A Model for Predicting Flow Regime Transitions in Horizontal and Near Horizontal Gas-Liquid Flow", AIChE Journal, Vol. 22, No. 1, 1976, pp. 47-55.
41. Wallis, G.B., "Flooding Velocities for Air and Water in Vertical Tubes", UKAEA Report AEE W-R-123, 1962, and "One-Dimensional Two-Phase Flow", McGraw-Hill, New York, 1969.
42. Soliman, H.M., "On the Annular-to-Wavy Flow Pattern Transition During Condensation Inside Horizontal Tubes", The Canadian Journal of Chemical Engineering, Vol. 60, August, 1982, pp. 475-481.
43. Soliman, H.M., "Correlation of Mist-to-Annular Transition During Condensation", The Canadian Journal of Chemical Engineering, Vol. 61, April, 1983, pp. 178-182.
44. Weisman, J., Duncan, D., and Gibson, J., "Effects of Fluid Properties and Pipe Diameter on Two-Phase Flow Patterns in Horizontal Lines", Int. J. Multiphase Flow, Vol. 5, 1979, pp. 437-462.
45. Mandhane, J.M., Gregory, G.A., and Aziz, K., "A Flow Pattern Map for Gas-Liquid Flow in Horizontal Pipes", Int. J. Multiphase Flow, Vol. 1, 1974, pp. 537-553.
46. Bell, K.J., Taborek, J., and Fenoglio, F., "Interpretation of Horizontal In-Tube Condensation Heat Transfer Correlation with a Two-Phase Flow Regime Map", Chem. Eng. Proc. Symp. Ser., Vol. 66, No. 102, 1970, pp. 150-163.

47. Goodykoontz, J.H. and Dorsch, R., "Local Heat Transfer Coefficients and Static Pressures for Condensation of High-Velocity Steam Within a Tube"., NASA Technical Note TN D-3953, May, 1967.
48. Goodykoontz, J.H., and Dorsch, R., "Local Heat Transfer Coefficients for Condensation of Steam in Vertical Downflow Within a 5/8-Inch-Diameter Tube, NASA Technical Note, TN D-3326, March, 1966.
49. Traviss, D.P., "Condensation in Refrigeration Condensers", Ph.D. Thesis, MIT, 1972.
50. "Steam Tables", An ASME Publication Distributed by Combustion Engineering, Inc., Windsor, Conn., 1967.

APPENDIX A

Determination of State Points in a Vapor Compression Cycle

The state points, shown in Fig. 1.1 and 1.2, of a real vapor compression cycle are calculated below. The property values are obtained from ASHRAE Handbook 1985 Fundamentals [2].

Refrigerant used	= R-502
Refrigerated space temperature	= -20°C
Ambient air temperature	= 32°C
Evaporator temperature	= 28.9°C
Condenser temperature	= 43°C

State Point Properties

State	Absolute Pressure MPa	Temperature $^{\circ}\text{C}$	Enthalpy kJ/kg	Entropy kJ/K
1	0.22	-27.8	239.0	1.156
2	0.19	-31.7	330.4	1.551
3	0.18	-24.0	335.2	1.567
4	0.17	-18.0	336.8	1.580
5	2.4	93.0	397.9	1.610
6	2.1	89.8	397.9	1.624
7	1.7	40.6	246.3	1.162
8	1.5	35.0	239.0	1.136

Refrigerant effect	= 330.4 - 239.0
	= 91.4 kJ/kg
Refrigerant mass flow	= 211/91.4
	= 2.31 kg/min
	= 38.6 g/s
Heat of compression	= (397.9-335.2) 2.31
	= 144.84 kJ/min
	= 2.4 kW
COP	= 211/144.84
	= 1.5
Heat rejected	= (397.9-239.0) 2.31
	= 367.1 kJ/min
	= 6.1 kW
Heat absorbed	= 211 kJ/min
	= 3.52 kW
Superheating in suction lines	= (335.2-330.4) 2.31
	= 11.1 kJ/min
	= 0.19 kW
Superheating in the compressor cylinder	= (336.8-335.12) 2.31
	= 3.88 kJ/min
	= 0.07 kW
Change in Entropy of the refrigerated space assuming Carnot Cycle operation, ΔS_R	= -211/253
	= -0.8340 kJ/K-min

Net work input for a Carnot cycle operation, W	$= S_R (T_O - T_R)$ $= 0.8340 (316.3 - 253)$ $= 52.82 \text{ kJ/min}$ $= 0.88 \text{ kW}$
Change in entropy at the evaporator due to finite temperature difference, S_{Qi}	$= 211/246.9$ $= 0.8546 \text{ kJ/K-min}$
Network input for an actual cycle (including superheat)	$= 367.1 - 211.0$ $= 156.1 \text{ kJ/min}$ $= 2.6 \text{ kW}$
Overall COP	$= 211/157$ $= 1.35$
Work input to the cycle, W	$= 156.1 - 52.82$ $= 103.28 \text{ kJ/min}$ $= 1.72 \text{ kW}$
Change of entropy of the atmosphere, S_o	$= 367.1/316.3$ $= 1.1605 \text{ kJ/K-min}$
Net increase in entropy, S_{univ}	$= 1.1605 - 0.8340$ $= 0.3265 \text{ kJ/K-min}$
Net irreversibility, $T_o S_{univ}$	$= 316.3 \times 0.3265$ $= 103.3 \text{ kJ/min}$ $= 1.72 \text{ kW}$

Available energy outflow from the refrigerant during heat rejection, $(E_u)_o$

$$= [(1.162-1.136) 2.31 + (1.567-1.551) 2.31 + (1.58-1.567) 2.31 + (1.624-1.567) 2.31] 316.3$$

$$= (1.1133) 316.3$$

$$= 352.14 \text{ kJ/min}$$

$$= 5.87 \text{ kW}$$

Available energy outflow from the refrigerant during its process of heat rejection rendered unavailable when absorbed by atmosphere, $(E_A)_o$

$$= 367.1 - 352.14$$

$$= 14.96 \text{ kJ/min}$$

$$= 0.25 \text{ kW}$$

Available and unavailable portion of energy inflow during evaporation and compression, $(E_u)_i$

$$= 316.3 \times 0.8546$$

$$= 270.3 \text{ kJ/min}$$

$$= 4.51 \text{ kW}$$

Available energy inflow to the refrigerant during compression

$$= 211 - 270.3$$

$$= -59.3 \text{ kJ/min}$$

$$= -0.99 \text{ kW}$$

Available energy that is degraded by the heat transfer from the refrigerated space when the process is accomplished through a finite temperature differences, $(E_{Ad})_i$

$$= -[-59.3 - (-52.82)]$$

$$= 6.49 \text{ kJ/min}$$

$$= 0.11 \text{ kW}$$

$$(E_{Ad})_o = (E_A)_o = 14.96 \text{ kJ/min}$$

Irreversibilities caused in
expansion valve and compressor
valves

$$= 316.3 (0.0601 + 0.0370 + 0.0300 + 0.1317)$$

$$= 81.83 \text{ kJ/min}$$

$$= 1.36 \text{ kW}$$

Sum of all the available energy
that has been degraded by the
refrigerant in its cyclical
operation, (ΣE_{Ad})

$$= 6.49 + 14.96 + 81.83$$

$$= 103.28 \text{ kJ/min}$$

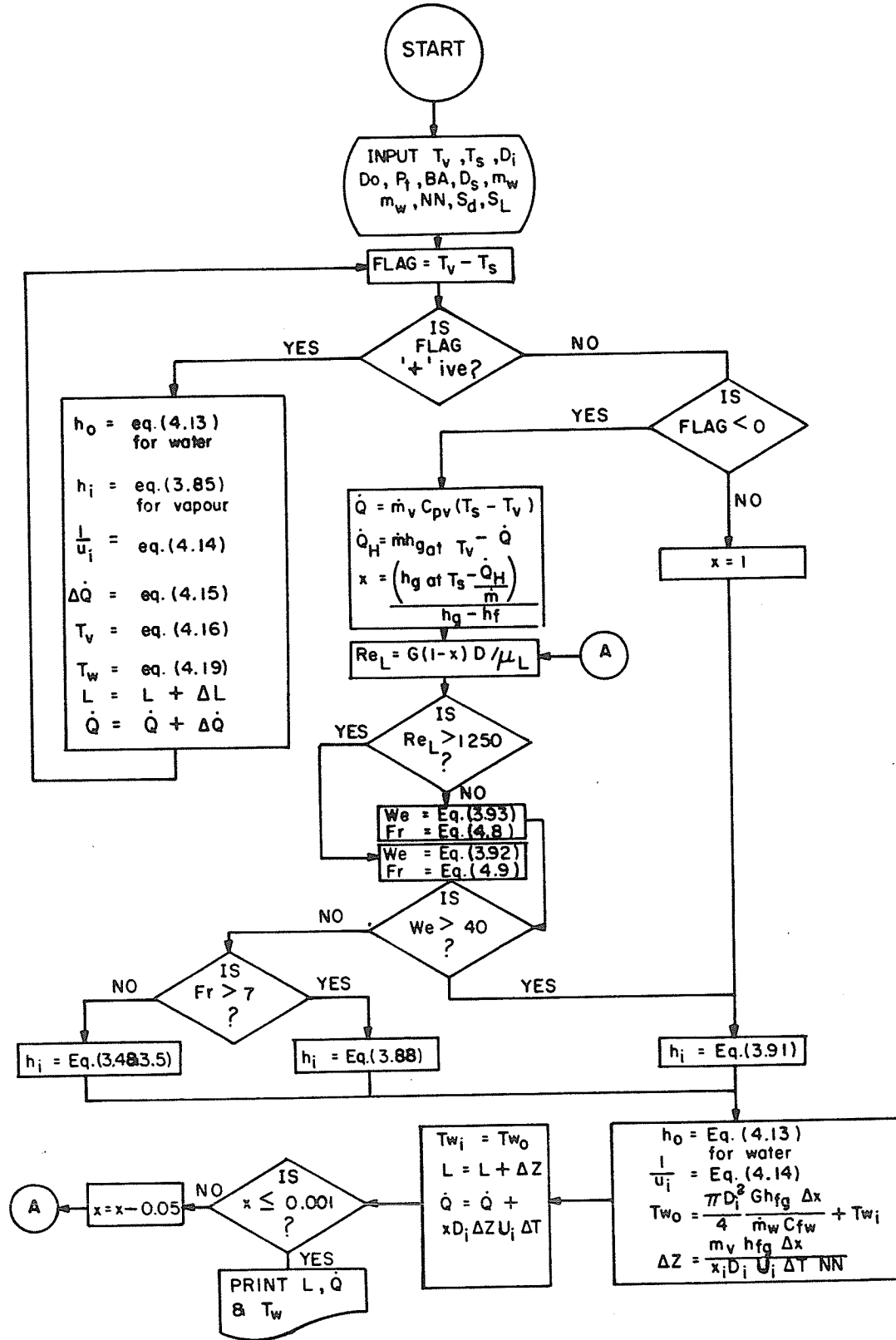
$$= 1.72 \text{ kW}$$

Energy	kJ/min	Area
Q_i	211.00	$q + t$
Q_o	367.10	$(a \rightarrow u)$
w	156.10	$(a \rightarrow u) - (q + t)$
$(E_A)_i$	-59.30	$-(l + m)$
$(E_U)_i$	270.30	$l + m + q + t$
$(E_A)_o$	14.96	$(a \rightarrow h)$
$(E_U)_o$	352.14	$(i \rightarrow u)$
$(E_{Ad})_r$	81.80	$i + (j+k) + (n+r+S+u) + (o+p+v)$

$$\begin{array}{rclcl}
 Q_i & + & W & = & Q_o \\
 211 & + & 156.1 & = & 367.1 \\
 \\
 Q_i & = & (E_A)_i & + & (E_U)_i \\
 211 & = & -59.3 & + & 270.3 \\
 \\
 Q_o & = & (E_A)_o & + & (E_U)_o \\
 367.1 & = & 14.96 & + & 352.14 \\
 \\
 W & + & (E_A)_i & = & (E_A)_o & + & (E_{Ad})_r \\
 156.1 & - & 59.3 & = & 14.96 & + & 81.83 \\
 & & 91.59 & = & 91.59 & & \\
 \\
 (E_U)_i & + & (E_{Ad})_r & = & (E_U)_o \\
 270.3 & + & 81.83 & = & 352.14
 \end{array}$$

APPENDIX B

Algorithm of the Design Procedure



APPENDIX C

Computer Listing of the BASIC Program

```

1 REM *****
2 REM          PROGRAM DEVELOPED BY T.NITHEANANDAN
3 REM *****
4 REM
5 REM *****
6 REM *THIS PROGRAM IS ABLE TO DESIGN A CONDENSER WHEN PARTICULARS REQUIRED IN*
7 REM *STATEMENTS 35 TO 48 ARE TYPED IN. TWO BUILT-IN SUBROUTINES SUPPLY THE *
8 REM *THERMODYNAMIC PROPERTY VALUES OF R-502 AND WATER. FOR ANY OTHER VAPORS *
9 REM *OTHER THAN R-502 A NEW SUBROUTINE TO HANDLE PROPERTIES MUST BE INCORPE-*
10 REM *RATED.THE DESIGN IS MADE IN SMALL SEGMENTS AS THE VAPOR CHANGES FROM A *
11 REM *SUPER HEATED VAPOR TO A SATURATED LIQUID,THEN THE SEGMENTS ARE SUMMED *
12 REM *TO OBTAIN THE FINAL DESIGN.
13 REM *****
14 DEFDBL A-H
15 DEFDBL K-Z
16 PRINT "DO YOU LIKE TO RUN THIS PROGRAMME WITH THE BUILT-IN INPUT DATA?"
17 PRINT "TYPE 'Y' IF THE ANSWER IS YES. ELSE TYPE ANY OTHER KEY"
18 INPUT A$
19 IF A$="Y" THEN GOTO 35
20 INPUT "VAPOR TEMPERATURE";TV
21 INPUT "SATURATION TEMPERATURE";TS
22 INPUT "INTERNAL DIAMETER OF TUBES";DI
23 INPUT "OUT SIDE DIAMETER OF TUBES";DO
24 INPUT "PITCH OF TUBES";PT
25 INPUT "BAFFLE SPACING";BA
26 INPUT "SHELL DIAMETER";DS
27 INPUT "MASS FLOW RATE OF SHELL SIDE FLUID";MW
28 INPUT "NUMBER OF TUBES";NN
29 INPUT "MASS FLOW RATE OF TUBE SIDE FLUID";MV
30 INPUT "INLET TEMPERATURE OF SHELL SIDE FLUID";TW
31 INPUT "TRANSVERSE SPACING OF TUBES";ST
32 INPUT "DIAGONAL SPACING OF TUBES";SD
33 INPUT "LONGITUDINAL SPACING TUBES";SL
35 TV=158
36 TS=104
37 DI=3.583333E-02
38 DO=4.166667E-02
39 PT=.0625
40 BA=2
41 DS=.5
42 MW=8000
43 NN=40
44 MV=4000
45 TW=41
46 ST=.0625
47 SD=.0625
48 SL=.649519
50 LPRINT "          DESIGN OF A CONDENSER FOR R-502"
51 LPRINT
52 LPRINT
111 GW=TW
112 TW=(TV+TS)/2
113 GOSUB 3000
114 FZ=FW
116 TW=GW
120 LE=0
121 J=0      :TF=TS
122 GOSUB 1100
124 LPRINT "Temperature of the super heated vapor=",TV,"Deg.F"
125 LPRINT "Saturation temperature          =",TS,"Deg.F"

```

```

126 LPRINT "Pitch                                =",PT,"feet" :LPRINT "Baffle s
pacing                                =",BA,"feet"
127 LPRINT "Outside diameter of tube          =",DO,"feet":LPRINT "Inside dia
. of tube                                =",DI,"feet"
128 LPRINT "Mass flowrate of water=" ,MW,"lbs/hr"
129 LPRINT "Mass flowrate of R-502=" ,MV,"lbs/hr"
130 U=0
131 LPRINT "No. of tubes=" ,NN
132 X=DS*(PT-DO)*BA/PT
133 LPRINT "Water inlet temperature=" ,TW,"Deg.F"
134 Y=(3.4641016##PT^2)/(3.1415927##DO)-DO
135 LPRINT
136 LPRINT "DETAILS OF THE CONDENSER PORTION COOLING SUPER HEATED VAPOR"
138 LPRINT
139 LPRINT
140 W=TV-TS
150 IF W < 0 THEN GOTO 396
160 IF W = 0 THEN GOTO 380
165 GOSUB 3000
166 G1=MW/(RW*X)
170 A=(SD-DO)*2
172 B=(ST-DO)
173 REM LPRINT "A=" ,A,"B=" ,B
174 IF A<B THEN GOTO 180
176 G=G1*ST/(ST-DO)
178 GOTO 210
180 G=G1*ST/(2*(SD-DO))
210 F9=RW*G*Y/VW
215 IF F9<1000 THEN GOTO 4430
216 IF F9>2000000! THEN GOTO 223
217 R1=ST/SL
218 IF R1>2 THEN GOTO 221
219 C=.35*(ST/SL)^.2 :M=.6
220 GOTO 230
221 C=.4 :M=.6
222 GOTO 230
223 IF F9>2000000! THEN GOTO 4430
224 C=.022 :M=.84
230 HO=C*(F9^M)*(PW^.36)*((PW/PZ)^.25)*KW/Y
234 TF=TV
235 J=1
240 GOSUB 1100
280 F=1.2732396##MV/(DI*VG*NN)
290 Z=CG*VG/KG
300 HI=.023*(F^.8)*(Z^.3)*KG/DI
310 UI=1/(1/HI+1/(HO*(DO/DI)))+(DO-DI)*DI/(231.70582##(DO+DI))
320 QL=1.5707963##DI*UI*(TV-TW)*NN
330 TV=TV-QL/(MV*CG)
340 TW=QL/(MW*CW)+TW
350 LE=LE+.5
360 U=U+QL
361 LPRINT
362 LPRINT "HO=" ,HO,"Btu/hr-sq.ft-F"
363 LPRINT "HI=" ,HI,"Btu/hr-sq.ft-F"
364 LPRINT "U=" ,UI,"Btu/hr-sq.ft-F"
365 LPRINT "SHELL SIDE REYNOLDS No.=" ,F9
366 LPRINT "M=" ,M,"C=" ,C
367 LPRINT "PW=" ,PW,"PZ=" ,PZ
368 LPRINT "TUBE SIDE REYNOLDS No.=" ,F
369 LPRINT "HEAT TRANSFERED IN HALF FEET LENGTH=" ,QL,"Btu/hr"
370 LPRINT "RATIO ST/SL=" ,R1,"G=" ,G

```

```

371 LPRINT "TV=",TV,"TW=",TW
373 GOTO 138
380 QA=1
385 LPRINT "LENGTH REQUIRED TO REMOVE SUPER HEAT=",LE,"feet"
386 LPRINT "Heat transfered while removing super heat=",U,"Btu/hr"
390 GOTO 410
396 QC=MV*CG*(TS-TV)
397 QH=MV*HG-QC
398 QA=(QH/MV-HE)/(HG-HE)
399 LPRINT "LENGTH REQUIRED TO REMOVE SUPER HEAT=",LE,"feet"
400 LPRINT "Heat transfered while removing super heat=",U,"Btu/hr"
410 GW=TW
411 TW=TS
412 GOSUB 3000
413 FZ=FW
414 TW=GW
423 LPRINT
424 LPRINT
425 LPRINT
426 LPRINT
427 LPRINT "DETAILS OF THE CONDENSER PORTION REMOVING LATENT HEAT OF SATURATED V
APOR"
428 J=2 :TF=TS :GOSUB 1100
429 LPRINT
430 LPRINT
435 RE=1.2732396##MV*(1-QA)/(DI*VL*NN)
450 XT=((VL/VV)^.1)*(((1-QA)/QA)^.9)*(RV/RL)^.5
460 XI=1+1.09*(XT^.039)
465 SI=451431.53#
470 S1=VL*VL/(RL*SI*DI)
480 BB=(S1^.3)*((RV/RL)^.0555)*((VL/VV)^.111)*(XT^-.711)*(XI^-.4)
485 IF RE>1250 THEN GOTO 500
490 FF=2.45247*(RE^.64)*BB
495 GOTO 550
500 FF=.853003*(RE^.79)*BB
550 LPRINT "MODIFIED WEB.NO.=",FF
600 IF FF<40 THEN GOTO 671
610 SS=(QA/VV)+(1-QA)/VL
620 SA=1.2732396##MV*SS/(DI*NN)
630 QC=MV*HF*(QA-.05)/NN
640 TT=(QC*LOG(DO/DI))/(1455.8506#)+TW
650 SE=VV*HF/(KV*(TS-TT))
660 HI=.00345*(SA^.9)*(SE^.333333)*KL/DI
670 GOTO 790
671 IF RE > 1250 THEN GOTO 674
672 FR=.024*(RE^1.6)*(((VL*VL)/(4.1731*(10^8)*(DI^3)*RL*RL))^.5)*((XI/XT)^1.5)
673 GOTO 675
674 FR=1.28*(RE^1.04)*(((VL*VL)/(4.1731*(10^8)*(DI^3)*RL*RL))^.5)*((XI/XT)^1.5)
675 LPRINT
676 LPRINT
677 LPRINT "FROUDE NUMBER=",FR
678 IF FR < 7 THEN GOTO 690
679 PR=CL*VL/KL
680 HL=.023*(((1.2732396##MV)/(VL*DI*NN))^.8)*(PR^.4)*KL/DI
681 H9=HL*((1-QA)^.8)
682 Z9=(((1/QA)-1)^.8)*((PS/619)^.4)
683 HI=H9*(1+(3.8/(Z9^.95)))
684 PRINT PS
685 GOTO 790
690 PR=CL*VL/KL

```

```

691 GX=1.2732396##MV/(DI*DI*NN)
692 GE=(1-QA)*GX+QA*GX*((RL/RV)^.5)
693 R9=DI*GE/VL
694 IF R9 > 50000! THEN GOTO 697
695 HI=5.03*(PR^.333333)*(R9^.333333)*KL/DI
696 GOTO 790
697 HI=.0265*(PR^.333333)*(R9^.8)*KL/DI
790 GOSUB 3000
800 F=RW*G*Y/VW
805 IF F<1000 THEN GOTO 4430
806 IF F>200000! THEN GOTO 813
807 R1=ST/SL
808 IF R1>2 THEN GOTO 811
809 C=.35*(ST/SL)^.2           :M=.6
810 GOTO 820
811 C=.4                       :M=.6
812 GOTO 820
813 IF F>2000000! THEN GOTO 4430
814 C=.022                   :M=.84
815 IF F<1000 THEN GOTO 4430
820 HO=C*(F^M)*(PW^.36)*((PW/PZ)^.25)*KW/Y
830 UI=1/(1/HI+1/(HO*(DO/DI))+(DO-DI)*DI/(231.70582##(DO+DI)))
840 T9=(MV*HF*.05)/(MW*CW) + TW
850 DT=((TS-T9)-(TS-TW))/(LOG((TS-T9)/(TS-TW)))
860 DZ=MV*HF*.05/(3.1415927##DI*UI*DT*NN)
870 TW=T9
880 LE=LE+DZ
890 U=U+3.1415927##DI*DZ*NN*UI*DT
892 LPRINT "HO=",HO,"Btu/hr-sq.ft-F"
894 LPRINT "HI=",HI,"Btu/hr-sq.ft-F"
896 LPRINT "U=",UI,"Btu/hr-sq.ft-F"
897 LPRINT
898 LPRINT "LENGTH OF HEAT EXCHANGER REQUIRED TO CONDENSE 5% QUALITY=",DZ,"FEET"
899 LPRINT "QUALITY=",QA
900 LPRINT "REYNOLDS NUMBER SHELL SIDE=",F
901 LPRINT "LIQUID REYNOLDS No.TUBE SIDE=",RE
902 LPRINT "M=",M,"C=",C
903 LPRINT "PW=",PW,"PZ=",PZ
909 QA=QA-.05
910 IF (QA < 0) THEN GOTO 930
920 GOTO 430
930 LPRINT
932 LPRINT
934 LPRINT "THE DETAILS OF THE FINAL DESIGN"
936 LPRINT
938 LPRINT "TOTAL LENGTH=",LE,"feet"
940 LPRINT "TOTAL HEAT TRANSFERED=",U,"Btu/hr"
950 LPRINT "WATER OUTLET TEMPERATURE=",TW,"Deg.F"
990 END
1100 TC=(TF-32)*5/9
1101 TC=(TF-32)*5/9
1170 T=TC+273
1175 TR=TF+459.67
1176 IF J >> 1 THEN GOTO 1180
1177 TJ=TS+459.67
1178 GOTO 2230
1180 IF T < 268 THEN GOTO 4410
1185 IF T > 320 THEN GOTO 4410
1190 VT=-13.586+6104.13/T-763533!/T^2
1200 VL=(EXP(VT))/.413
1250 KL=(.0742-.000391*TC)/1.728
1260 KV=5.32444*.001+1.8*.00001*TF
1280 CL=(.94098-9.297479*.0001*T+6.58114*10^(-6)*T^2)/4.19
1290 CV=(-15.5795+.1871*T-7.2396*10^(-4)*T^2+9.41629*10^(-7)*T^3)/4.19

```

```

2210 V1=-8.517301E+02+1.02897*.001+1-0.802824.000001*TR+4.89888*1E-09*TR+3
2220 VV=V1/.413
2230 V2=T^5/(.6997+192.77/T+20.394/T^2)
2240 V6=(V2*.001)/.413
2270 K6=(-.01118+1.25755*.0001*TR-2.68221*.0000001*TR^2+3.44533*10^(-10)*TR^3)/1.72
8
2272 IF J=1 THEN GOTO 2302
2300 C6=(.415949+1.53046*10^(-4)*TR+4.53163*10^(-6)*TR^2-6.37086*10^(-9)*TR^3)/4.19
2301 GOTO 2305
2302 TR=TJ
2305 A=10.64495-3671.153/TR-.3698349*LOG(TR)*.434294481903#
2307 B=654-TR
2310 PS=10^(A-.0017463519#*TR+.8161139*B*LOG(B)*.434294481903#/TR)
2315 IF J=1 THEN GOTO 2345
2330 T1=1-TR/639.56
2340 RL=35!+53.48437*T1^(1/3)+63.86417*T1^(2/3)-70.08066*T1+48.47901*T1^(4/3)
2344 GOTO 2350
2345 TR=TF+459.67
2350 E0=EXP(-4.2*TR/639.56)
2360 E1=PS
2370 E2=.096125*TR
2380 E3=-3.2613344#+.0020576287#*TR-24.24878*E0
2390 E4=.034866748#-.86791313#*.00001*TR+.33274779#*E0
2400 E5=-8.5765677#*.0001-7.0240549#*.0000001*TR+.022412368#*E0
2410 E6=8.8368967#*.000001-7.9168095#*1E-09*TR-3.7167231#*.0001*E0
2420 E7=-3.8253726#*10000000#+5.5816094#*10000*TR+1.5378377#*1000000000#*E0
2430 E8=2*E3
2440 E9=3*E4
2450 F1=4*E5
2460 F2=5*E6
2470 VN=.096125*TR/PS
2480 I=0
2485 TT=9999999999999#
2490 I=I+1
2500 IF I > 50 THEN GOTO 2703
2510 V=VN
2520 V2=V^2
2530 V3=V^3
2540 V4=V^4
2550 V5=V^5
2560 V6=V^6
2570 F3=EXP(-609*(V+.00167))
2580 F4=F3^2
2590 F=E1-E2/V-E3/V2-E4/V3-E5/V4-E6/V5-E7*F4/(F3+.0000007)
2600 FV=E2/V2+E8/V3+E9/V4+F1/V5+F2/V6+E7*609*F4*(F3+2*.0000007)/(F3+.0000007)^2
2610 VN=V-F/FV
2620 Z=(VN-V)/V
2630 Z1=ABS(Z)
2635 IF Z1 < TT THEN TT=Z1 :LL=VN
2640 IF Z1 > 1E-08 THEN GOTO 2490
2650 RV=1/(VN+.00167)
2655 IF J=1 THEN GOTO 2661
2660 HF=(1/RV-1/RL)*PS*2.302585093#*(3671.15381257#/TR-.36983496#/2.302585093#-
0017463519#*TR-.81611391#*(.4342944819#+654*.434294481903#*LOG(654-TR)/TR))*185
053
2661 T2=TR^2
2662 T3=TR^3
2663 T4=TR^4
2664 VR=1/RV-.00167
2665 V1=2*VR^2
2666 V2=3*VR^3
2667 V3=4*VR^4
2668 KT=4.2*TR/639.56

```

```

2669 EK=EXP(-KT)
2670 EM=EXP(-609/RV)
2671 H1=.020419*TR+2.996802*.0001*T2/2-1.409043*.0000001*T3/3+2.210861*1E-11*T4/
4-64.058511#/TR
2672 H2=.185053*PS/RV
2673 H3=-3.2613344#/VR+.034866748#/V1-8.5765677#*.0001/V2+8.8368967#*.000001/V3
2674 H4=-24.24879/VR+.33274779#/V1+.022412368#/V2-3.7167231#*.0001/V3
2675 H0=1/609*(EM-7*.0000001*LOG(1+EM/.0000007))
2676 H3=H3-3.8253726#*10000000#*H0
2677 H4=H4+1.5378377#*1000000000#*H0
2678 HG=H1+H2+.185053*H3+.185053*EK*(1+KT)*H4+35.308
2679 HE=HG-HF
2680 IF J=0 THEN GOTO 2683
2681 IF J=1 THEN GOTO 2685
2682 GOTO 2690
2683 HJ=HG
2684 GOTO 2690
2685 CG=(HG-HJ)/(TF-TS)
2690 LPRINT
2691 LPRINT
2692 LPRINT "          PROPERTIES OF R-502"
2693 LPRINT "VL=",VL,"VV=",VV
2694 LPRINT "VG=",VG,"KL=",KL
2695 LPRINT "KV=",KV,"KG=",KG
2696 LPRINT "CL=",CL,"CV=",CV
2697 LPRINT "CG=",CG,"PS=",PS
2698 LPRINT "RL=",RL,"RV=",RV
2699 LPRINT "HFG=",HF,"HF=",HE
2700 LPRINT "HG=",HG,"TF=",TF
2701 GOTO 2900
2703 LPRINT
2704 LPRINT
2705 LPRINT "*** WARNING *** VAPOUR DENSITY CONVERGES AT A REDUCED TOLARENCE OF"
,TT,"THE ACCEPTED TOLARENCE= 1.0 E-08"
2706 RV=1/(LL+.00167)
2707 GOTO 2655
2900 RETURN
3000 O=(TW-32)*5/9+273.15
3100 IF O<273.15 THEN GOTO 4410
3110 IF O>275 THEN GOTO 3180
3120 B1=0          :B2=1
3130 B3=-.0012    :B4=4.217
3140 B5=19.6     :B6=1750
3150 B7=1        :B8=569
3160 B9=.154     :C1=12.99          :O1=O-273.15
3170 GOTO 4350
3180 IF O>280 THEN GOTO 3250
3190 B1=0          :B2=1
3200 B3=-.0026    :B4=4.211
3210 B5=46        :B6=1652
3220 B7=1.6       :B8=574
3230 B9=.392     :C1=12.22          :O1=O-275
3240 GOTO 4350
3250 IF O>285 THEN GOTO 3320
3260 B1=0          :B2=1
3270 B3=-.0018    :B4=4.198
3280 B5=39.4     :B6=1422
3290 B7=1.6       :B8=582
3300 B9=.29      :C1=10.26          :O1=O-280
3310 GOTO 4350
3320 IF O>290 THEN GOTO 3390
3330 B1=.0002     :B2=1
3340 B3=-.001     :B4=4.189
3350 B5=29        :B6=1225
3360 B7=1.6       :B8=590

```

```

3380 GOTO 4350
3390 IF 0>295 THEN GOTO 3460
3400 B1=.0002 :B2=1.001
3410 B3=-6.000001E-04:B4=4.184
3420 B5=24.2 :B6=1080
3430 B7=1.6 :B8=598
3440 B9=.188 :C1=7.56 :01=0-290
3450 GOTO 4350
3460 IF 0>300 THEN GOTO 3530
3470 B1=.0002 :B2=1.002
3480 B3=-.0004:B4=4.181
3490 B5=20.8 :B6=959
3500 B7=1.4 :B8=606
3510 B9=.158 :C1=6.62 :01=0-295
3520 GOTO 4350
3530 IF 0>305 THEN GOTO 3600
3540 B1=.0004 :B2=1.003
3550 B3=-.0002:B4=4.179
3560 B5=17.2 :B6=855
3570 B7=1.4 :B8=613
3580 B9=.126 :C1=5.83 :01=0-300
3590 GOTO 4350
3600 IF 0>310 THEN GOTO 3670
3610 B1=.0004 :B2=1.005
3620 B3=0 :B4=4.178
3630 B5=14.8 :B6=769
3640 B7=1.6 :B8=620
3650 B9=.116 :C1=5.2 :01=0-305
3660 GOTO 4350
3670 IF 0>315 THEN GOTO 3740
3680 B1=.0004 :B2=1.007
3690 B3=.0002 :B4=4.178
3700 B5=12.8 :B6=695
3710 B7=1.2 :B8=628
3720 B9=.092 :C1=4.62 :01=0-310
3730 GOTO 4350
3740 IF 0>320 THEN GOTO 3810
3750 B1=.0004 :B2=1.009
3760 B3=.0002 :B4=4.179
3770 B5=10.8 :B6=631
3780 B7=1.2 :B8=634
3790 B9=.078 :C1=4.16 :01=0-315
3800 GOTO 4350
3810 IF 0>325 THEN GOTO 3880
3820 B1=.0004 :B2=1.011
3830 B3=.0004 :B4=4.18
3840 B5=9.8 :B6=577
3850 B7=1 :B8=640
3860 B9=.07 :C1=3.77 :01=0-320
3870 GOTO 4350
3880 IF 0>330 THEN GOTO 3950
3890 B1=6.000001E-04 :B2=1.013
3900 B3=.0004 :B4=4.182
3910 B5=7.8 :B6=528
3920 B7=1 :B8=645
3930 B9=.054 :C1=3.42 :01=0-325
3940 GOTO 4350
3950 IF 0>335 THEN GOTO 4020
3960 B1=.0004 :B2=1.016
3970 B3=.0004 :B4=4.184
3980 B5=7.2 :B6=489
3990 B7=1.2 :B8=650

```

```

4000 B9=.054 :C1=3.15 :01=0-330
4010 GOTO 4350
4020 IF 0>340 THEN GOTO 4090
4030 B1=6.000001E-04 :B2=1.018
4040 B3=.0004 :B4=4.186
4050 B5=6.6 :B6=453
4060 B7=.8 :B8=656
4070 B9=.044 :C1=2.88 :01=0-335
4080 GOTO 4350
4090 IF 0>345 THEN GOTO 4160
4100 B1=6.000001E-04 :B2=1.021
4110 B3=6.000001E-04 :B4=4.188
4120 B5=6.2 :B6=420
4130 B7=1.6 :B8=660
4140 B9=.042 :C1=2.66 :01=0-340
4150 GOTO 4350
4160 IF 0>350 THEN GOTO 4230
4170 B1=6.000001E-04 :B2=1.024
4180 B3=.0008 :B4=4.191
4190 B5=4.8 :B6=389
4200 B7=0 :B8=668
4210 B9=.032 :C1=2.45 :01=0-345
4220 GOTO 4350
4230 IF 0>355 THEN GOTO 4290
4240 B1=6.000001E-04 :B2=1.027
4250 B3=.0008 :B4=4.195
4260 B5=4.4 :B6=365
4270 B7=.6 :B8=668
4280 B9=.03 :C1=2.29 :01=0-350
4285 GOTO 4350
4290 IF 0>360 THEN GOTO 4410
4300 B1=.0008 :B2=1.03
4310 B3=.0008 :B4=4.199
4320 B5=3.8 :B6=343
4330 B7=.6 :B8=671
4340 B9=.024 :C1=2.14 :01=0-355
4350 RW=(1/((B1*01+B2)*10^-3))*0.062428
4360 CW=(B3*01+B4)*.23886
4370 VW=(-B5*01+B6)*2419.1*10^-6
4380 KW=(B7*01+B8)*10^-3*.57782
4390 PW=(-B9*01+C1)
4400 GOTO 4420
4410 LPRINT "ERROR IN PROPERTY LIMITS"
4420 LPRINT
4421 LPRINT " PROPERTIES OF WATER"
4422 LPRINT "RW=",RW,"CW=",CW
4423 LPRINT "VW=",VW,"KW=",KW
4424 LPRINT "PW=",PW,"TW=",TW
4425 RETURN
4430 LPRINT "***ERROR***THIS PROGRAM HAS NO CORRELATIONS TO PREDICT NUSSELT NUMB
ER WHEN THE REYNOLDS NUMBER IS LESS THAN 1000 AND WHEN GREATER THAN 2000000."
4440 END

```